2006

Sulfonamide-induced cutaneous drug reactions: role of bioactivation, oxidative stress and folate deficiency

Piyush Manhur Vyas
University of Iowa

SULFONAMIDE-INDUCED CUTANEOUS DRUG REACTIONS: ROLE OF BIOACTIVATION, OXIDATIVE STRESS AND FOLATE DEFICIENCY

by

Piyush Manhar Vyas

An Abstract

Of a thesis submitted in partial fulfillment
of the requirements for the Doctor of
Philosophy degree in Pharmacy (Pharmaceutics)
in the Graduate College of
The University of Iowa

December 2006

Thesis Supervisor: Professor Craig K. Svensson

ABSTRACT

Sulfonamide- and sulfone-induced hypersensitivity reactions are thought to be mediated through bioactivation of parent drug molecule(s) to their respective reactive metabolite(s). In order to explain the cutaneous drug reactions caused by sulfonamides and sulfone, a mechanism can be proposed by which the bioactivation of these drugs in keratinocytes of the skin forms reactive hydroxylamine metabolites that can covalently bind to cellular proteins, which in turn act as antigens leading to the cascade of immune reactions resulting in a cutaneous drug reaction.

In order to probe the proposed mechanism, we determined the enzymes responsible for the bioactivation of these parent drugs to their hydroxylamine metabolites in cultured human keratinocytes. It was found that flavin containing monooxygenases and peroxidases play an important role in the bioactivation of these drugs in keratinocytes. We also confirmed the presence of these enzymes in keratinocytes. Interestingly, though cytochrome P450s are important in the oxidation of parent arylamine xenobiotics to their hydroxylamine metabolites in the liver, they do not appear to play a significant role in the bioactivation of these drugs in keratinocytes.

The hydroxylamine metabolites of sulfamethoxazole and dapsone can undergo autooxidation, generating reactive free radicals. Our studies showed that both of these metabolites elevate oxidative stress in keratinocytes by forming reactive oxygen species. Though the cytotoxicity induced by these metabolites is not correlated with the extent of oxidative stress, the generation of reactive

oxygen species may be important finding as these species can act as danger signals that activate antigen presenting cells in the skin.

As a possible explanation for the idiosyncratic nature of these reactions, folate deficiency was studied as a potential risk factor. However, the results of these studies suggested that deficiency of folic acid in keratinocytes does not predispose such cells to the toxicity associated with the parent drugs or their metabolites. Unexplored is the potential role of such deficiency on the immune response itself.

Abstract Approved: _____

Thesis Supervisor

_____

Title and Department

_____

Date

SULFONAMIDE-INDUCED CUTANEOUS DRUG REACTIONS: ROLE OF BIOACTIVATION, OXIDATIVE STRESS AND FOLATE DEFICIENCY

by

Piyush Manhar Vyas

A thesis submitted in partial fulfillment
of the requirements for the Doctor of
Philosophy degree in Pharmacy (Pharmaceutics)
in the Graduate College of
The University of Iowa

December 2006

Thesis Supervisor: Professor Craig K. Svensson

Graduate College
The University of Iowa
Iowa City, Iowa

CERTIFICATE OF APPROVAL

_____

PH.D. THESIS

_____

This is to certify that the Ph.D. thesis of

Piyush Manhar Vyas

has been approved by the Examining Committee
for the thesis requirement for the Doctor of
Philosophy degree in Pharmacy (Pharmaceutics)
at the December 2006 graduation.

Thesis Committee: _____
Craig Svensson, Thesis Supervisor

_____
Michael Duffel

_____
Kevin Rice

_____
Peter Veng-Pedersen

_____
Philip Wertz

To my parents, with their love, motivation and support, I have the inspiration to strive for my goals and be the best to reach my dreams!

ACKNOWLEDGEMENTS

First and foremost, I bow in front of almighty GOD for all the blessings and for making this possible.

I am eternally indebted to my mentor Dr. Craig K. Svensson, who as my advisor has been a firm pillar of support, guidance and encouragement during tenure of my Ph.D. studies. Always the epitome of patience and perfection; he has painted brilliantly on the canvas of my life and sculpted my skills with finesse, making me a better person and a scientist.

I would like to thank my dissertation committee members, Drs. Duffel, Rice, Veng-Pedersen and Wertz for their wonderful insights, suggestions and providing their valuable time in my research project. Appreciation also goes to Drs. Nauseef, Hines, Kerns, Prisinzano, Dutta, Woster, Williams, Krueger, Goldstein, Schalinske and Schuetz for their assistance in my research work. My acknowledgements to the Division of Pharmaceutics, College of Pharmacy, University of Iowa, Department of Pharmaceutical Sciences at Wayne State University for providing the necessary institutional facilities and for a grant from the National Institutes of Health to Dr. Svensson which provided financial support.

I am highly obliged to my family, my parents, my late grandfather (Dada) and late grandmother (Ba), my sister, Madhvi and brother, Harish and also to Giju Faiba, Tinaben, Bharatbhai, Jaybhai, Naniba, Tichukmama, Anilmama and other members of my family for encouraging me to work in right prospective.

My special thanks to dearest Rakhi for her love and support to achieve my goals. I am deeply gratified to you for staying beside me in ups and downs of my life.

For always helping me in my difficulties, I am very grateful to my colleagues and friends, especially Sanjoy, Rania, Farah, Payal, Sree, Mike, Sujit, Maya, Rohit, Rajesh, Jayant, Suraj, Jesil, Mani, Keith, Denise, Steve and Judith who made my tenure an enjoyable experience.

I wish to thank Josie Birtcher, Judy Putney, IT office members and other office members at University of Iowa for their timely help and support in my academic career.

And finally, I thank all my well wishers without whom this would not have being possible.

ABSTRACT

Sulfonamide- and sulfone-induced hypersensitivity reactions are thought to be mediated through bioactivation of parent drug molecule(s) to their respective reactive metabolite(s). In order to explain the cutaneous drug reactions caused by sulfonamides and sulfone, a mechanism can be proposed by which the bioactivation of these drugs in keratinocytes of the skin forms reactive hydroxylamine metabolites that can covalently bind to cellular proteins, which in turn act as antigens leading to the cascade of immune reactions resulting in a cutaneous drug reaction.

In order to probe the proposed mechanism, we determined the enzymes responsible for the bioactivation of these parent drugs to their hydroxylamine metabolites in cultured human keratinocytes. It was found that flavin containing monooxygenases and peroxidases play an important role in the bioactivation of these drugs in keratinocytes. We also confirmed the presence of these enzymes in keratinocytes. Interestingly, though cytochrome P450s are important in the oxidation of parent arylamine xenobiotics to their hydroxylamine metabolites in the liver, they do not appear to play a significant role in the bioactivation of these drugs in keratinocytes.

The hydroxylamine metabolites of sulfamethoxazole and dapsone can undergo autooxidation, generating reactive free radicals. Our studies showed that both of these metabolites elevate oxidative stress in keratinocytes by forming reactive oxygen species. Though the cytotoxicity induced by these metabolites is not correlated with the extent of oxidative stress, the generation of reactive

oxygen species may be important finding as these species can act as danger signals that activate antigen presenting cells in the skin.

As a possible explanation for the idiosyncratic nature of these reactions, folate deficiency was studied as a potential risk factor. However, the results of these studies suggested that deficiency of folic acid in keratinocytes does not predispose such cells to the toxicity associated with the parent drugs or their metabolites. Unexplored is the potential role of such deficiency on the immune response itself.

TABLE OF CONTENTS

LIST OF FIGURES ix

LIST OF ABBREVIATIONS xiii

CHAPTER ONE: INTRODUCTION 1

1.1 Adverse Drug Reactions (ADRs) 1
1.1.1 Introduction and epidemiology of ADRs 1
1.1.2 Classification of ADRs 2
1.2 ADRs affecting the skin 4
1.2.1 Common agents associated with CDRs 7
1.2.2 Potential role of bioactivation in CDRs 9
1.2.3 Role of reactive metabolites in the series of immune events leading to CDRs 10
1.3 Proposed mechanism of CDRs 12
1.4 Specific Aims in the proposed mechanism of CDRs 13

CHAPTER TWO: DETERMINATION OF THE ENZYME WHICH IS RESPONSIBLE FOR THE BIOACTIVATION OF SMX AND DDS IN NHEK. 17

2.1 Enzyme-mediated protein haptenation of dapsone and sulfamethoxazole in human keratinocytes - 1. Expression and role of Cytochromes P450. 17
2.1.1 Introduction 17
2.1.2 Materials and Methods 19
2.1.3 Results 27
2.1.4 Discussion 29

2.2 Enzyme-mediated protein haptenation of dapsone and sulfamethoxazole in human keratinocytes - 2. Role of human cyclooxygenase-2. 47
2.2.1 Introduction 47
2.2.2 Materials and Methods 48
2.2.3 Results and Discussion 50

2.3 Enzyme-mediated protein haptenation of dapsone and sulfamethoxazole in human keratinocytes - 3. Expression and role of flavin containing monooxygenase and peroxidases. 56
2.3.1 Introduction 56
2.3.2 Materials and Methods 57
2.3.3 Results 69
2.3.4 Discussion 74

CHAPTER THREE: DETERMINATION OF THE ROLE OF REACTIVE OXYGEN SPECIES (ROS) GENERATION BY THE HYDROXYLAMINE METABOLITES OF SMX AND DDS LEADING TO CELL DEATH. 88

3.1 Introduction 88
3.2 Materials and Methods 90
3.3 Results 96
3.4 Discussion 100

CHAPTER FOUR: ROLE OF FOLATE DEFICIENCY AS A PREDISPOSING FACTOR IN CDRs. 117

4.1 Introduction 117
4.2 Materials and Methods 119
4.3 Results 124
4.4 Discussion 127

CHAPTER FIVE: SUMMARY AND CONCLUSION 136

REFERENCES 141

LIST OF FIGURES

Figure 1.1 Proposed bioactivation-dependent pathway for SMX induced idiosyncratic reactions. 14

Figure 1.2 Proposed mechanism for SMX/DDS leading to cutaneous drug reactions following its bioactivation and immune response in skin. 15

Figure 1.3 Proposed scheme representing the specific aims. 16

Figure 2.1 Protein haptenation in NHEK incubated with DDS or MADDS. 34

Figure 2.2 Protein haptenation in NHEK incubated with SMX or NASMX. 36

Figure 2.3 Blot analysis for CYP2C9 mRNA expression in NHEK and HaCaT cells. 38

Figure 2.4 Immunoblot analysis for CYP2C9 protein expression in NHEK and HaCaT cells. 39

Figure 2.5 Analysis for CYP3A4 and CYP3A5 expression in NHEK and HaCaT cells. 40

Figure 2.6 Quantitative RT-PCR assessment of CYP2E1 mRNA in NHEK and HaCaT cells. 41

Figure 2.7 Protein haptenation of DDS in NHEK in the presence of inhibitors of CYP450s and cyclooxygenase. 42

Figure 2.8 Protein haptenation of SMX in NHEK in the presence of inhibitors of CYP450s and cyclooxygenase. 44

Figure 2.9 Scheme for the bioactivation of SMX and DDS giving rise to protein haptenation. 46

Figure 2.10 Bioactivation and subsequent adduct formation of DDS by human recombinant COX-2. 53

Figure 2.11 Determination of arylhydroxylamine formation of DDS and SMX by HPLC in the incubation containing COX-2 activating system.. 54

Figure 2.12 Determination of H_2O_2 mediated arylhydroxylamine formation of DDS and SMX by HPLC. 55

Figure 2.13 DDS-dependent protein haptenation in NHEK in the presence of peroxidase inhibitors. 79

Figure 2.14 Presence of Peroxidases in NHEK. 81

Figure 2.15 Immunoblot analysis for MPO protein expression in NHEK. 82

Figure 2.16 Northern blot analysis for LPO mRNA expression in NHEK. 83

Figure 2.17 SMX- and DDS-dependent protein haptenation in NHEK in the presence of an FMO competitive substrate. 84

Figure 2.18 Human recombinant FMO mediated DDS and SMX adduct formation. 85

Figure 2.19 FMO3 and FMO1 protein expression in NHEK. 86

Figure 2.20 D-NOH dependent protein haptenation in NHEK to determine the sequential bioactivation of DDS to D-NO. 87

Figure 3.1 Scheme for ROS generation and increase in oxidative stress by arylhydroxylamines. 106

Figure 3.2 Identified and potential metabolites of DDS and SMX giving rise to ROS. 107

Figure 3.3 Structures of dapsone dihydroxylamine (DDS-diNOH), monoacetyldapsone hydroxylamine (MADDS-NOH), and 4-nitrophenyl-*p*-tolyl sulfone hydroxylamine (NPTS-NOH). 108

Figure 3.4 Fluorescence of 2′,7′-dichlorofluorescein (DCF) in the presence of various compounds in a cell-free system. 109

Figure 3.5 Increase of DCF fluorescence per minute in presence of various compounds in a cell-free system. 110

Figure 3.6 Fluorescence of 2′,7′-dichlorofluorescein (DCF) in the presence of various compounds and horseradish peroxidase in a cell-free system. 111

Figure 3.7 Fluorescence of 2′,7′-dichlorofluorescein (DCF) in NHEK incubated with SMX-NOH and DDS-NOH. 112

Figure 3.8 Fluorescence of 2′,7′-dichlorofluorescein (DCF) in NHEK preloaded/postloaded with DCHF-DA exposed to various metabolites and analogues. 113

Figure 3.9 ROS generation in NHEK incubated with SMX-NOH or DDS-NOH in presence and absence of ROS scavengers. 114

Figure 3.10 Cytotoxicity of various compounds in presence and absence of ascorbic acid in NHEK. 115

Figure 3.11 Metabolite-protein adducts formation by SMX-NOH and DDS-NOH in presence and absence of ascorbic acid (AA) in NHEK. 116

Figure 4.1 Folate, Methionine and Homocysteine Metabolism 130

Figure 4.2 Measurement of 5-MTHF in folate deficient and folate supplemented NHEK. 131

Figure 4.3 Protein haptenation by DDS-NOH in folate deficient and folate supplemented NHEK. 132

Figure 4.4 Cytotoxicity of SMX-NOH and DDS-NOH in folate deficient and folate supplemented NHEK. 133

Figure 4.5 ROS formation of SMX-NOH and DDS-NOH in folate deficient and folate supplemented NHEK. 134

Figure 4.6 Formation of the parent drugs from the arylhydroxylamines in folate deficient and folate supplemented NHEK cells by HPLC..... 135

LIST OF ABBREVIATIONS

AA	:	Ascorbic acid
ABH	:	4-aminobenzoicacid hydrazide
ABT	:	1-aminobenzotriazole
ACD	:	Allergic contact dermatitis
ADRs	:	Adverse drug reactions
APC	:	Antigen presenting cells
BSA	:	Bovine serum albumin
CDR	:	Cutaneous drug reaction
CYP450	:	Cytochrome P450
COX	:	Cyclooxygenase
DAB	:	3,3’ – diaminobenzidine tetrahydrochloride
DC	:	Dendritic cells
DCHF	:	2’,7’-dichorodihydrofluorescein
DDS	:	Dapsone
DDS-NOH	:	Dapsone hydroxylamine
D-NO	:	Dapsone nitroso
DHSS	:	Drug hypersensitivity syndrome
DMAP	:	4-dimethylaminopyridine
DRESS	:	Drug eruption with eosinophilia and systemic symptoms syndrome
DTH	:	Delayed type hypersensitivity
EM	:	Erythema multiforme

FMO	:	Flavinmonooxygenase
Hcy	:	Homocysteine
HHcy	:	Hyperhomocysteinemia
HEK	:	Human embryonic kidney -293 cells
HSR	:	Hypersensitivity reactions
INDO	:	Indomethacin
KBM	:	Keratinocyte basal media
KGM	:	Keratinocyte growth media
KCZ	:	Ketoconazole
LC	:	Langerhans cells
LPO	:	Lactoperoxidase
MADDS	:	Monoacetyl dapsone
MMZ	:	Methimazole
MPO	:	Myeloperoxidase
MTHF	:	Methyl tetrahydrofolate
NASMX	:	N-acetyl sulfamethoxazole
NSAIDs	:	Nonsteroidal anti-inflammatory drugs
NHEK	:	Normal human epidermal keratinocytes
PBS	:	Phosphate buffered saline
PCR	:	Polymerase chain reaction
PRX	:	Peroxidase
RT	:	Reverse transcriptase
RT-PCR	:	Reverse transcription polymerase chain

		reaction
SJS	:	Stevens-Johnson syndrome
SMX	:	Sulfamethoxazole
SMX-NOH	:	Sulfamethoxazole hydroxylamine
SSLR	:	Serum sickness–like reaction
TEN	:	Toxic epidermal necrolysis
THF	:	Tetrahydrofolate
THFR	:	Tetrahydrofolate reductase
TPO	:	Thyroid peroxidase
TBS	:	Tris buffered saline

CHAPTER ONE

INTRODUCTION

1.1 Adverse Drug Reactions (ADRs)

1.1.1 Introduction and epidemiology of ADRs

An adverse drug reaction is any response to a drug which is noxious and unintended and which occurs at doses or overdoses used in man for prophylaxis, diagnosis, or therapy, excluding therapeutic failures. In its broadest sense, it includes the undesirable effects which might be due to the pharmacological effects of the drug or might be due to unpredictable mechanisms where the pharmacology of the xenobiotic is not directly related to the observed adverse effect.

With the advent of modern drug therapy, we have the benefits of novel molecules for treating different diseases, but at the same time, we have the disadvantage of ADRs caused by these drugs. ADRs affect an individual not only in terms of illness, but also in terms of social and economic status and thus are a very important concern.

Regarding the frequency of ADRs, reports vary from 6 to 30%[1 2] in studies done in the USA. The incidence of ADRs in hospitalized patients is generally 10 to 20%[3-5], however, studies have also reported frequencies ranging from 1.5 to 44%[6]. For those hospital admissions which are due to ADRs, the incidence ranges from 3-8%[7-9]. Certain factors appear responsible for making some individuals predisposed to ADRs. For example, women have a greater chance of ADRs as compared to men, while elderly patients are also reported to be more

vulnerable to ADRs[10]. The number of elderly patients which are hospitalized due to ADRs is 10-17%[8, 11]. AIDS patients have been reported to be prone to ADRs by drugs such as sulfamethoxazole and amoxicillin[12, 13]. Apart from patient characteristics, factors associated with medication and their therapeutic categories also appear to be important in determining the frequency of ADRs. For example, among the top 10 drugs reported for causing the ADRs by the yellow card system to the UK Committee on Safety of Medicines in 1986, 7 were nonsteroidal anti-inflammatory drugs (NSAIDs), causing 74% of the reported ADRs. Other drugs reported were angiotensin converting enzyme inhibitors (enalepril, captopril) and cotrimoxazole, which accounted for 19% and 7% of ADRs respectively[7]. Though there are many other therapeutic categories which might be responsible for causing ADRs, the mechanism for the prevelance of certain therapeutic/pharmacologic categories of drugs is unclear.

1.1.2 Classification of ADRs

ADRs are mainly classified as Type A and Type B reactions. Type A are reactions that arise due to the pharmacological action of the drug and, hence, they are predictable. About 80% of ADRs are of Type A, where it is easy to identify the responsible factor, though sometimes they are unavoidable at the normal prescribed dose. Some of the common factors for Type A reactions are inappropriate dose and drug interactions[14].

Type B reactions are those which do not reflect the expected pharmacological action of the drug and thus they are unpredictable. These are also called idiosyncratic reactions as they represent unusual reactions within

normal population. Certain genetic and immunological factors might be responsible for the cause of these reactions. For example glutathione (GSH) deficiency may be responsible for the increased toxicity of sulfonamides in AIDS patients[13].

Type B immune mediated reactions or allergic hypersensitivity reactions (HSR) are further classified into 4 groups:

IgE-dependent (Type I) drug reactions: Urticaria and anaphylaxis[15]. In these reactions, mast cells or leukocytes release variety of chemical mediators including histamine, leukotrienes, prostaglandin and a variety of pro-inflammatory cytokines upon their activation by the complexation of drug-protein conjugates with two or more specific IgE molecules on the cell surface [16].

Antibody-mediated (Type II) drug reactions. Reactions of this nature demonstrate binding of antibody directly to cells leading to complement-mediated cytolysis and resultant cell damage. Purpura caused by quinidine is a good example of this reaction[17].

*Immune complex-dependent (Type III) drug reaction*s. In this type of reaction, drug/antigen results in the generation of IgG or IgM antibodies, which combine with drug to form immune complexes. These immune complexes activate the complement cascade forming complement protein fragments C3a and C5a, which trigger release of chemical mediators from mast cells and basophils resulting in variety of reactions such as serum sickness reaction and vasculitis[18].

Cell mediated (Type IV) reactions. These involve the T and B lymphocytes and cells of monocytes-macrophage lineage[19]. The interactions are under the control

of the immune response or MHC genes to generate the final response. The contact drug hypersensitivity observed with penicillin has been demonstrated to be a delayed type, cell mediated cutaneous drug reaction (CDR)[20].

The above mentioned immune mediated type B (type I to IV) reactions may be manifested as eruptions in skin, which is not unexpected since skin contains all the elements of the immune system that are required to generate such responses.

1.2 ADRs Affecting the Skin

Drug eruptions in skin are very frequent manifestations of ADRs. The reaction rate has been reported to be about 2%[21, 22]. Antimicrobials, NSAIDs and anticonvulsants are the major therapeutic categories associated with reactions in skin. The idiosyncratic nature of these reactions might be attributed to some of the factors which affect the metabolic and detoxification pathways of these drugs. For example, AIDS patients are more vulnerable to (CDRs) from sufonamides such as co-trimoxazole[13] [combination of trimethoprim (TMP) and sulfamethoxazole (SMX)] and ß-lactam antibiotics such as amoxicillin[12]. AIDS patients may have a deficiency in GSH, which is very important to the cellular antioxidant system. Due to the deficiency of GSH, the hydroxylamine metabolite of SMX may not get detoxified and, thereby, may result in toxic reactions manifested as CDRs in these patients[13].

Variaties of mild to severe CDRs, such as purpura, exanthema, toxic epidermal necrolysis (TEN), fixed drug eruptions and other types, are manifested in skin. Some of these reactions and their clinical pattern are discussed below.

Purpura is a common CDR caused by many drugs and arises due to hemmorhage of blood in the skin. Purpuric rashes are also common clinical manifestations in these conditions. Many drugs have been reported to cause these reactions. For example, cephalosporins and bleomycin cause allergic thrombocytopenia and valproic acid causes this reaction by an alteration in platelet function[23, 24]. Purpuric rashes caused by quinidine is a standard example for type III allergic reactions where drug antigen combines with IgG class of antibody to activate the complement system[17].

Exanthematic reactions are another type of mild CDRs which are very common. They are caused by many different drugs, but the most common agents are sulfonamides, ampicillin and amoxicillin. These reactions are manifested after 7-14 days from the initiation of administration of the drug and it is often difficult to identify the offending agent due to similarities in the clinical patterns of these reactions with viral-induced skin rashes[25]. The primary lesions in these reactions are of scarlatiniform, rubelliform or morbilliform. Purpuric lesions on the legs, large macules, reticular eruptions and erosive stomatitis are rare, but might be manifested. Continuation of medication may lead to exfoliative dermatitis, further confluency of eruptions may stop even if the drug continued[26]. Histological examinations do not show major signs except red blood cell extravasation and lymphohistiocytic and eosinophil infiltration[27].

Stevens-Johnson syndrome (SJS) is a severe type of CDR. Drugs which are commonly associated with SJS are sulfonamides and other antibiotics (e.g., tetracycline and penicillin derivatives)[28]. In the US, NSAIDs have been reported

as an offending agent to cause this serious CDR[29]. Another toxic reaction which overlaps with SJS is TEN. Epidermal sloughing and intestinal involvement are common in TEN, however, the extent at which the skin is involved differentiate these two reactions[30]. The clinical features of these reactions include arthralgia, myalgia, fever and malaise.[30]. Sheet-like erosions covering more than 10% of the body surface area and involvement of mucous membrane of conjunctiva, cornea, oral cavity and genitalia are manifested. Though rare, liver toxicity might be present[31]. Re-exposure of the drug should be avoided as it might lead to a fatal condition[30]. Histological evaluation shows the presence of perivascular infiltration of lymphocytes, eoisinophils and papillary oedema in the dermal lesions. In epidermal lesions, infiltration of mononuclear cells and necrotic keratinocytes with extravasation of red cells is manifested[32, 33].

From the histological evaluation of these CDRs, it is clear that these reactions are mediated by the immune system. The presence of lymphocytes, mast cells, mononuclear cells, along with immune mediators such as cytokines, provides evidence of involvement of the immune system[34, 35]. Also, when lymphocytes from allergic individuals are isolated and incubated with the specific drug in vitro, there is a clear proliferation of lymphocytes. This response is absent in those individuals who are not allergic to these drugs, which provides evidence of a drug-specific response by the immune system in these reactions[36-38]. Studies in which slow increases in the dosage of an offending agent induced tolerance in allergic patients gives further proof for immune mediated nature of these reactions[39].

1.2.1 Common agents associated with CDRs

Many antibacterial, antifungal, antimalarial, NSAID, anticoagulant and anticancer drugs are associated with CDRs. Some of the important agents are described below.

ß-lactam antibiotics, such as penicillin, amoxicillin and related agents, are reported as a frequent cause of CDRs. Penicillin has been shown to cause all 4 types of immunological reaction including urticaria and anaphylaxis (type I), hemolytic anemia (type II), vasculitis (type III) and contact dermatitis (type IV) reactions[40]. The epidemiology of penicillin-induced CDRs shows that 2% of patients receiving the drug experience a maculopapular rash, which increases to 10% if there is prior history of the reaction[41, 42]. The frequency of anaphylactic reactions to peniciilin is estimated at 0.015%, while 0.0015-0.002% are fatal reactions[43]. Penicillin undergoes hydrolysis and the resulting release of a penicilloyl group on the molecule is responsible for the generation of and binding to IgE antibody [42]. With in 1 hour of its administration, a variety of reactions such as anaphylactic shock, urticaria, laryngeal edema and bronchospasm has been manifested[44]. Other reactions, such as neutropenia, a maculopapular rash, serum sickness and erythema multiforme do not occur until at least 72 hours after administration[20]. Cross reactivity of the penicillin-generated antibodies with other ß-lactam antibiotics (e.g., amoxicillin, ampicillin) is common and results in cross-sensitivity to numerous agents[42].

NSAIDs are among the most common agents to cause CDRs, especially the more serious forms, such as SJS and TEN[29]. Piroxicam has been reported to

cause CDRs in 2-3% of patients receiving the drug[45, 46]. A variety of CDRs, including urticaria, erythema multiforme, vasculitis, and fixed drug eruption are provoked by this drug[47]. Piroxicam is metabolized to a phototoxic metabolite, which causes phototoxicity in up to two-thirds of patients receiving the drug and is the most common toxicity of its adminstration[48]. Other drugs, such as ibuprofen, sulindac and indomethacin, are also known to induce these reactions [49, 50].

The anticancer agent bleomycin is associated with symptoms of buccal ulceration, glossitis, alopecia and fever, and may also result in cutaneous erythema or hyperpigmentation[51]. Other manifestations include ischemic ulceration and systemic sclerosis, localized erythematous, infiltrated plaques, and darkening of the nail cuticle[52]. Progressive pulmonary fibrosis is a major problem of systemic therapy of this drug[53]. The rash caused by bleomycin resolves even with the continuation of therapy with this medication, though the exact mechanism behind this is still not certain[54].

Another therapeutic category which causes frequent CDRs are sulfonamides. Up to 5% of patients treated with these drugs show evidence of a HSR in skin[22, 55]. Some of the common reactions caused by these drugs are a lupus-like syndrome, allergic vasculitis, morbilliform rashes[56, 57], fixed eruptions, exfoliative dermatitis, phototoxic and photoallergic reactions, erythema nodosum, erythema multiforme[58], SJS and TEN[22, 55]. Factors such as acetylator status and HIV infection appear to act as risk factors for these reactions[13, 59].

Sulfonamides appear to be metabolized to reactive metabolites and these resultant metabolites are responsible for mediating the CDRs. For example, SMX is bioactivated to reactive arylhydroxylamine and arylnitroso metabolites, which are believed to be responsible for its ability to cause HSR[60].

1.2.2 Potential role of bioactivation in CDRs

It is clearly evident from the above discussion that numerous therapeutic agents cause severe CDRs. However, the mechanism behind these reactions is still uncertain. It is believed that bioactivation of certain drugs to their reactive metabolites is the initial step in mediating these reactions. For example, abacavir is bioactivated to reactive aldehyde metabolites with the help of alcohol dehydrogenase and possibly other human liver cytosolic enzymes[61]. Lamotrigine, phenytoin and carbamezipine have been reported to bioactivate to reactive arene oxide metabolites [62-64]. Drugs such as SMX and dapsone (DDS) have been known to be converted to their respective arylhydroxymine and arylnitroso metabolites via cytochrome P450 enzymes (CYP450s) and myeloperoxidases (MPO)[65-69] (Figure 1.1). Other oxidizing enzymes such as cyclooxygenases (COX), peroxidases (PRXs) and flavin containing monooxygenases (FMOs) have also been reported to mediate the bioactivation of the various chemical moeities to their toxic reactive intermediates[70-73].

In order to explain the mechanism behind the presence of these reactive metabolites in the skin, it might be hypothesized that these metabolites are generated in liver and then subsequently enter the skin during their circulation. However, it might also be possible that after the distribution of a xenobiotic and

during its passage through the skin, the drug is bioactivated by skin cells to reactive metabolites. As in the epidermis 90-95% of the cells are keratinocytes, it possible that in addition to being target cells for these reactions, keratinocytes may also be a site of metabolism for these drugs. Moreover, keratinocytes have been reported to contain a variety of oxidizing enzymes such as CYP450s, COX, and FMOs[74-76] which are capable of oxidizing the drugs to their reactive metabolites. Thus, our laboratory has postulated the bioactivation of the drugs to their reactive metabolites in keratinocytes of the skin as an initial step in the manifestation of CDRs.

1.2.3 Role of reactive metabolites in the series of immune events leading to CDRs

Subsequent to the formation of reactive metabolites, further events lead to the generation of an immune response resulting in CDRs. The first step after the formation of reactive metabolites is the covalent binding of these metabolites to cellular proteins to form the protein-hapten conjugate or an antigen, which is then capable of generating an immune response[77]. According to the hapten hypothesis, small molecular compounds are not capable of generating an immune response on their own. They need to be activated by the process of metabolism to generate reactive electrophilic species which are capable of oxidizing the cellular proteins resulting in covalently bound drug-protein complex. The formed antigen is a large molecular weight species which is now capable of generating an immune response[39].

Formation of reactive species results in diversified toxic effects. Some of these reactive metabolites are capable of generating free radicals which have a short life span and are capable of oxidizing any cellular protein in the vicinity[78]. Reactive arylhydroxylamine metabolites of SMX (SMX-NOH) and DDS (DDS-NOH) can undergo autooxidation to form the respective arylnitroso metabolites which are believed to be the final reactive moieties to form the hapten-protein conjugate. During the conversion of arylhydroxylamine to the arylnitroso species, a variety of free radicals or reactive oxygen species (ROS) such as superoxide, hydrogen peroxide and hydroxyl radicals are generated. These ROS, being highly toxic electrophiles, can oxidize cellular lipids, proteins and chromosomal DNA, causing mutations[79, 80].

In skin, the increase in the oxidative stress and ROS due to reactive metabolites may result in the induction of various danger signals in the form of heat shock proteins and cytokines leading to antigen presenting cell (APC) activation/maturation and T-cell activation[81, 82]. The generation of ROS by these reactive metabolites leads to a cascade of responses. For example, superoxide generation has been shown to upregulate cell surface markers CD80, CD83, and CD86 on APC[83] that are required signals for the clonal expansion of T-cells. H_2O_2 generation by these metabolites may upregulate cytokines such as TNF-α and IL-8 by human APC[84]. Reactive metabolite mediated ROS generation might be important in the activation of T-cells when APCs present antigen to T-cells, as ROS have been reported to influence the APC-T cell interaction[85] (one of the essential criteria for antigen presentation). Further, upregulation of adhesion

molecules such as E-selectin and ICAM-1 due to ROS[86] might lead to the homing of T-cells to the specific site of insult in the skin where the antigen is present. Thus, induction of oxidative stress by the reactive metabolites and subsequent expression of danger signals is believed to be an important step leading to the immune response.

1.3 Proposed mechanism of CDRs

Based on the above mentioned phenomena of bioactivation mediated reactive metabolite formation, the mechanism outlined in Figure 1.2 is proposed to explain the development of these reactions.

As shown in the scheme in Figure 1.2, arylamine xenobiotics such as SMX or DDS, after their administration and distribution to the skin, can diffuse into keratinocytes, which are the most abundant cells in the epidermis. As these cells have been reported to express variety of oxidizing enzymes (e.g., CYP450s, COX, PRX and FMOs) the arylamine drugs SMX or DDS are metabolized to their respective arylhydroxylamine and arylnitroso metabolites in these cells. Being reactive in nature, these metabolites oxidize cellular proteins in keratinocytes and form the covalent adducts leading to protein haptenation, which can then act as an antigen capable of initiating an immune response. Alternatively, the metabolites formed in liver and distributing to the skin may form covalent adducts after diffusion into these cells. Subsequent to protein haptenation, keratinocytes release the danger signals such as heat shock proteins and cytokines which will activate the APC. The antigen formed in keratinocytes will be taken up by skin APCs. Antigen uptake by APCs results in the expression of specific surface

molecules (e.g., major histocompatability complex [MHC]), cytokines and costimulatory molecules (e.g., CD80)[87]. Activation of APCs will lead to their migration from the skin to the draining lymph node where it can present the antigen to the T-cells in an MHC–restricted fashion. The cross-talk between the T-cells and APCs by the T-cell receptor and costimulatory molecules (CD28 / CD80) leads to the clonal expansion of drug reactive T-cells. Expression of skin homing receptors on T-cells and its subsequent distribution to the target site in the skin results in inflammation and killing of those keratinocytes; ultimately giving rise to the clinical manifestations of a CDR.

1.4 Specific Aims in the proposed mechanism of CDRs

The scheme in figure 1.3 represents the proposed specific aims in this dissertation:

Specific Aim 1: To determine the enzyme responsible for the bioactivation of the SMX and DDS to their hydroxylamine metabolites in NHEK (Chapter-2).

Specific Aim 2: To determine the role of reactive oxygen species (ROS) generation by the hydroxylamine metabolites of SMX and DDS leading to cell death (Chapter 3).

Specific Aim 3: To determine the role of folate deficiency as a predisposing factor in the SMX and DDS mediated CDRs (Chapter 4).

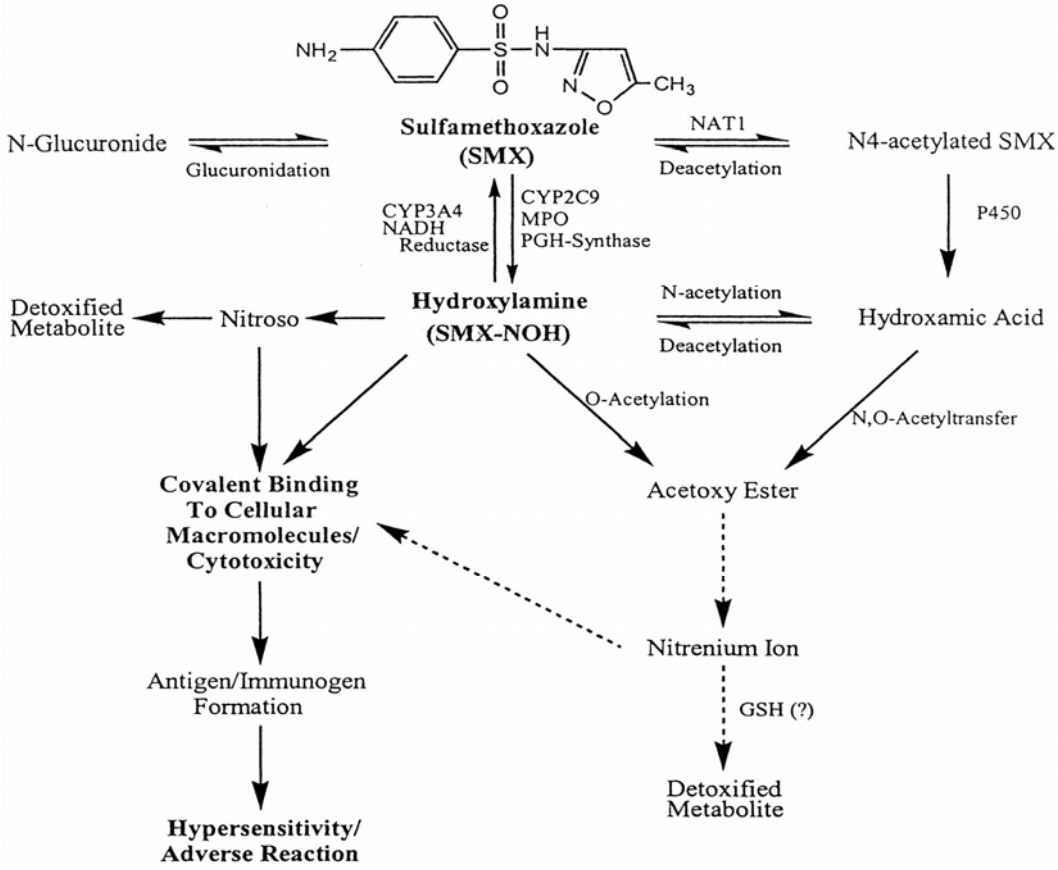

Figure 1.1. Proposed bioactivation-dependent pathway for SMX induced idiosyncratic reactions. CYP, cytochrome P450; MPO, myeloperoxidase; NAT1, N-acetyltransferase 1; PGH-synthase, prostaglandin H synthase[88] .

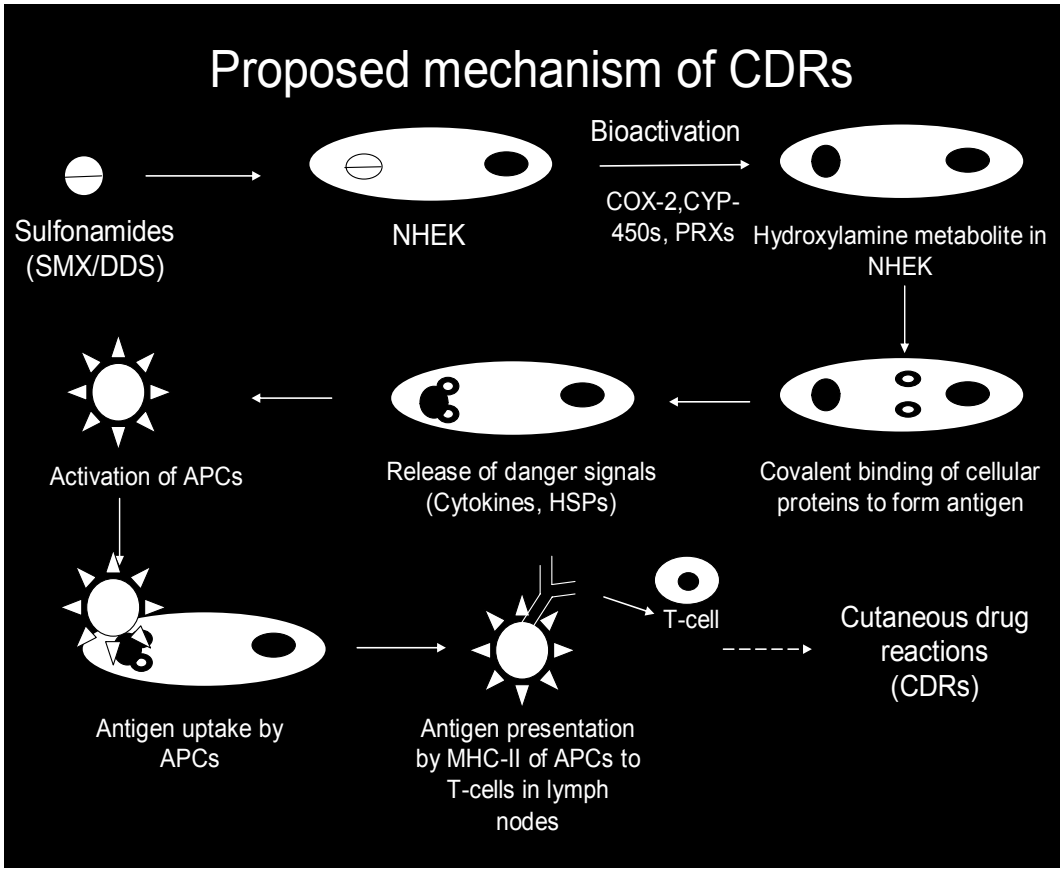

Figure 1.2. Proposed mechanism for SMX/DDS leading to cutaneous drug reactions following its bioactivation and immune response in skin. SMX, sulfamethoxazole: DDS, dapsone; NHEK, normal human epidermal keratinocytes; COX-2, cyclooxygenase 2; CYP450s, Cytochrome P450s; PRXs, peroxidases; HSPs, heat shock proteins; APCs, antigen presenting cells; MHC-II, major histocompatibility complex-II.

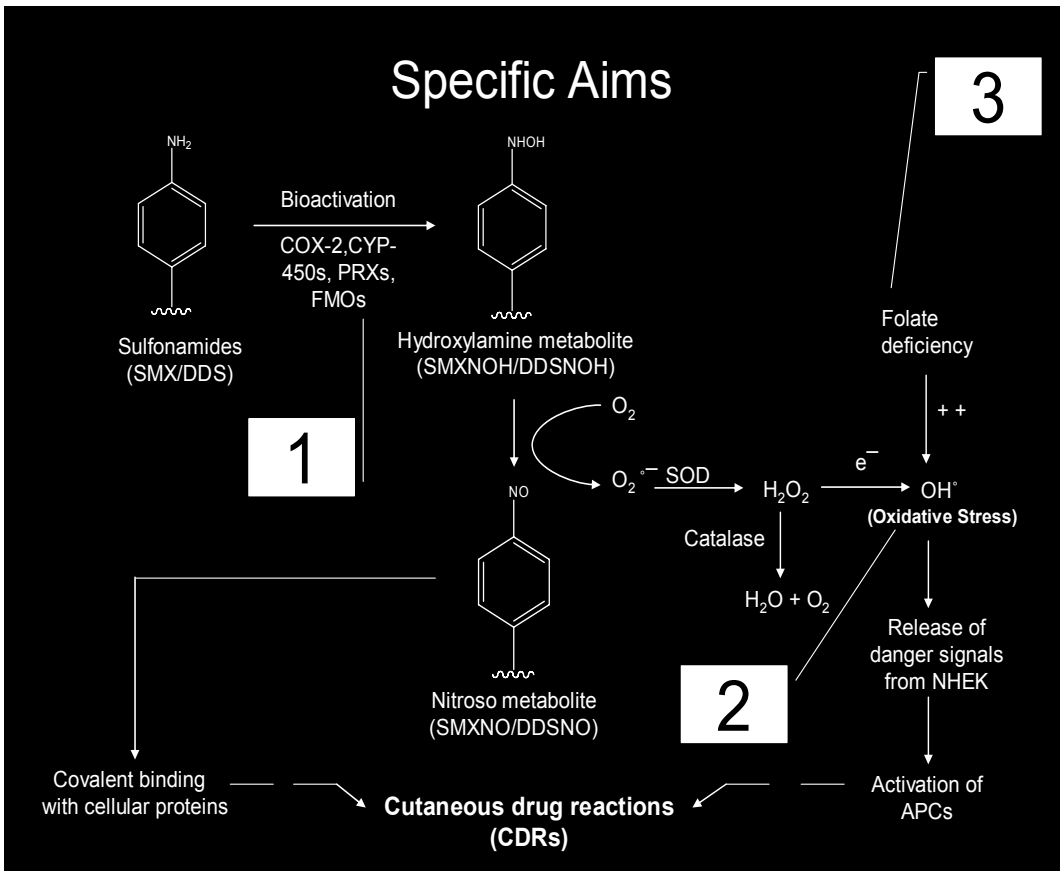

Figure 1.3. Proposed scheme representing the specific aims in this dissertation.

CHAPTER TWO

DETERMINATION OF THE ENZYME RESPONSIBLE FOR THE BIOACTIVATION OF THE SMX AND DDS TO THEIR HYDROXYLAMINE METABOLITES IN NHEK.

In order to study the enzyme responsible for the bioactivation of the parent arylamine drugs, SMX and DDS in NHEK, we determined the role of CYP450s, COX-1 & COX-2, PRXs and FMOs. Each of these studies has been published and can be accessed online and are presented here as sub-chapters.

2.1 Enzyme-mediated protein haptenation of dapsone and sulfamethoxazole in human keratinocytes - 1. Expression and role of cytochromes P450*.

2.1.1 Introduction

Sulfonamides are used in the treatment of numerous infectious diseases. Their effectiveness in the treatment of *Pneumocystis carinii* pneumonia (PCP), especially in AIDS patients, has increased their importance as therapeutics agents in the modern antimicrobial era [89]. Sulfamethoxazole (SMX) and the sulfone dapsone (DDS) are widely used antimicrobials for the treatment of PCP resulting in the recovery of approximately 75% of the patients suffering from this ailment [90, 91]. However, adverse drug reactions, especially those of a cutaneous nature, limit their use. These reactions most commonly occur 7-10 days after

---

* Note: Published as: Vyas PM, Roychowdhury S, Khan FD, Prisinzano TE, Lamba JK, Schuetz EG, Blaisdell J, Goldstein JA, Munson KL, Hines RN, Svensson CK. Enzyme-mediated protein haptenation of dapsone and sulfamethoxazole in human keratinocytes - 1. Expression and role of cytochromes P450. *Journal of Pharmacology and Experimental Therapeutics*. (Published online July 20, 2006; doi: 10.1124/jpet.106.105858**)**

initiation of therapy and are associated with fever and skin rash. Morbilliform or maculopapular, non-urticarial types of skin rash are most commonly observed with these agents. Some patients, however, progress to Stevens-Johnson syndrome (SJS) or toxic epidermal necrolysis (TEN), which can have a mortality rate as high as 40-50%. A multi-organ syndrome, manifested as fever, rash, eosinophilia, and hepatotoxicity, has also been reported in patients receiving these drugs [92-95].

Several studies have demonstrated that SMX and DDS undergo biotransformation to form reactive N-arylhydroxylamine metabolites, which are believed to be responsible for causing cutaneous drug reactions (CDRs) [89, 96, 97]. It has been proposed that the bioactivation of these drugs at the site of manifestation (i.e., skin) may be a critical element in the initiation of these reactions [98]. Indeed, we have previously demonstrated that normal human epidermal keratinocytes (NHEK) are able to bioactivate SMX and DDS to their respective arylhydroxylamine metabolites (SMX-NOH and DDS-NOH) [98] and that such bioactivation results in protein haptenation [99].

Studies have demonstrated that skin cells express a variety of drug metabolizing enzymes, such as cytochrome P450s (CYP450s), cyclooxygenase (COX), flavin-containing monooxygenase (FMO) and peroxidases, which may bioactivate numerous chemical agents [100-104]. Hydroxylation of SMX and DDS by various CYP450s has been reported [105-108]. Several arylamine drugs, including procainamide, are oxidized to arylhydroxylamine metabolites by COX-2 [109, 110].

In the present investigation, we sought to identify the enzyme(s) that catalyze the bioactivation of SMX and DDS leading to protein haptenation in NHEK. Our studies demonstrate that while COX-1/-2, CYP3A4 and CYP2E1 are able to catalyze the bioactivation of SMX and DDS *in vitro*, inhibitors of these enzymes do not reduce adduct formation when NHEK are exposed to either SMX or DDS. These data suggest that these enzymes do not play an important role in the bioactivation and subsequent protein adduction of SMX and DDS in NHEK.

2.1.2 Materials and Methods

Materials. Monoacetyl dapsone (MADDS) was generously provided by Parke-Davis (now Pfizer, Ann Arbor, MI). DDS, SMX, 4-dimethylaminopyridine (DMAP), 1-aminobenzotriazole (ABT), troleandomycin, disulfiram and indomethacin (INDO) were obtained from Sigma (St. Louis, MO). 7-benzyloxyquinoline (7-BQ) and 7- hydroxyquinoline (7-HQ) were purchased from Gentest (Bedford, MA). DDS and SMX hydroxylamine metabolites were synthesized as described previously [111]. 1,2-trans dichloroethylene (DCE) was obtained from TCI America (Portland, OR). Rabbit anti-sera was raised against SMX- and DDS-keyhole limpet hemocyanine conjugates and specificity assessed as described previously [98]. Rat tail collagen (type-I) was obtained from Sigma (St. Louis, MO). Normal human epidermal keratinocytes (as 1st passage cells) and keratinocyte culture media were obtained from CAMBREX (Walkersville, MD). HaCaT cell line was generated by Dr. N. Fusenig (DKFZ Heidelberg, Heidelberg, Germany) and obtained from Dr. Michael Southhall (Johnson & Johnson; Skillman, NJ). Microtiter ELISA plates (96 well) were obtained from Rainin

Instruments (Woburn, MA). Rabbit anti-CYP2C9 antibody was custom made from Covance Research Products Inc. (Denver, PA). Donkey anti-rabbit IgG conjugated to horseradish peroxidase was obtained from Amersham Pharmacia Biotech Inc. (Piscataway, NJ). SuperSignal West Pico Chemiluminescent Substrate was purchased from Pierce (Rockford, IL) and a SynGene GeneGnome chemiluminescence detection system was obtained from Synoptics (Cambridge, UK). Monoclonal anti-CYP3A4 K03 [112] or α-3A5 primary antibodies were purchased from Gentest, Goat-anti-rabbit IgG conjugated with Alexafluor 488 and goat anti-rabbit antibody conjugated with alkaline phosphatase and YoYo-1 were purchased from Molecular Probes (Eugene, OR). Bradford assay reagent was purchased from Pierce Chemical Company (Rockford, IL). Immunomount was obtained from Vector Laboratories (Burlingame, CA). Trizol was purchased from Invitrogen (Carlsbad,CA). All other chemicals and reagents were purchased from Sigma (St. Louis, MO) or Fisher Scientific (Chicago, IL).

Synthesis of N-acetylsulfamethoxazole (NASMX). SMX (250 mg) was dissolved in 1 ml of acetic anhydride in presence of 0.5 g of DMAP and 10 ml of dichloromethane. The reaction was carried out for 1 h at room temperature with continuous stirring to obtain NASMX. Excess of acetic anhydride was removed by neutralizing the reaction mixture with saturated sodium bicarbonate solution and NASMX obtained by re-crystallizing the product in an acetone and hexane (1:3) mixture. NASMX was characterized by NMR and the purity was determined by HPLC-UV. Product purity was 98% while the observed yield was 79%.

Cell Culture. Adult normal human keratinocytes (NHEK) and immortalized HaCaT cells were cultured as detailed previously [98]. In brief, cells were propagated in 75 cm^2 flasks using basal media (KBM-2) supplemented with bovine pituitary extract (7.5 mg/ml), human epidermal growth factors (0.1 ng/ml), insulin (5 μg/ml), hydrocortisone, (0.5 μg/ml), epinephrine, transferrin, gentamicin (50 μg/ml) and amphotericin (50 ng/ml) at 37°C in an atmosphere containing 5% CO_2. Media was replaced every 2-3 days. When cell cultures reached near confluency (70-90%), cells were disaggregated using 0.025% Trypsin/0.01% EDTA in HEPES followed by neutralization with 2 volumes of Trypsin neutralizing solution. Cell suspensions were then centrifuged at 220 x g for 5 min followed by washing in basal media and re-suspension in KGM-2 (Supplemented growth medium). Cells were then either subjected to subculturing or cryo-preservation for further purposes. All experiments were performed using 3rd to 4th passage cells.

Determination of mRNA for CYP2C9 in NHEK. Total RNA was isolated from 4th passage NHEK and 7th passage HaCaT cells using Trizol (Invitrogen) following the manufacturer's protocol. cDNA was generated using 500 ng total RNA in a synthesis reaction using SuperScript™ II RT with random hexamers according to the supplier's protocol. PCR was performed using the CYP2C9 specific primers 5'-GATCTGCAATAATTTTTCTC-3' and 5'-TCTCAGGGTTGTGCTTGTC-3' with diluted amounts of cDNA from the keratinocytes resulting in a 280 bp product. Plasmid CYP2C9 cDNA in pCW was used as a positive control for amplification. Actin was also amplified from the

keratinocyte cDNA using the primers 5'-TCATGAAGTGTGACGTTGACATCCGT-3' and 5'-CCTAGAAGCATTTGCGGTGCACGATG-3' resulting in a 285 bp fragment. Amplifications were performed in 20 μl reactions using Amplitaq Gold (Applied Biosystems) according to the manufacturer's protocol with a final concentration of $MgCl_2$ of 2 mM. Cycling conditions consisted of an initial denaturation at 94° for 5 min followed by 40 cycles of 94° for 30 s, 53° for 10 s and 72° for 10 s. Reactions were analyzed on 4% agarose gels stained with ethidium bromide.

Determination of protein for CYP2C9 in NHEK. Cell lysates and partially purified recombinant proteins were electrophoresed in SDS-10% (w/v) polyacrylamide gels and transferred to nitrocellulose membranes. Membranes were immunoblotted with custom rabbit anti-CYP2C9 antibody (1:500) and donkey anti-rabbit IgG conjugated to horseradish peroxidase. Specific bands were visualized with SuperSignal West Pico Chemiluminescent Substrate and a SynGene GeneGnome chemiluminescence detection system.

Determination of mRNA for CYP3A4 and CYP3A5 in NHEK. Total RNA was isolated from NHEK and HaCaT cells using Trizol Reagent (Invitrogen) and first strand cDNA was synthesized from 3 μg of total RNA according to the manufacturer's instructions (SuperScript First Strand cDNA Synthesis kit, Invitrogen). Amplification of CYP3A4 cDNA (Genbank no. AF182273) from first strand cDNA was performed using (f) 5'-CCCAGACTTG GCCATGGAAACC-3' and (r) 5'-GAGGTCTCTGGTGTTCTCAG-3' primers that annealed to nucleotides in exon 1 and 13. PCR was carried out in a total reaction volume of 50 μl

consisting of 5 × PCR buffer with 1.5 mM $MgCl_2$, 1 µl , 5 pmol of each primer, 0.2 mM dNTP (Life Technologies, Gaithersburg, MD, USA), and 2.5 U of Taq DNA Polymerase (Boehringer Mannheim Expand High Fidelity PCR system, Mannheim, Germany). PCR consisted of at initial denaturation at 94 °C for 3 min followed by 35 cycles of denaturation at 94 °C for 30 s, annealing at 55 °C for 30 s and synthesis at 72 °C for 90 s and a final extension at 72 °C for 10 min. Second Round PCR was carried out under similar amplification conditions to detect if very small amounts of mRNA were present. CYP3A5 was amplified using (P1-f) 5'−AACAGCCCAGCAAACAGCAGC−3' (f), and (P2-r), 5'−TAAGCCCATCTTTATTTCAAGGT−3' primers as described previously [113].

Determination of protein for CYP3A4 and CYP3A5 in NHEK. NHEK, HaCaT cell and human liver samples were resuspended in storage buffer (100 mM potassium phosphate, pH 7.4, 1.0 mM EDTA, 20% glycerol, 1 mM dithiothreiotol, 20 µM butylated hydroxytoluene, 2 mM phenylmethylsulfonyl fluoride), lysates were generated by sonication, and protein concentrations determined using the Bio-Rad protein assay. 30 µg of lysate was separated on 10% SDS-polyacrylamide gels and immunoblotted with monoclonal anti-CYP3A4 K03 or α-3A5 (Gentest), followed by an appropriate secondary antibody coupled with peroxidase. The blot was developed with the ECL detection system (Amersham Biosciences).

Determination of catalytic activity for CYP3A4 in NHEK. NHEK (10^6 cells) were incubated in KGM-2 overnight. After 24 h, the media was discarded and replaced with fresh media. NHEK cells were then incubated with the inhibitors of

CYP3A4 enzymes, 1-aminobenzotriazole (ABT-1 mM) and troleandomycin (TMC- 100 μM) for 3 h. After 3 h, 7-benzyloxyquinoline (7-BQ - 50 μM), a substrate for CYP3A4 activity, was added to measure the catalytic activity of CYP3A4 in these cells. The plate was incubated for 30 min. at 37°C after the addition of 7-BQ followed by the fluorescence measurement using the Cytofluor multiwell fluorescent plate reader using the excitation wavelength of 410 nm and emission wavelength of 538 nm. The final concentration of DMSO was 1% (10 μl in 1 ml of assay). Control cells were treated with only 7-BQ. Fluorescence of NHEK cells was also measured as a measure of background fluorescence. Standard curve using the fluorescent metabolite 7-hydroxyquinoline (7-HQ- 0, 5, 10, 25 and 50 μM) which is the metabolite product of 7-BQ was also measured in NHEK cells.

Determination of CYP2E1 in NHEK. CYP2E1 mRNA expression was quantified in NHEK and HaCaT cells essentially as described by Haufroid et al [114]. Briefly, total RNA was isolated from keratinocytes using Trizol reagent (Invitrogen, Carlsbad, CA) and quantified using a Quant-iT RiboGreen kit (Invitrogen) as per the manufacturer's instructions. Using 2 μg of total RNA from each cell preparation, cDNA was prepared using random hexamer primers and ImProm-II reverse transcriptase following the procedures outlined in the ImProm-II Reverse Transcription System kit (Promega, Madison, WI). RT-PCR reactions to quantify CYP2E1 mRNA concentrations were carried out in a total volume of 40 μl containing 5.5 mM $MgCl_2$, 0.2 mM each deoxyribonucleotide, 0.3 μM of each PCR primer and 0.2 μM fluorescent probe, 5 or 25 ng of keratinocyte cDNA,

0.01 U/µl uracil N-glycosylase and 0.025 U/µl AmpliTaq Gold Polymerase (TaqMan PCR Core Reagents kit, Applied Biosystems, Foster City, CA) in a MJ Research Opticon System (MJ Research, Watertown, MA). 18S rRNA concentrations were determined using the TaqMan Ribosomal RNA Control Reagents (ABI) which were designed to generate an 187 bp product. Each 40 µl PCR reaction contained 5.5 mM $MgCl_2$, 0.2 mM each deoxyribonucleotide, 0.05 µM of each PCR primer and 0.2 µM fluorescent probe, 5 or 25 ng of keratinocyte cDNA, 0.01 U/µl uracil N-glycosylase and 0.025 U/µl AmpliTaq Gold Polymerase (TaqMan PCR Core Reagents kit, ABI).

Determination of the Cytotoxicity of Inhibitors in NHEK. To determine the maximal non-cytotoxic concentrations of various inhibitors in NHEK for the inhibition of the respective enzymes, the cytotoxicity of concentrations ranging from 25 µM to 25 mM were examined. Cytotoxicity was determined using an impermeable DNA binding dye (YoYo - 1), as we have described previously [111].

ELISA Analysis of Drug/metabolite-protein Adducts. Formation of covalent adducts following SMX or DDS exposure, in the presence or absence of the selective enzyme inhibitors, was determined by cultivating NHEK (1 X 10^6 cells) for 24 h in 50 ml centrifuge tubes containing 10 ml of complete growth medium. The concentrations of the selective inhibitors used were the maximum non-cytotoxic concentrations of those inhibitors in NHEK. Cells were then incubated with selective enzyme inhibitors for 3 h followed by SMX (1 mM ascorbic acid was added prior to the addition of SMX) or DDS treatment for 3 h (concentrations specified in Results). Following total 6 h incubation, tubes were

centrifuged at 220 x g for 5 min to pellet the cells. Covalent adducts were determined as previously described [111].

Immunocytochemistry. Drug/metabolite-protein covalent adduct formation was visualized using immunofluorescence confocal microscopy as described previously[115]. Cells were grown on collagen-coated (0.1 mg/ml) coverslips placed in petri-dishes containing 2 ml of complete growth medium. After 24 h, cultures were subjected to different selective enzyme inhibitors for 3 h (maximum non-cytotoxic concentrations were used), followed by SMX or DDS treatment for 3 h (concentrations specified in Results). After the 3 h incubation, cells were washed (three times) with phosphate buffered saline (PBS, 0.05M sodium phosphate, 0.15M NaCl, pH 7.4) and fixed for 20 min with 4% paraformaldehyde (PFA) in PBS. After fixation, cultures were washed 3 times with PBS followed by blocking for 60 min with Tris-casein buffer containing 0.3% Triton-X-100 and overnight incubation with the anti-DDS or anti-SMX antisera (1:500 diluted in blocking buffer) at 4^{o}C. Coverslips were then washed with PBS, incubated for 3 h at 37^{o}C with the fluorochrome-conjugated secondary antibody (Alexa fluor-488 labeled goat-anti-rabbit IgG, 1:500 diluted in blocking buffer), and mounted on glass slides using Immunomount® containing anti-fade reagent.

Fluorescence images were acquired with a Zeiss Laser Scanning Microscope (LSM 510, Zeiss Axiovert stand, Zeiss 63x and 20x objective lens) using excitation at 488 nm. Emission was set to a long pass filter at 505 nm.

Image analysis. For imaging with the confocal laser scanning microscope, laser attenuation, pinhole diameter, photomultiplier sensitivity and offset were

kept constant for every set of experiments. Images were acquired from 3 different view fields of each slide. The obtained images were quantitatively analyzed for changes in fluorescence intensities within regions of interests (boxes drawn over cell somata) using the Image J software. Fluorescence values from minimum of 3 view fields consisting of 15-20 NHEK cells in each field from 3 different slides of each treatment were averaged and expressed as mean (SD) fluorescence intensity.

Statistical analysis. Data are presented as mean (SD). Data were analyzed using SIGMASTAT (USA). Statistical comparisons between two groups were made using either student t-test (parametric method) for normalized data or Friedman's rank sum test (nonparametric method) for the data which did not pass the normality test. For the comparison between more than two groups, ANOVA and the Holm-Sidak method for multiple pair wise comparisons was used. A value of $p<0.05$ was considered to be significant.

2.1.3 Results

Covalent adduct formation of DDS and SMX and their acetylated metabolites in NHEK. Protein haptenation of the parent arylamine drugs, DDS and SMX, was readily detected by both confocal microscopy and ELISA (Fig. 2.1. and 2.2). N-acetylation of SMX or DDS resulted in marked attenuation of protein haptenation. As we have noted previously, the amount of adduct formed with DDS appears to be greater than that seen with SMX, though this may represent differences in antisera affinity for the respective adducts.

Expression of various cytochrome P450s in keratinocytes. NHEK and an immortalized keratinocyte cell line (HaCaT) were probed for the presence of various CYP450s known to catalyze the formation of the arylhydroxylamine metabolites of SMX and DDS *in vitro*. As shown in Fig. 2.3, CYP2C9 mRNA essentially was absent in cells from cultures of primary keratinocytes (NHEK) and HaCaT cells.

In addition, immunoblot analysis failed to detect the presence of CYP2C8, CYP2C9, CYP2C18, or CYP2C19 (Fig. 2.4).

The recombinant CYP2C proteins were expressed in a yeast cDNA expression system as described previously [116]. Interestingly, while both CYP3A4 and CYP3A5 mRNA were observed in NHEK, only CYP3A5 mRNA was observed in HaCaT cells (Fig. 2.5A). Immunoblot analysis using an antibody specific for CYP3A5 yielded positive results in both NHEK cells, and a monoclonal antibody that recognizes both CYP3A4 and CYP3A5 detected an immunoreactive CYP3A protein in NHEK cells (Fig. 2.5B). However, the levels of CYP3A4 and CYP3A5 proteins were much lower as compared to the human livers.

CYP2E1 mRNA was also found to be expressed in both NHEK and HaCaT cells (Fig. 2.6), while CYP2E1 protein was barely detectable (data not shown).

Determination of catalytic activity for CYP3A4 in NHEK. Catalytic activity of CYP3A4 was not observed in NHEK as there was no difference between the fluorescence of either control NHEK cells (NHEK+7-BQ) or the cells treated with

the CYP3A4 inhibitors (NHEK+ABT or TMC+7-BQ) or even NHEK cells without any treatment indicating the lower or substantial reduced activity of these enzymes in these cells. The standard curve using the 7-HQ in NHEK, however, showed the correlation coefficient of 0.987 indicating the positive response and higher sensitivity of this assay.

Covalent adduct formation of DDS and SMX in presence and absence of inhibitors of various enzymes. The effect of various enzyme inhibitors on protein haptenation in NHEK exposed to SMX or DDS was evaluated by both confocal microscopy and ELISA. For each inhibitor, we utilized the highest concentration that did not cause cytotoxicity in NHEK. As shown in Fig. 2.7, a broad inhibitor of CYP450 (ABT) which inhibits CYP3A4, a selective inhibitor of CYP2E1 (DCE), and an inhibitor of COX (INDO) failed to reduce the protein haptenation of DDS in NHEK cells.

Similar results were observed with SMX by ELISA (Fig. 2.8).

Similar results were obtained when inhibitors were added simultaneously with SMX or DDS and incubated for 3 h (data not shown). We also found that troleandomycin (a potent inhibitor of CYP3A4) and disulfiram (CYP2E1 inhibitor) did not attenuate the protein haptenation with either DDS or SMX (data not shown).

2.1.4 Discussion

The biotransformation of xenobiotics to reactive metabolites is believed to be responsible for a wide range of adverse reactions. Sulfonamides such as SMX and the sulfone DDS have been reported to be bioactivated to

arylhydroxylamine metabolites, which readily autooxidize to arylnitroso species (Fig. 2.9).

These metabolites are believed to initiate the cascade of events that ultimately provoke a CDR [97, 117]. We have previously proposed that bioactivation in the skin may play an important role in these reactions [98]. Indeed, incubation of NHEK with SMX or DDS results in protein haptenation [99].

In vitro studies have shown that the bioactivation of these parent arylamine drugs to their arylhydroxylamine metabolites may be mediated by various oxidizing enzymes such as CYP2C9, CYP2E1, CYP3A4, and MPO [105-108, 118, 119]. Several arylamine drugs, including procainamide, are oxidized to arylhydroxylamine metabolites by COX-2 *in vitro* [109, 110]. Which of these enzymes, if any, mediates the bioactivation of SMX and DDS in NHEK is unknown.

To assess the importance of arylamine oxidation, we evaluated the impact of SMX and DDS N-acetylation on protein haptenation in NHEK. We found that the N-acetyl metabolites gave rise to a lower level of protein haptenation as measured by both ELISA and confocal microscopy (Fig. 2.1 and 2.2). It should be noted that it is possible that the apparent reduction in adduct formation could be secondary to a reduced affinity of the antisera for the adduct in the presence of an acetyl group on the drug, as opposed to an actual reduction in the amount of adduct formed. Differentiation of these two potential explanations could only be accomplished by the characterization of and development of chemical methods for the quantification of the drug-protein adducts.

Prior to evaluating the effect of various enzyme inhibitors on protein haptenation with these drugs, we sought to confirm the presence of the most probable enzymes for bioactivation in NHEK. As HaCaT cells are widely used as an alternative to primary cultures of NHEK, together with our previous observation of protein haptenation in these cells when exposed to SMX or DDS [99], we also examined the presence of CYP450 enzymes in this cell line. While CYP2C9 appears to be the most important enzyme for bioactivating SMX and DDS in the human liver [105-107], we did not detect the presence of CYP2C9 message or protein in either cell type (Fig. 2.3 & 2.4). In addition, there was no evidence of other members of the CYP2C family of enzymes in either NHEK or HaCaT cells when probed by immunoblot. Yengi et al [120] have previously reported the expression of CYP2C9, CYP2C18, and CYP2C19 transcripts in human skin samples. As these investigators probed full thickness skin, it is not possible to determine which skin cells gave rise to these transcripts. Saeki et al., have observed the presence of CYP2C transcripts in human keratinocytes from several subjects[121]. However, their use of non-specific primers does not permit identification of the specific CYP2C genes that were expressed in these cells. While our data demonstrate protein haptenation with SMX and DDS in the absence of detectable CYP2C9 in NHEK, further studies are needed to more carefully determine the expression of this enzyme in human skin.

As shown in Figure 2.5, both CYP3A4 and CYP3A5 mRNA and protein were readily detected in NHEK. Interestingly, only CYP3A5 mRNA was detectable in HaCaT cells. While our antibodies were not specific for CYP3A4,

the blot analysis using antibody specific for CYP3A5, combined with the mRNA results, suggest that the protein detected using the nonspecific CYP3A antibody was due to recognition of CYP3A5 in HaCaT cells (Fig. 2.5B). To our knowledge, this differential expression of CYP3A enzymes has not been demonstrated previously in keratinocytes. The differential expression of CYP3A4/5 proteins, especially much lower expression in NHEK and HaCaT cells as compared to liver, might suggest the minor role of these enzymes for the bioactivation of these parent drugs in skin. We were also able to demonstrate the presence of CYP2E1 mRNA in both NHEK and HaCaT cell types (Fig. 2.6). This is consistent with the reports of other investigators who have demonstrated the presence of CYP2E1 transcripts and protein in NHEK[74, 121].

Based on the mRNA and protein data, we concluded that CYP2C9 was not a likely mediator of the bioactivation of these drugs in NHEK. Indeed, preliminary studies demonstrated that sulfaphenazole, an inhibitor of CYP2C9, did not inhibit protein adduction in NHEK exposed to SMX or DDS [122].To evaluate the role of CYP3A4/5 and CYP2E1 in the generation of drug-protein adducts, we evaluated the effect of inhibitors of these enzymes (at their maximum non-cytotoxic concentration) on protein haptenation in NHEK exposed to SMX or DDS. Our results indicate that a general inhibitor of CYP450s, ABT (which has been shown to completely (~ 90%) inhibit most of the major CYP450s, such as CYP1A2, 2B6, 2C9, 2C19, 2D6, and 3A4) [123], did not reduce the covalent adducts formed after exposure of NHEK to DDS and SMX (Fig. 2.7 and 2.8). The selective inhibitor of CYP2E1 (DCE) also failed to decrease adduct

formation. Other inhibitors of CYP3A4 (troleandomycin) and CYP2E1 (disulfiram) also did not reduce the protein haptenation of DDS and SMX in NHEK (data not shown). These results suggest that CYP450 does not play a major role in the oxidative metabolism of these drugs in NHEK. In addition, though COX-2 has been shown to mediate the oxidation of arylamines *in vitro*, an inhibitor of cyclooxygenase (indomethacin) did not attenuate the protein haptenation in NHEK exposed to either DDS or SMX (Fig. 2.7 and 2.8). This is consistent with our recent observation that recombinant COX-2 does not mediate the oxidation of these drugs [124].

Hence, our studies confirm our previous observations that NHEK are able to bioactivate SMX and DDS giving rise to haptenated proteins. We found that CYP450s that are important in the bioactivation of these drugs in the liver do not appear to play a significant role in their bioactivation in NHEK. It should be noted, however, that recent data suggests the level of CYP450 expression may differ as keratinocytes differentiate [125]. Nevertheless, we observed significant protein haptenation in NHEK in the absence of involvement of CYP450. These studies demonstrate that the role of various drug metabolizing enzymes in the bioactivation of drugs may vary from tissue to tissue. Likewise, though COX-2 has been reported to oxidize arylamines, neither COX-1 nor COX-2 appears to contribute to the bioactivation of these drugs in NHEK. In our companion paper to this current investigation, we demonstrate the role of FMO and peroxidases in the bioactivation of these arylamine drugs in keratinocytes.

Figure 2.1. Protein haptenation in NHEK incubated with DDS or MADDS. A. NHEK were incubated in the presence of vehicle (1% DMSO) or 800 μM of DDS or MADDS for 24 h. Cells were then imaged using confocal microscopy (objective lens: 20x) as described in Materials and Methods. Micrographs are representative images from each incubation condition. B. ages for control, DDS and MADDS in figure 2.1A were analyzed by Image J software and fluorescence intensity from a minimum of 3 view fields of 3 different slides of each treatment (with 15 – 20 cells per field) were averaged and expressed as mean (SD) fluorescence intensity (arbitrary units). Results were analyzed using ANOVA with the Holm-Sidak method for multiple pairwise comparisons. $^{*}p < 0.05$ compared to control; $^{**}p < 0.05$ compared to control or MADDS. C. Determination of covalent adducts of DDS and MADDS (800 μM, 24h) in NHEK by ELISA as described in Materials and Methods. Data presented represent the mean (SD) optical density of three different experiments having three replicates in each experiment. Data were analyzed using ANOVA with the Holm-Sidak test for multiple pairwise comparisons. $^{*}p< 0.05$ compared to NHEK incubated with vehicle or MADDS.

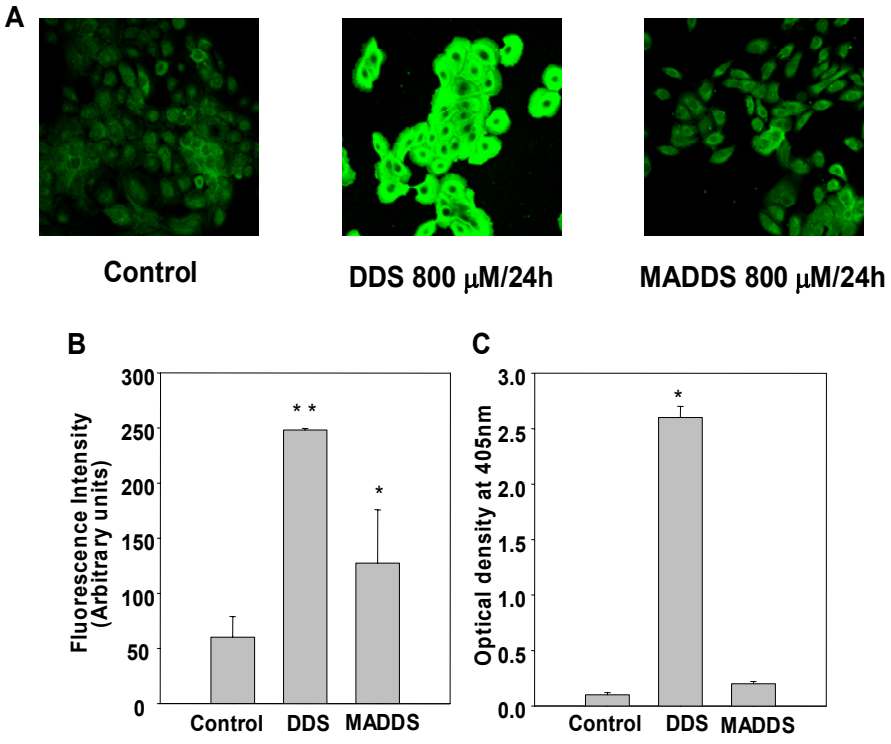
A
Control
DDS 800 μM/24h
MADDS 800 μM/24h
B
Fluorescence Intensity (Arbitrary units)
300
250
200
150
100
50
0
* *
*
Control
DDS
MADDS
C
Optical density at 405nm
3.0
2.5
2.0
1.5
1.0
0.5
0.0
*
Control
DDS
MADDS

Figure 2.2. Protein haptenation in NHEK incubated with SMX or NASMX. A. NHEK were incubated in the presence of vehicle (1% DMSO) or 800 μM of SMX or NASMX for 24 h. Cells were then imaged using confocal microscopy (objective lens: 63x) as described in Materials and Methods. Micrographs are representative images from each incubation condition. B. Images for control, SMX and NASMX in figure 2.2A were analyzed by Image J software and fluorescence intensity from a minimum of 3 view fields of 3 different slides of each treatment (with 5 – 10 cells per field) were averaged and expressed as mean (SD) fluorescence intensity (arbitrary units). Results were analyzed using ANOVA with the Holm-Sidak method for multiple pairwise comparisons. $^{*}p < 0.05$ compared to control and NASMX. C. Determination of covalent adducts of SMX and NASMX (800 μM, 24h) in NHEK by ELISA as described in Materials and Methods. Data presented represent the mean (SD) optical density of three different experiments having three replicates in each experiment. Data were analyzed using ANOVA with the Holm-Sidak test for multiple pairwise comparisons. $^{*}p< 0.05$ compared to NHEK incubated with vehicle or NASMX.

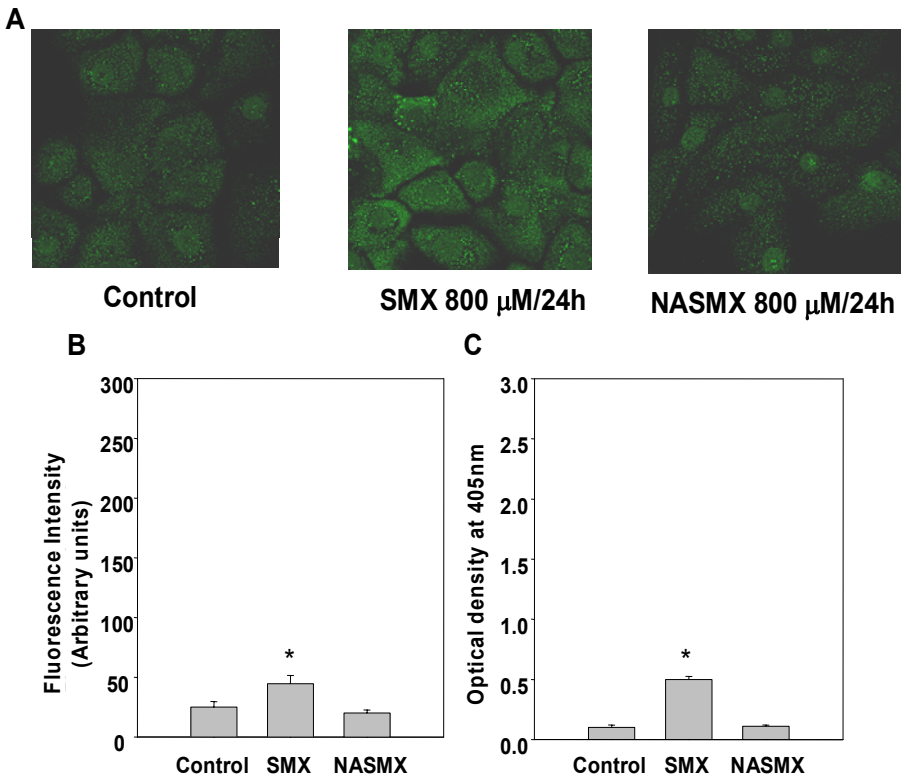
A
Control
SMX 800 μM/24h
NASMX 800 μM/24h
B
Fluorescence Intensity (Arbitrary units)
300
250
200
150
100
50
0
*
Control
SMX
NASMX
C
Optical density at 405nm
3.0
2.5
2.0
1.5
1.0
0.5
0.0
*
Control
SMX
NASMX

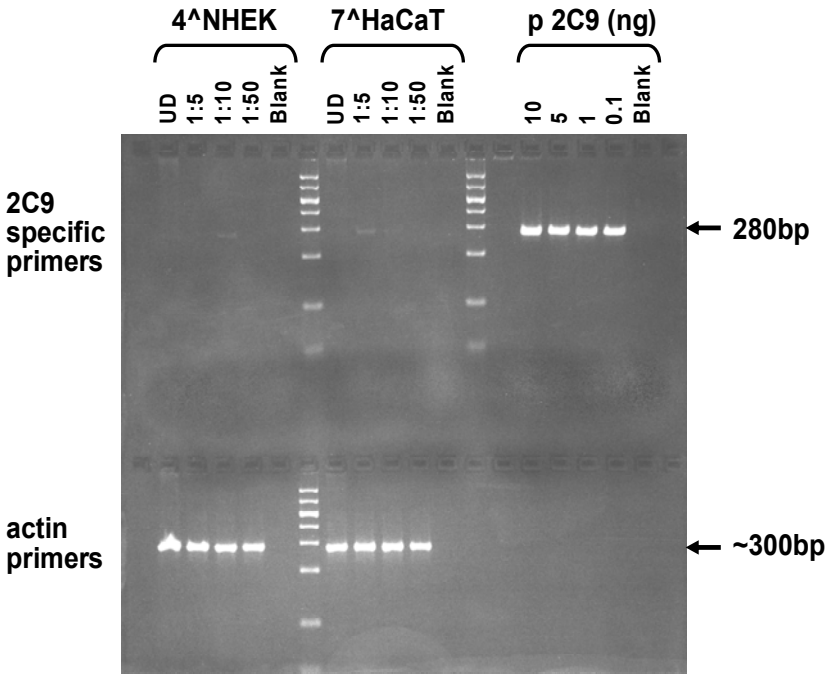

Figure 2.3. Blot analysis for CYP2C9 mRNA expression in NHEK and HaCaT cells. 4th passage NHEK (designated as 4^NHEK) and HaCaT (designated 7^HaCaT) cells were probed for mRNA expression using CYP2C9 specific primers, as described in Materials and Methods. Various dilutions were evaluated as denoted. Note the absence of a band in both cell types corresponding to CYP2C9.

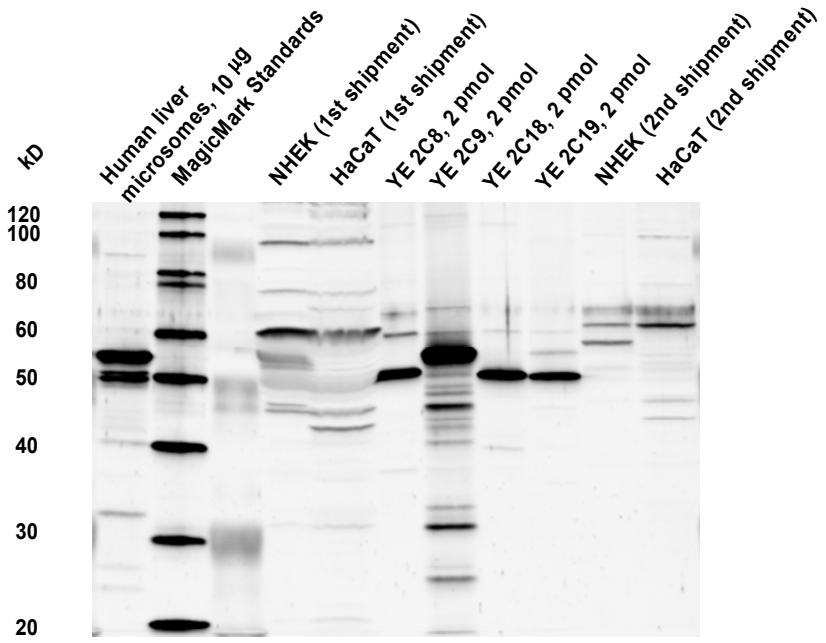

Figure 2.4. Immunoblot analysis for CYP2C9 protein expression in NHEK and HaCaT cells. 4th passage NHEK and HaCaT cells were probed for CYP2C proteins using specific antibodies. Replicate sets of cells were analyzed (designated as 1st and 2nd shipment). Note the absence on immunoblot of bands in either cell type corresponding to CYP2C8, CYP2C9, CYP2C18 or CYP2C19. YE stands for Yeast expressed.

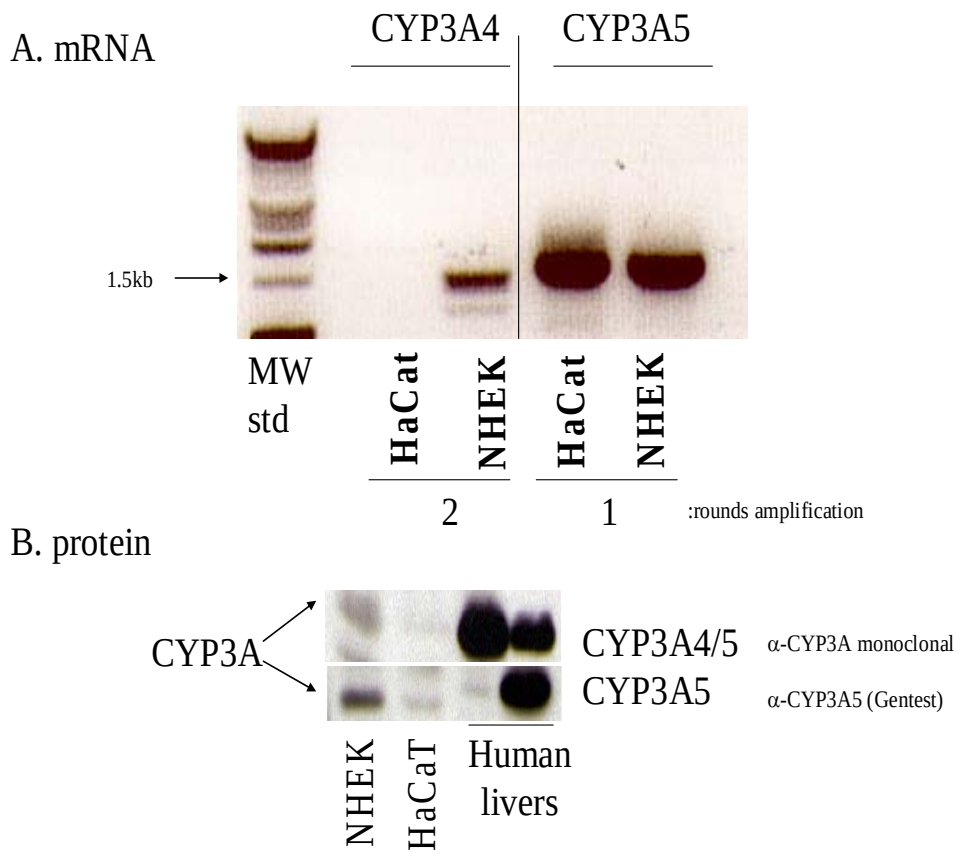

Figure 2.5. Analysis for CYP3A4 and CYP3A5 expression in NHEK and HaCaT cells. A) Northern blot analysis for CYP3A4 and CYP3A5 mRNA expression in NHEK and HaCaT cells. 4th passage NHEK and HaCaT cells were probed for mRNA expression using CYP3A4 and CYP3A5 specific primers as described in Materials and Methods. Note the absence of CYP3A4 mRNA in HaCaT cells. B) Immunoblot analysis for CYP3A expression in NHEK, HaCaT cells and human livers. 4th passage NHEK, HaCaT cells and human livers were probed for CYP3A proteins using monoclonal antibodies. Anti-CYP3A antibody recognizes both CYP3A4 and CYP3A5.

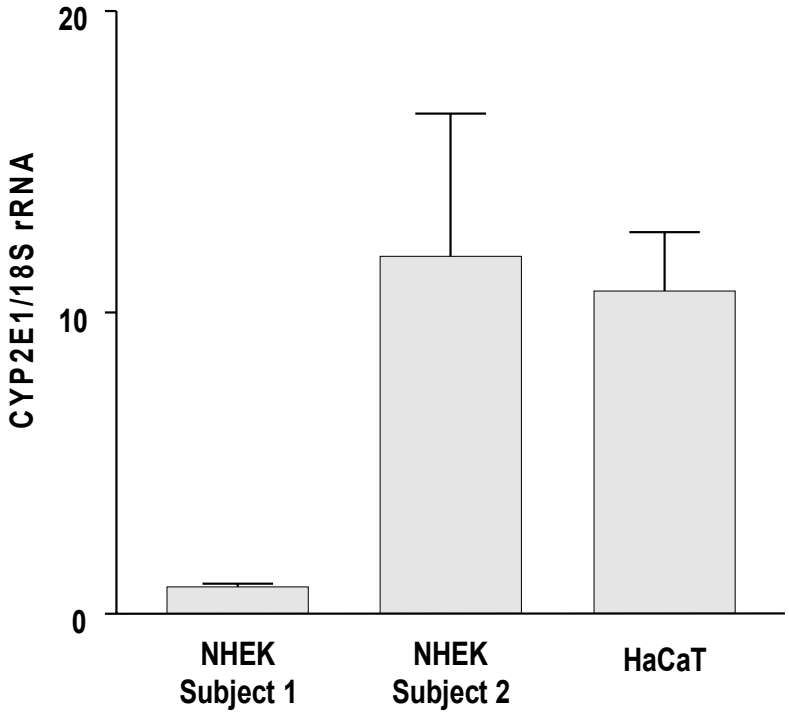

Figure 2.6. Quantitative RT-PCR assessment of CYP2E1 mRNA in NHEK and HaCaT cells. CYP2E1 mRNA was quantified in NHEK and HaCaT cells as described in Materials and Methods. CYP2E1 mRNA was normalized to 18S rRNA. NHEK represent data from 2nd passage cells from one patient (Subject 1) and 3rd passage cells from a different patient (Subject 2).

Figure 2.7. Protein haptenation of DDS in NHEK in the presence of inhibitors of CYP450s and cyclooxygenase. NHEK were incubated for 3 h in the presence of vehicle (1% DMSO), 5 mM aminobenzotriazole (ABT), 5 mM trans-dichloroethylene (DCE), or 100 μM indomethacin (INDO). The concentrations of inhibitors selected were the maximal concentrations that did not increase cell death in NHEK under the incubation conditions. After pre-incubation with inhibitors, cells were incubated for an additional 3 h with 250 μM DDS. Covalent adducts were quantified using confocal microscopy (A) or ELISA (B), as described in Materials and Methods. A. Quantification of adducts was performed as described in Materials and Methods. Control represents NHEK incubated with vehicle (1% DMSO) alone. Results were analyzed using ANOVA with Holm-Sidak method for multiple pairwise comparisons. $^{*}p < 0.05$ compared to NHEK incubated with vehicle alone. B. Covalent adducts were determined by the ELISA as described in Materials and Methods. Data presented represent the mean (SD) optical density of three different experiments having three replicates in each experiment. Data were analyzed statistically using ANOVA with the Holm-Sidak test for multiple pairwise comparisons. $^{*}p< 0.05$ compared to NHEK incubated with vehicle alone.

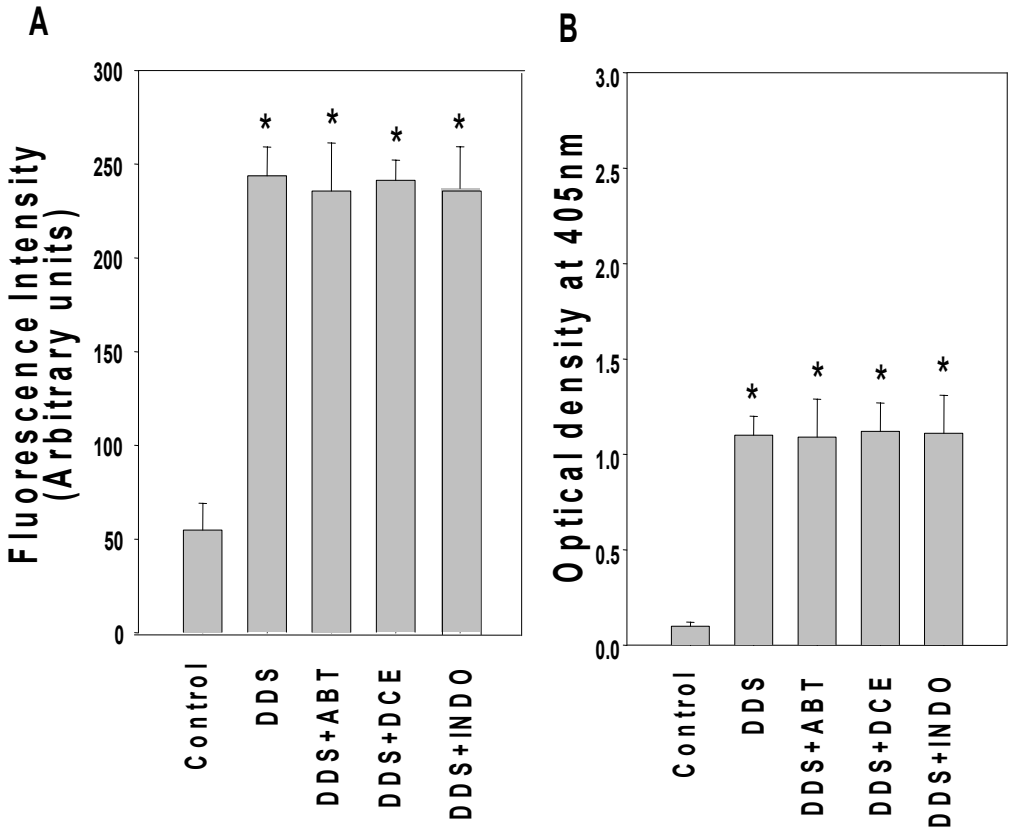
A
Fluorescence Intensity (Arbitrary units)
300
250
200
150
100
50
0
*
*
*
*
Control
DDS
DDS+ABT
DDS+DCE
DDS+INDO
B
Optical density at 405nm
3.0
2.5
2.0
1.5
1.0
0.5
0.0
*
*
*
*
Control
DDS
DDS+ABT
DDS+DCE
DDS+INDO

Figure 2.8. Protein haptenation of SMX in NHEK in the presence of inhibitors of CYP450s and cyclooxygenase. NHEK were incubated for 3 h in the presence of vehicle (1% DMSO), 5 mM aminobenzotriazole (ABT), 5 mM trans-dichloroethylene (DCE), or 100 μM indomethacin (INDO). The concentrations of inhibitors selected were the maximal concentrations that did not increase cell death in NHEK under the incubation conditions. After pre-incubation with inhibitors, cells were incubated for an additional 3 h with 250 μM SMX. Covalent adducts were quantified using ELISA as described in Materials and Methods. Data presented represent the mean (SD) optical density of three different experiments having three replicates in each experiment. Data were analyzed statistically using ANOVA with the Holm-Sidak test for multiple pairwise comparisons. $^{*}p< 0.05$ compared to NHEK incubated with vehicle alone.

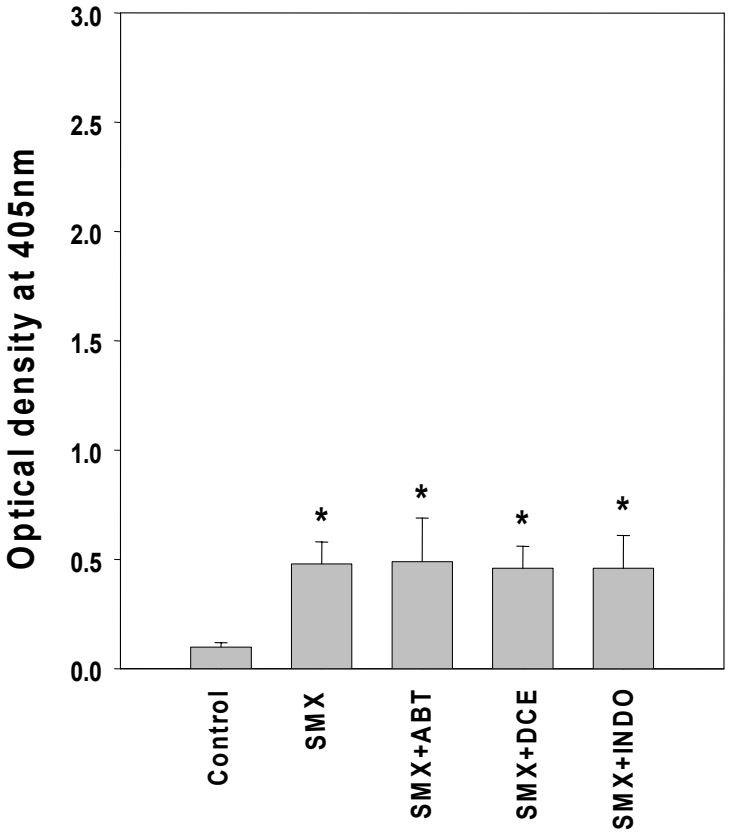
Optical density at 405nm
3.0
2.5
2.0
1.5
1.0
0.5
0.0
*
*
*
*
Control
SMX
SMX+ABT
SMX+DCE
SMX+INDO

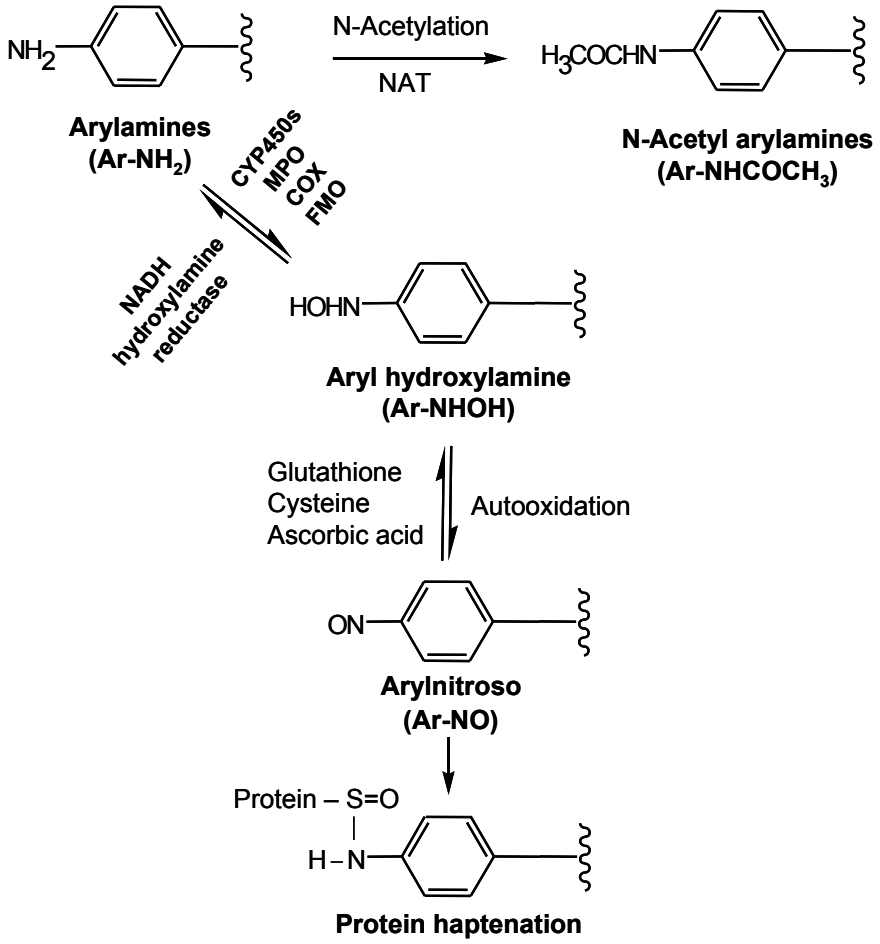

Figure 2.9. Scheme for the bioactivation of SMX and DDS giving rise to protein haptenation. Abbreviations: COX – cyclooxygenase; CYP450s – cytochromes P450; MPO – myeloperoxidase; NAT – N-acetyltransferase; FMO – Flavin containing monooxygenases**.**

2.2 Enzyme-mediated protein haptenation of dapsone and sulfamethoxazole in human keratinocytes – 2. Role of human cyclooxygenase-2*.

2.2.1 Introduction

Administration of sulfonamide antimicrobials such as sulfamethoxazole (SMX) and the sulfone dapsone (DDS) has been associated in humans with hypersensitivity reactions that include fever, skin eruptions, hepatotoxicity, and blood dyscrasias [92, 93]. The mechanism of sulfonamide hypersensitivity is not well understood, but has been hypothesized to be secondary to the generation of the reactive oxidative metabolites such as SMX-hydroxylamine (SMX-NOH) and DDS-hydroxylamine (DDS-NOH) and their respective nitroso derivatives [97]. The arylhydroxylamine metabolites of DDS and SMX, unlike the parent sulfonamides, are cytotoxic to a variety of cells *in vitro* and have been shown to generate reactive oxygen species [98, 111, 126]. The parent drugs and their arylhydroxylamine metabolites have been demonstrated to haptenize cellular proteins, which may lead to immune mediated cutaneous reactions [99, 127, 128]. Thus, the bioactivation of these arylamine xenobiotics to their respective arylhydroxylamine metabolites may be the first and most important step in initiation of these reactions.

Previous studies have demonstrated the ability of various oxidizing enzymes, including cytochrome 450 (CYP) 2C9, CYP2E1 and CYP3A4 as well

---

* Note: Published as: Vyas PM, Roychowdhury S, Svensson CK. Role of cyclooxygenases-2 in the bioactivation of dapsone and sulfamethoxazole. *Drug Metabolism and Disposition* 34(1): 16-18, 2006.

as myeloperoxidase (MPO) to bioactivate arylamines *in vitro* [105, 107, 108, 118, 129]. Cyclooxygenases (COX), or prostaglandin H synthase, have also been shown to bioactivate heterocyclic amines to their hydroxylamine metabolites [109]. Procainamide, an arylamine antiarrhythmic agent, has also been found to be oxidized to its arylhydroxylamine and arylnitroso metabolites by COX-2 [110]. The N-oxidation of 4-chloroaniline has also been reported to be mediated by COX [130]. Based upon these observations, we tested the hypothesis that COX-2 may bioactivate SMX and DDS resulting in protein haptenation.

2.2.2 Materials and Methods

Materials. Unless specified otherwise, all chemicals and reagents were purchased from Sigma (St. Louis, MO) or Fisher Scientific (Chicago, IL). DDS and SMX hydroxylamine metabolites were synthesized as described previously [111]. Human recombinant COX-2 was obtained from Cayman Chemical (Ann Arbor, MI). Rabbit anti-sera was raised against SMX- and DDS-keyhole limpet hemocyanine conjugates and specificity assessed as described previously [98]. Goat anti-rabbit antibody conjugated with alkaline phosphatase was purchased from Molecular Probes (Eugene, OR). Microtiter ELISA plates (96 well) were obtained from Rainin Instruments (Woburn, MA).

Adduct formation of DDS by human recombinant COX-2. An incubation mixture containing COX-2 (100 units), arachidonic acid (1 mM), hematin (1 μM), EDTA (5 mM) and H_2O_2 (1 mM) in Tris-HCl buffer (50 mM, pH 8.00), with and without INDO or DDS (100 μM each) was incubated for 1 h at 37°C. A control incubation containing only buffer was also included to account for non-specific

binding to the microtiter plate. After 1 h incubation, the reaction mixture was left overnight at 4°C for complete adhesion of protein to the microtiter plate. In addition, a DDS-bovine serum albumin adduct was added to a set of wells at this time to serve as a positive control for adduct detection. After 24 h, covalent adducts were determined by an adduct-specific ELISA as described previously [98].

Determination of arylhydroxylamine formation of DDS and SMX by HPLC in the incubation containing COX-2 activating system. DDS or SMX (800 μM) were added to the incubation mixture described above with and without COX-2 (100 units), for 1 h at 37°C. Ascorbic acid (1 mM) was included in all incubations to stabilize the arylhydroxylamine formed. After 1 h, the reaction was terminated by addition of 3 ml of ethyl acetate and the arylhydroxylamine metabolites determined as described previously [98]. As a positive control to determine the activity of COX-2, oxidation of a fluorescent dye 2',7'-dichorodihyrofluorescein (DCHF-5 μM) was measured [111].

Determination of H_2O_2 mediated arylhydroxylamine formation of SMX or DDS via high performance liquid chromatography (HPLC). SMX or DDS (800 μM) were incubated in Tris-HCl buffer (50 mM, pH 8.00) and ascorbic acid (1mM) with increasing concentration of H_2O_2, ranging from 0.01 μM to 10 mM. The incubation mixtures were kept for 1 h at 37°C. After 1h, the metabolites formed were extracted and quantified via HPLC.

Statistical analysis. Data are presented as mean (SD). Statistical comparisons between two groups were made using either student t-test

(parametric method) for normalized data or Friedman's rank sum test (nonparametric method) for the data which did not pass the normality test. For the comparison between more than two groups, ANOVA and the Holm-Sidak method for multiple pairwise comparisons was used. A value of $p<0.05$ was considered to be significant.

2.2.3 Results and Discussion

Antimicrobial sulfonamides, such as SMX, and the sulfone DDS are important drugs for the treatment of *Pneumocystis carinii* pneumonia, especially in AIDS patients [90]. However, in this patient population, these drugs are commonly associated with minor to severe CDRs, which are believed to be secondary to their metabolism to reactive arylhydroxylamine and arylnitroso derivatives [97]. As COX-2 is induced in the presence of various forms of environmental and pathological stress [131, 132], we hypothesized that the increased frequency of these reactions observed in AIDS patients may be secondary to elevated levels of these reactive metabolites formed as a result of COX-2 induction. As an initial test of this hypothesis, we sought to determine if COX-2 was capable of generating these reactive metabolites.

Using an adduct specific ELISA assay, we found that addition of DDS to an incubation mixture containing COX-2, hematin, EDTA, arachidonic acid and H_2O_2 resulted in covalent adduct formation (Fig. 2.10).

Importantly, however, a non-selective inhibitor for COX-1 and COX-2 (INDO) did not attenuate the formation of drug/metabolite-protein adducts. In addition, use of lower concentrations of H_2O_2 in the incubation mixture did not

give rise to detectable covalent adducts. Various controls ruled out non-specific binding of the primary antisera or secondary antibody as causing artifactual results. We confirmed the catalytic activity of COX-2 in this incubation mixture using a reactive oxygen species generation as a positive control, as described in Materials and Methods. There was 2.3 fold increase in the fluorescence of incubations with COX-2 as compared to incubations without COX-2 (data not shown); confirming the catalytic activity of the enzyme.

Formation of the arylhydroxylamine metabolites of DDS and SMX in the incubation mixture was confirmed via HPLC. However, removal of the enzyme in the assay gave rise to similar amount of the NHOH metabolites (Fig. 2.11).

This observation suggested that some other component in the incubation mixture was resulting in the chemical oxidation of DDS and SMX. Since removal of H_2O_2 from the incubation mixture prevented the formation of the arylhydroxylamine (data not shown), we suspected that we were observing a chemical oxidation of the arylamines. Indeed, we found that H_2O_2 alone gave rise to a concentration dependent oxidation of SMX and DDS (Fig. 2.12).

Our results indicate that enzymatic oxidation of SMX and DDS by COX-2 is negligible, but that chemical oxidation via H_2O_2 may occur. These results are consistent with the report of Rubin and Curnette [133], who demonstrated that H_2O_2 was able to oxidize procainamide giving rise to an arylhydroxylamine metabolite. Additionally, Goebel et al [110] found that the covalent binding of procainamide arising from an incubation mixture almost identical to that used in the present study was markedly attenuated when H_2O_2 was removed from the incubation.

However, these investigators found that in addition to H_2O_2, hematin was required to obtain similar levels of covalent binding in the absence of COX-2. In contrast, we did not find hematin to be an essential component for the N-oxidation of SMX or DDS (data not shown).

Taken together, these data suggest that COX-2 is unlikely to play a significant role in mediating the formation of reactive metabolites of sulfonamides. Indeed, we have recently found that the protein haptenation observed when SMX and DDS are incubated with normal human keratinocytes is not altered by the addition of non-specific and specific inhibitors of COX [122]. In addition, incubation of keratinocytes with pro-inflammatory cytokines, which results in the induction of COX-2, does not enhance the covalent binding of SMX or DDS in these cells[134]. These observations indicate that induction of COX-2 in the presence of environmental or pathological stress is unlikely to play a role in the increased frequency of adverse reactions to sulfonamides in AIDS patients.

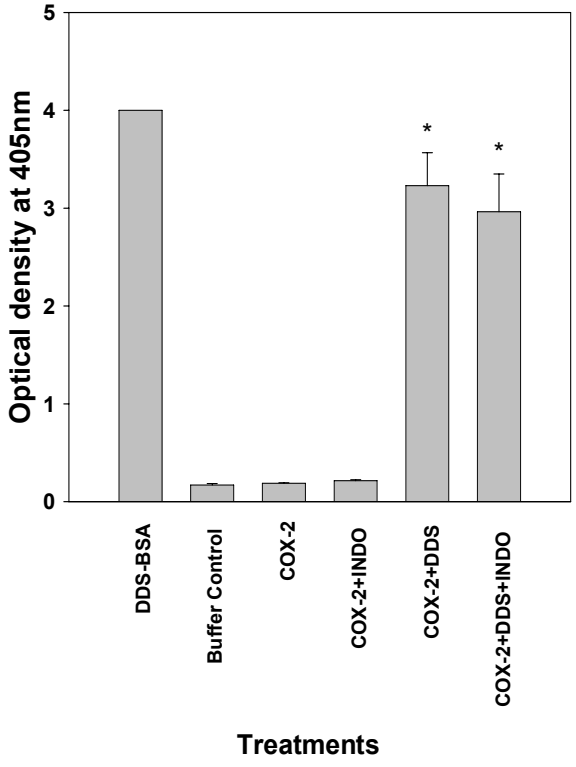

Figure 2.10. Bioactivation and subsequent adduct formation of DDS by human recombinant COX-2. DDS (100 μM) was incubated in a mixture containing COX-2 (100 units), arachidonic acid (1 mM), hematin (1 μM), EDTA (5 mM) and H_2O_2 (1 mM) in Tris-HCl buffer (50 mM, pH 8.00) with and without INDO (100 μM) for 1 h at 37°C. Controls containing buffer, COX-2 and COX-2+INDO were used to determine the non-specific binding of anti-DDS rabbit sera. Covalent adducts were determined using adduct specific ELISA as described in Materials and Methods. Data presented represent the mean (SD) optical density of 6 replicates. Data were analyzed statistically using ANOVA and Holm-Sidak test for multiple pairwise comparisons. $^{*}p< 0.05$ compared to buffer control, COX-2 and COX-2+INDO. DDS-BSA was used as positive control.

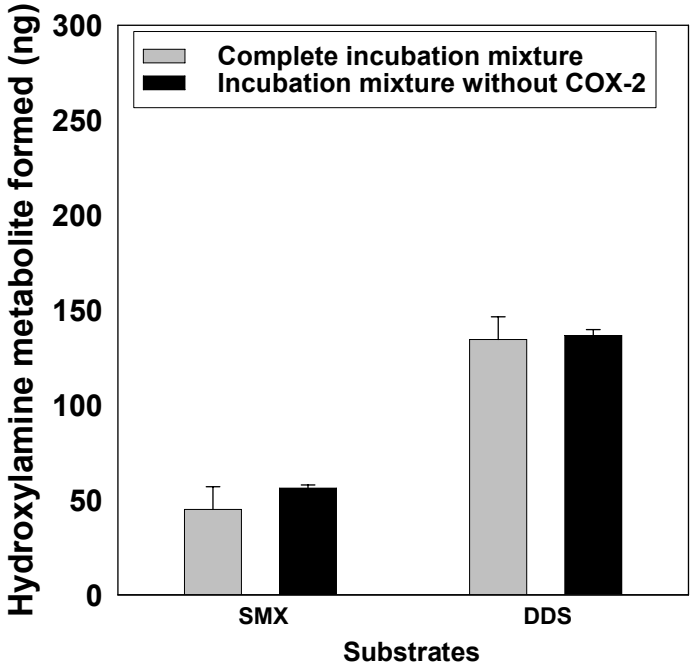

Figure 2.11. Determination of arylhydroxylamine formation of DDS and SMX by HPLC in the incubation containing COX-2 activating system. SMX or DDS (800 μM) were incubated in a mixture containing arachidonic acid (1 mM), hematin (1 μM), EDTA (5 mM), ascorbic acid (1 mM) and H_2O_2 (1 mM) in Tris-HCl buffer (50 mM, pH 8.00), with and without COX-2 (100 units), for 1 h at 37°C. After 1 h, the formed SMX-NOH or DDS-NOH was extracted and quantified via HPLC as described in Materials and Methods. Data presented represent the mean (SD) amount of SMX-NOH formed of 9 replicates of each condition. Data were analyzed statistically using the Student's t-test, with no differences between incubation conditions observed.

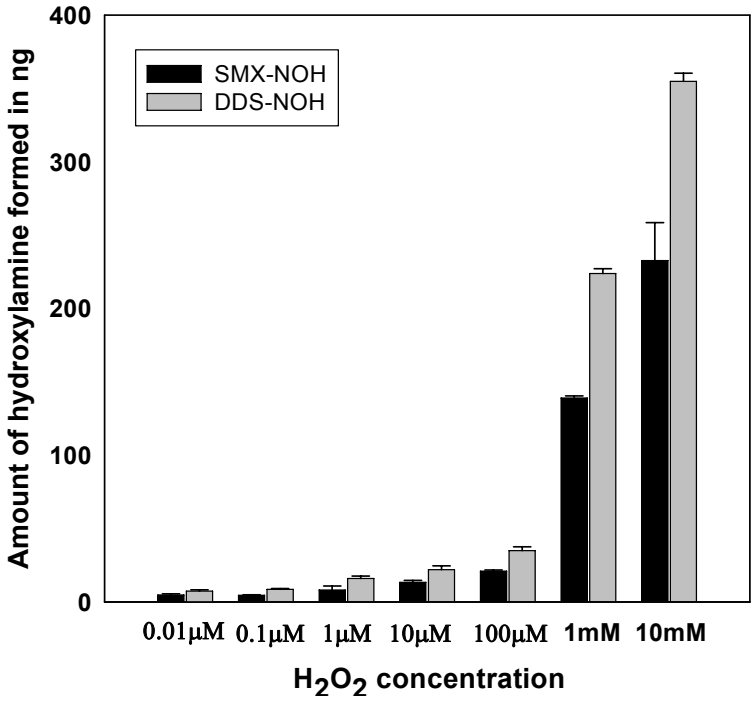

Figure 2.12. Determination of H_2O_2 mediated arylhydroxylamine formation of DDS and SMX by HPLC. DDS and SMX (800 μM) were incubated with increasing concentrations of H_2O_2 with ascorbic acid (1 mM) in Tris-HCl buffer (50 mM, pH 8.00) for 1 h at 37°C. After 1 h, the formed hydroxylamine metabolites were extracted and quantified via HPLC as described in Materials and Methods. Data presented represent the mean (SD) amount of DDS-NOH and SMX-NOH formed for 9 replicates of each condition.

2.3 Enzyme-mediated protein haptenation of dapsone and sulfamethoxazole in human keratinocytes – 3. Expression and role of flavin-containing monooxygenases and peroxidases*.

2.3.1 Introduction

Biotransformation of non-reactive drugs or chemicals to reactive intermediates or metabolites is believed to be an important step in the provocation of numerous adverse drug reactions, especially those that appear to be immune-mediated. Whereas the liver is the major site for the generation of reactive metabolites, organs other than the liver are often the primary or secondary target for toxicity. As the ability of unstable metabolites to distribute from the liver to other organs is questionable, it has been proposed that extrahepatic metabolism (e.g., in circulating cells) may be important in mediating such toxic events [135].

Skin eruptions after systemic drug administration represent one of the most commonly reported adverse drug reactions. Many drugs associated with cutaneous drug reactions (CDRs) are known to be metabolized to reactive metabolites [82]. However, the survival of such metabolites during transit from liver to the skin is undocumented. We have suggested that bioactivation of drugs in

---

* Note: Published as: Vyas PM, Roychowdhury S, Koukouritaki SB, Hines RN, Krueger SK, Williams DE, Nauseef WM, Svensson CK. Enzyme-mediated protein haptenation of dapsone and sulfamethoxazole in human keratinocytes - 2. Expression and role of flavin-containing monooxygenases and peroxidases. *Journal of Pharmacology and Experimental Therapeutics*. (Published online July 20, 2006; doi: 10.1124/jpet.106.105874)

the skin may play an important role in the initiation of CDRs [136]. Utilizing sulfonamides as model compounds to test this hypothesis, we have shown the bioactivation of sulfamethoxazole (SMX) and dapsone (DDS) to their respective arylhydroxylamine metabolites (SMX-NOH, DDS-NOH) in normal human epidermal keratinocytes (NHEK) [136]. Moreover, we have demonstrated that incubation of such cells with the parent compounds gives rise to protein haptenation [115].

Whereas the formation of the arylhydroxylamine metabolites of these compounds in the liver is mediated primarily via cytochromes P450 [65, 66, 69], it is unclear what enzyme(s) bioactivate these drugs in NHEK. In the first of these two companion papers, we demonstrate that cytochromes P450 do not play a major role in the protein haptenation observed in NHEK exposed to SMX or DDS. In addition, though other investigators have reported that cyclooxygenase-2 is able to oxidize arylamine compounds [72], our results indicate that neither cyclooxygenase-1 nor -2 is involved in the protein haptenation observed in these cells [137]. Hence, we probed the role of flavin-containing monooxygenases (FMOs) and peroxidases (PRXs) in this phenomenon. Our results indicate that FMOs and PRXs are the primary enzymes that bioactivate these drugs in NHEK and thereby generate haptenated proteins. Based on these findings, extrapolation of observations in one organ of bioactivation to another (e.g., liver to skin) must be made cautiously.

2.3.2 Materials and Methods

Materials. DDS, SMX, ketoconazole (KCZ), methimazole (MMZ), 4-aminobenzoic acid hydrazide (ABH), magnesium chloride, $NADP^+$, glucose-6-phosphate, glucose-6-phosphate dehydrogenase, 3, 3'-diaminobenzidine tetrahydrochloride (DAB), and rat tail collagen (type-I) were obtained from Sigma (St. Louis, MO). DDS and SMX hydroxylamine metabolites were synthesized as described previously [80]. Rabbit anti-sera was raised against SMX- and DDS-keyhole limpet hemocyanin conjugates and specificity assessed as described previously [136]. Normal human epidermal keratinocytes and keratinocyte culture media were obtained from CAMBREX (Walkersville, MD). Microtiter ELISA plates (96 well) were obtained from Rainin Instruments (Woburn, MA). Goat-anti-rabbit IgG conjugated with Alexafluor 488 and goat anti-rabbit antibody conjugated with alkaline phosphatase, Amplex red reagent and YoYo-1 were purchased from Molecular Probes (Eugene, OR). Mouse monoclonal antibody to human thyroid peroxidase (TPO) and rabbit polyclonal anti-mouse IgG antibody conjugated to alkaline phosphatase was purchased from Abcam (Cambridge, MA). Pure TPO was obtained from Fitzgerald Industries International, Inc. (Concord, MA). Human salivary gland mRNA, used as a positive control for lactoperoxidase (LPO), was obtained from Clontech (Mountain view, CA). A human promyelocytic cell line (PLB-985 cells) known to express myeloperoxidase (MPO) was obtained from Dr. Tom Redo [138] and used as a positive control for MPO. Polyclonal antibodies raised against human FMO1 and FMO3 peptides and horseradish peroxidase-conjugated goat anti-rabbit IgG were obtained from Gentest (Woburn, MA).

Protein molecular weight standards (bench mark prestained protein ladder) were from Invitrogen (Carlsbad, CA). Donkey anti-rabbit – HRP antibody, nitrocellulose membranes and enhanced chemiluminescence Western blotting kits were purchased from Amersham Pharmacia Biotech (Arlington Heights, IL). The 1-step NBT/BCIP substrate, micro bicinchoninic acid protein assay and Bradford assay reagent were purchased from Pierce Chemical Company (Rockford, IL). Immunomount was obtained from Vector Laboratories (Burlingame, CA). The pCEL1001 plasmid containing the Celera 19600414014330 cDNA representing full-length human FMO1, position +61 to +2172 inserted into pCMVSport 6 at the *Spe*I site, Trizol reagent, TOPO cloning kits, and all reagents for baculovirus protein expression were purchased from Invitrogen (Carlsbad,CA). RNeasy and One-Step RT-PCR kits were obtained from Qiagen (Valencia, CA). Criterion precast acrylamide gels and the Criterion Gel Electrophoresis system were purchased from Bio-Rad (Hercules, CA). All other chemicals and reagents were purchased from Sigma (St. Louis, MO) or Fisher Scientific (Chicago, IL).

Cell Culture. Normal human epidermal keratinocytes (NHEK) cells were cultured as detailed previously [136]. In brief, cells were propagated in 75 cm^2 flasks using basal media (KBM-2) supplemented with bovine pituitary extract (7.5 mg/ml), human epidermal growth factor (0.1 ng/ml), insulin (5 μg/ml), hydrocortisone, (0.5 μg/ml), epinephrine, transferrin, gentamicin (50 μg/ml) and amphotericin (50 ng/ml) (KGM-2) at 37°C in a humidified atmosphere containing 5% CO_2. Media was replaced every 2-3 days. When the cultures were nearly confluent (70-90%), cells were disaggregated using 0.025% trypsin/0.01% EDTA

in HEPES buffer followed by neutralization with 2 volumes of trypsin neutralizing solution. Cell suspensions were then centrifuged at 220 x *g* for 5 min followed by washing in KBM-2 and re-suspension in KGM-2. Cells were then either subcultured or cryo-preserved for further purposes. All experiments were performed using 3rd to 4th passage cells.

Determination of Inhibitor cytotoxicity in NHEK. To determine the maximal non-cytotoxic concentrations of various inhibitors in NHEK to block the respective enzymes, the cytotoxicity of concentrations ranging from 25 μM to 25 mM was examined. Cytotoxicity was determined using an impermeable DNA binding dye (YoYo - 1), as we have described previously [80].

ELISA Analysis of Drug/Metabolite-Protein Adducts. Formation of covalent adducts following SMX or DDS exposure, in the presence or absence of the selective enzyme inhibitors, was determined by cultivating NHEK (1 X 10^6 cells) for 24 h in 50 ml centrifuge tubes containing 10 ml of complete growth medium. The caps of the tubes were slightly loosened to maintain the aerobic conditions. The concentrations of the inhibitors used were the maximum non-cytotoxic concentrations determined in NHEK. Cells were then incubated with enzyme inhibitors 3 h prior to or immediately before addition of SMX (1 mM ascorbic acid was added prior to the addition of SMX as we have previously reported that ascorbic acid increases the protein haptenation in NHEK[115]) or DDS treatment for 3 h (concentrations specified in Results). Following the total 6 h or 3 h incubation, tubes were centrifuged at 220 *g* for 5 min to pellet the cells. Covalent adducts were determined as previously described [80].

Immunocytochemistry. Drug/metabolite-protein covalent adducts formation was also visualized using immunofluorescence confocal microscopy as described previously[115]. Cells were grown on collagen-coated (0.1 mg/ml) coverslips placed in petri-dishes containing 2 ml of complete growth medium. After 24 h, cultures were subjected to different selective enzyme inhibitors for 3 h (maximum non-cytotoxic concentrations were used), followed by SMX or DDS treatment for 3 h (concentrations specified in Results). After the total 6 h incubation, cells were washed (three times) with phosphate buffered saline (PBS: 0.05M sodium phosphate, 0.15M NaCl, pH 7.4) and fixed for 20 min with 4% paraformaldehyde in PBS. After fixation, cultures were washed 3 times with PBS followed by blocking for 60 min with Tris-casein buffer containing 0.3% Triton X-100 and overnight incubation with the anti-DDS or anti-SMX antisera (1:500 diluted in blocking buffer) at 4^{o}C. Coverslips were then washed with PBS, incubated for 3 h at 37^{o}C with the fluorochrome-conjugated secondary antibody (Alexa fluor-488 labeled goat-anti-rabbit IgG, 1:500 diluted in blocking buffer), and mounted on glass slides using Immunomount® containing anti-fade reagent.

Fluorescence images were acquired with a Zeiss Laser Scanning Microscope (LSM 510, Zeiss Axiovert stand, Zeiss 63x and 20x objective lens) using excitation at 488 nm. Emission was set to a long pass filter at 505 nm.

Image Analysis. For confocal laser scanning microscopy; laser attenuation, pinhole diameter, photomultiplier sensitivity and offset were kept constant for every set of experiments. Images were acquired from 3 different view fields of each slide. The obtained images were quantitatively analyzed for

changes in fluorescence intensities within regions of interests (boxes drawn over cell somata) using the Image J software (National Institutes of Health). Fluorescence values from a minimum of three view fields consisting of 15-20 NHEK cells in each field from three different slides of each treatment were averaged and expressed as mean ± SD fluorescence intensity.

Peroxidase Assay in NHEK. Peroxidase activity was determined using the fluorescent dye, Amplex red. Briefly, $5x10^6$ NHEK cells were lysed in 0.5 ml of 10 mM sodium phosphate buffer (pH 7.4). The cell lysate was centrifuged at 2040 *g* for 2 min in a microcentrifuge to obtain the supernatant fraction. Protein content of the supernatant fraction was determined using Bradford assay. Various amount of protein of the supernatant fraction (10 µg – 50 µg) was mixed with 50 µM Amplex red reagent and 1 mM H_2O_2 in a microtiter plate and then incubated in the dark at room temperature for 1 h. Following the incubation period of 1 h, the reactions were read in a fluorescence plate reader (Cytofluor®) at an excitation wavelength of 530 nm and an emission wavelength of 580 nm. The peroxidase activity was determined by measuring the observed fluorescence intensity.

The presence of peroxidases was also determined by mixing 300 µl of cell lysate supernatant with 0.27 mM of 3,3' – diaminobenzidine tetrahydrochloride (DAB) and 1.4 mM H_2O_2 in 100 mM potassium acetate buffer (pH 5.0) in a microtiter plate. Following incubation in the dark at room temperature for 24 h, absorbance at 450 nm was measured to assess the presence of peroxidases in the NHEK cell lysate.

MPO Immunoblot Analysis. Lysates of NHEK or PLB-985 cells and purified MPO were solubilized in SDS sample buffer and separated by SDS-PAGE in 9% acrylamide gel. Immunoblots were probed with rabbit polyclonal antibody to human MPO [139] followed by secondary donkey anti-rabbit antibody conjugated to HRP (Amersham).

Reverse Transcription Polymerase Chain Reaction (RT-PCR) Amplification for MPO and LPO. Total RNA was isolated from human salivary glands, NHEK, PLB and human embryonic kidney-293 (HEK) cells using a Qiagen RNeasy kit (Qiagen, Valencia, CA) following the manufacturer's protocol. cDNA was generated using 1750 ng total RNA in a synthesis reaction using Qiagen One Step reverse transcriptase (RT) with random hexamers according to the supplier's protocol. PCR amplification was performed using the MPO-specific forward primer, 5' – AAC ATC ACC ATC CGC AAC CAG AT - 3', and reverse primer, 5' – AAT GCA GGA AGT GTA CTG CAG TT - 3', resulting in a 1.2 kbp product, and the LPO specific forward primer, 5'-TCA TGC AG T GGG GTC AGA TTG TGG A-3', and reverse primer, 5'-CGG AAG GCG AAG GTG AAG ACA TTG G-3', resulting in a 744 bp product. PLB cells and human salivary glands were used as a positive control for MPO and LPO, respectively, and HEK cells were used as negative control for both reactions. GAPDH was used as housekeeping gene and was amplified from the keratinocyte cDNA using the primers 5'-CCA CCA CCC TGT TGC TGT AGC-3' and 5'-GGA TCC CCA CAG TCC ATG CCA-3' resulting in a 455 bp fragment. Amplifications were performed in 50 μl reactions. Cycling conditions for MPO and GAPDH consisted of an initial

incubation at 50° for 30 min followed by denaturation at 95° for 15 min, then 25 cycles of 94° for 1 min, 53° for 30 s, and 72° for 2 min, and a final 72° extension for 10 min. Cycling conditions for LPO consisted of an initial incubation at 50° for 30 min followed by 37 cycles of 94° for 2.5 min, 68° for 30 s, and 72° for 1 min, and a final extension at 72° for 10 min. Reactions were analyzed on 0.7% agarose gels stained with ethidium bromide.

MPO Chlorination Assay. MPO-mediated hypochlorous acid formation was measured using a previously reported method for quantification of taurine chloramine [140]. Briefly, 5 X 10^7 NHEK cells suspended in 10 ml Hanks balanced salt solution (HBSS) without Ca^{+2} or Mg^{+2} were incubated with 1 mM of diisopropylfluorophosphate to inhibit endogenous serine proteases. Cells were washed, resuspended in 0.5 ml relaxation buffer (10 mM PIPES, 3 mM NaCl, 3.5 mM $MgCl_2$, 100 mM KCl at pH 7.3) containing 1 mM $ATP(Na)_2$, and cavitated in 350 psi N_2, as previously described for neutrophils [141] The cavitate was collected in relaxation buffer containing 1 mM EGTA and centrifuged at 200 *g* for 10 min to remove unbroken cells and nuclei. The postnuclear supernatant was centrifuged at 100,000 *g* x 20 minutes to obtain cytosol and membrane for subsequent study. Reaction buffer (Dulbecco's PBS + 20 mM taurine + 1 mM glucose) was added to cytosol and supernatant and one hundred µl of each were incubated at 37°C for 90 minutes in the presence or absence of a cell-free H_2O_2-generating system, composed of 10 mM acetaldehyde and 0.01 U of xanthine oxidase in reaction buffer. The reaction was terminated by adding 200 U of catalase and the reaction mixture was cooled on ice for 10 min prior to the

addition of 1 mM 5-thio-2-nitrobenzoic acid (TNB, extinction coefficient = 14,100 /M/cm) and incubated for 5 min in the dark at room temperature. The absorbance was measured at 412 nm (A_{412}) to assess the concentration of TNB in solution and the hypochlorous acid produced was calculated by determining the loss in A_{412} of the sample without acetaldehyde compared to the A_{412} of the sample with acetaldehyde and dividing by 28200, the molar extinction coefficient for two moles of yellow TNB reacting with one mole of taurine chloramine to form one mole of colorless 5,5'-dithiobis(2-nitrobenzoic acid) (DTNB).

TPO Immunoblot Analysis. NHEK cell lysate (75 µg) and purified TPO were solubilized in SDS sample buffer and separated by PAGE in 10% SDS gel. Immunoblots were probed with mouse monoclonal antibody to human TPO followed by secondary rabbit anti-mouse – alkaline phosphatase conjugated antibody. NBT/BCIP was used as substrate for the secondary antibody to determine the presence of TPO.

Expression of Human Recombinant FMO3 and FMO1. A baculovirus/insect cell system was used for cloning and expression of FMO3 and FMO1. FMO1 cDNA was amplified by PCR from pCEL1001 using the forward primer, 5'-CAC CAT GGC CAA GCG AGT TGC-3', and the reverse primer, 5'-TTT TAC TTA TAG GAA AAT CAG AAA AAT AG-3' (underlined sequences correspond to the start and stop codon positions in the forward and reverse primers, respectively). The resulting 1606 bp amplicon representing FMO1 sequences from +98 to +1703 (accession number NM_002021) was cloned into the pENTR/SD/D-TOPO plasmid using a TOPO cloning kit (Invitrogen).

The original full-length FMO3 cDNA was amplified from an adult liver RNA sample using RT-PCR and the forward primer, 5'-TTG GAC AGG ACG TAG ACA CA-3', and reverse primer, 5'-TGG GTA TTG TCA GTA ACT TTC A-3'. The resulting 1711 bp amplicon was cloned into the pCR2.1 vector using AT cloning, resulting in pRNH696.

To move the FMO3 cDNA into the pENTR shuttle vector, PCR amplification was performed using linearized pRNH696 as a template and the forward primer, 5'-CAC CAT GGG GAA GAA AGT G-3', and reverse primer, 5'-GAT GAT TAG GTC AAC ACA AG-3'. The resulting 1604 bp amplicon was then cloned into the pENTR/SD/D-TOPO plasmid using the TOPO cloning kit, The resulting cDNA clone, pRNH829, contains FMO3 sequences from position +91 to +1697 (accession number NM_001002294). For both the FMO1 and FMO3 shuttle vectors, the fidelity of the amplified products were verified by complete DNA sequence analysis of the cDNA inserts.

Baculovirus and proteins were produced in ovary cells from *Spodoptera frugiperda* (Sf9) with the BaculoDirect system that utilizes lambda phage integration sites for the recombination reaction with BaculoDirect linear DNA. Once the primary virus was produced, it was amplified and proteins were expressed as described elsewhere [142, 143]. FAD was added (10 μg/ml) to the cell culture media during protein production to ensure that the level of this essential cofactor would not be limiting. Microsomes were prepared from cells harvested at approximately 96 h post-infection. Protein concentration was determined by the Bradford method, while the FMO content was determined by an HPLC based

method [142] that measures the FAD concentration. Substrate dependent NADPH oxidation by FMO1 and FMO3 was performed as previously described [142].

DDS- and SMX-Dependent Adduct Formation Catalyzed by Human Recombinant FMO3 and FMO1. An incubation mixture containing FMO3 or FMO1 (50 µg microsomal protein), $MgCl_2$ (3.3 mM), $NADP^+$ (0.065 mM), glucose-6-phosphate (3.3 mM), glucose-6-phosphate dehydrogenase (0.1 U) and DDS or SMX (100 µM) in Tris-glycine buffer (50 mM, pH 9.5) was incubated for 1 h at 37°C. Heat-inactivated FMO3 and FMO1 (90°C for 5 min) was utilized as a negative control to account for non-specific binding of the antisera in this experiment. After 1 h incubation, the reaction mixture was left overnight at 4°C for complete adhesion of protein to the microtiter plate. After 24 h, covalent adducts were determined by an adduct-specific ELISA as described previously [136].

Determination of FMO3 and FMO1 Protein in NHEK. SDS-PAGE, using 10% resolving gels and a Tris-glycine running buffer, was performed according to the method of Laemmli [144]. Fractionation was carried out using the Criterion Precast Gel Electrophoresis System (Bio-Rad, Hercules, CA.), followed by electrophoretic transfer to a nitrocellulose membrane using the Criterion Blotter (Bio-Rad) [145]. Twenty micrograms of microsomal protein were used for each sample of NHEK. Nonspecific binding sites were blocked by overnight incubation at 4°C with 5% nonfat dry milk in Tris-buffered saline (TBS; 25 mM Tris, pH 7.5, 150 mM NaCl). The blots were then incubated for 1 h at room temperature with FMO1 or FMO3 primary antibody diluted 1:5000 in TBS containing 0.5% nonfat

dry milk. After extensive washing with several changes of TBS supplemented with 0.1% Tween-20, the blots were incubated for 1 h at room temperature with horseradish peroxidase-conjugated goat anti-rabbit IgG diluted 1:10,000 in TBS containing 0.5% nonfat dry milk. Blots were then washed with several changes of TBS supplemented with 0.1% Tween-20 and processed for detection by enhanced chemiluminescence according to the manufacturer's instructions. The luminescence produced was detected by exposure of Fuji Super RX film (Fisher Scientific, Pittsburgh, PA) and after digitizing the image using a Hewlett Packard 6300C scanner (Boise, ID), the integrated OD of immunoreactive protein bands was determined using a Kodak DC120 digital camera and Digital Science 1D V 3.0 software (New Haven, CT). In all blots, bands corresponding to the protein of interest (FMO1 or FMO3) were identified by reference to the baculovirus-expressed FMO1 and FMO3 and molecular weight standards.

D-NOH Dependent Adduct Formation in Presence of Peroxidase Inhibitor and FMO Competitive Subtrate. Protein haptenation following D-NOH exposure to NHEK cells, in the presence or absence of ABH or MMZ was determined. Briefly, NHEK (1 X 10^6 cells) were incubated for 24 h in 50 ml centrifuge tubes containing 10 ml of complete growth medium maintaining the sterile aerobic conditions. Cells were then incubated with D-NOH (100 μM) and immediate addition of the PRX inhibitor (ABH, 5 mM) or the FMO competitive substrate (MMZ, 5 mM). The samples were incubated for 3 h more followed by ELISA analysis for the covalent adducts as described previously [80].

Statistical analysis. Data are presented as mean ± SD. Data were analyzed using SIGMASTAT (San Rafael, CA). Statistical comparisons between two groups were made using either the Student t-test (parametric method) for normalized data or Friedman's rank sum test (nonparametric method) for the data which did not pass the normality test. For comparisons between more than two groups, ANOVA and the Holm-Sidak method for multiple pairwise comparisons was used. A p value <0.05 was accepted as significant.

2.3.3 Results

DDS- and SMX-Dependent Protein Haptenation in the Presence and Absence of Peroxidase Inhibitors in NHEK. We have previously observed that DDS- and SMX-dependent protein haptenation is dose-dependent [115]. Various oxidizing enzymes including cytochromes P450, COX, FMOs and PRXs might play an important role in the bioactivation of these drugs in NHEK. In our previous studies, we found that cytochrome P450s and COX do not play major role in the bioactivation of these drugs in NHEK, which led to the focus in this study on the role of PRXs and FMOs in mediating the bioactivation leading to protein haptenation. In order to determine the role of PRX-mediated bioactivation of DDS and SMX, the effect of the PRX inhibitors ABH and KCZ [146, 147] on protein haptenation in NHEK exposed to DDS was evaluated by both confocal microscopy and ELISA. ABH has been generally used for MPO inhibition, but as a hydrazide inhibitor, it also inhibits non-specific PRXs [148, 149]. KCZ, though usually utilized for CYP3A inhibition, has also been reported to inhibit PRXs [146].

For each inhibitor, we utilized the highest inhibitor concentration that did not cause NHEK cytotoxicity. As shown in Figure 2.13 A and B, ABH and KCZ reduced DDS-dependent protein haptenation in NHEK cells by 35 to 45% and 16 to 24%, respectively.

ABH and MMZ caused similar reductions in SMX-dependent protein haptenation (data not shown). Similar results were obtained when inhibitors were added simultaneously with SMX or DDS and incubated for 3 h (data not shown).

Presence of Peroxidases in NHEK. Reduction of covalent adduct formation by PRX inhibitors ABH and KCZ suggested the presence of PRXs in NHEK. To further explore the presence of PRX activity in NHEK, we utilized the Amplex red reagent for measurement of PRX activity. In the presence of H_2O_2, the Amplex red reagent reacts with PRXs to produce the red-fluorescent oxidation product, resorufin, which has absorption and fluorescence emission maxima of approximately 571 nm and 585 nm, respectively. As shown in Figure 2.14, fluorescence increased with increasing amount of NHEK cell lysate, confirming the presence of PRX activity in these cells.

Horse radish peroxidase (HRP; 100 μU) was used as a positive control for activity and the ability of ABH (5 mM) to inhibit HRP confirmed the ability of ABH to inhibit PRXs (Figure 2.14). The presence of PRXs in NHEK was also demonstrated by the DAB assay, which gave rise to the brown precipitate expected from the oxidation of DAB (data not shown).

MPO in NHEK. The reduction in protein haptenation by the PRX inhibitors, ABH and KCZ, together with the presence of PRX activity in NHEK, suggested a

role for PRXs in DDS and SMX bioactivation. As MPO has been shown to bioactivate arylamines to their hydroxylamine metabolites [68], we probed for the presence of MPO in NHEK. Immunoblot analysis (Figure 2.15) failed to detect the presence of MPO. In contrast, MPO was readily detected in a myeloid cell line known to express this PRX.

The band in NHEK that co-migrated with a band in pure MPO is believed to be that of degradation products due to the heat treatment of these samples. Thus, to probe further for the presence of MPO, we also used RT-PCR amplification and were unable to observe MPO mRNA in NHEK (data not shown). In addition, we also failed to find evidence of MPO-like activity in NHEK using the chlorination assay (data not shown).

LPO in NHEK. The absence of MPO suggested other PRXs may be responsible for DDS and SMX bioactivation. As LPO also has been shown to oxidize arylamines to their nitroso metabolites [150], we sought to determine the presence of LPO in NHEK. LPO mRNA was readily detected in human salivary glands by RT-PCR amplification (positive control), but was non-detectable in NHEK. The human embryonic kidney (HEK) cells also showed the absence of LPO mRNA (negative control) (Figure 2.16).

TPO in NHEK. The absence of MPO and LPO lead us to assess whether or not TPO was present in NHEK. TPO has been shown to oxidize SMX to SMX-NOH [151]. Thus, we probed the presence of TPO in NHEK by immunoblot analysis. TPO was absent in NHEK. Using purified TPO as a positive control, the expected signal at 105 kDa was observed, along with another less intense

band at 35 kDa. Neither protein was present in NHEK lysates from three separate patient samples (data not shown).

DDS- and SMX-Dependent Protein Haptenation in the Presence and Absence of FMO Inhibitors in NHEK. The effect of MMZ as a prototypical FMO substrate was used to probe the potential role of this enzyme family on SMX- and/or DDS-dependent protein haptenation in NHEK. The highest concentration of MMZ that did not cause cytotoxicity in NHEK was used. As shown in Figure 2.17, MMZ reduced the DDS- and SMX-dependent protein haptenation by 40-50% in NHEK cells when measured by ELISA.

Similar results were obtained when MMZ was added simultaneously with SMX or DDS and incubated for 3 h (data not shown). Moreover, using confocal microscopy to detect haptenated proteins (as opposed to ELISA) yielded similar results (data not shown).

DDS- and SMX-Dependent Adduct Formation Catalyzed by Human Recombinant FMO3 and FMO1. To further elucidate the possible role of FMO in metabolizing these drugs, we studied the *in vitro* bioactivation of DDS and SMX with recombinant FMO enzymes. Both recombinant FMO3 and FMO1 were able to bioactivate DDS and SMX, as shown by the formation of covalent adducts detected by ELISA (Figure 2.18). Incubation of DDS with FMO3 showed higher adduct formation compared to FMO1. Heat inactivation of recombinant FMO3 and FMO1 reduced adduct formation by 53 to 60% and 40 to 46%, respectively, compared to non-inactivated enzyme.

Despite heat inactivation, significant absorbance was observed. This may be due to incomplete inactivation of the enzymes or non-specific binding of the antisera to the recombinant proteins. Alternatively, there may be some level of chemical-mediated oxidation of DDS that results in protein haptenation in the absence of enzyme activity. Preliminary studies have shown this latter effect occurs to a low degree with BSA (Farley M, Roychowdhury S, Vyas PM, and Svensson CK; personal communication). Significantly, no inhibition of FMO1 or FMO3 catalyzed DDS-dependent protein haptenation was observed when co-incubated with ABH. The optical density representing the protein haptenation of DDS by recombinant FMO3 or FMO1 was 2.83 (±0.18) and 0.54(±0.11), respectively; while the same incubations in the presence of ABH exhibited an optical density of 2.84(±0.11) for FMO3 and 0.55(±0.14) for FMO1.

Analysis of FMO in NHEK. Immunoblot analysis was used to determine the presence of FMO1 and FMO3 in NHEK. Other FMOs were not evaluated as FMO3 and FMO1 are the major FMOs which play a role in the oxidation of various xenobiotics [152]. As shown in Figure 2.19, FMO3 was readily detected, while FMO1 was undetectable in NHEK cells.

Thus, it appears that only FMO3 is involved in the observed bioactivation of DDS and SMX to their respective hydroxylamine metabolites in human keratinocytes.

D-NOH Dependent Adduct Formation in Presence of a PRX Inhibitor and an FMO Competitive Substrate. Since the combination of MMZ and ABH were found to inhibit protein haptenation in NHEK to the same level as that seen with

either agent alone, we sought to determine if these compounds inhibited sequential steps in the bioactivation leading to protein haptenation. For this reason, we examined protein haptenation following D-NOH exposure in NHEK cells, in the presence or absence of MMZ or ABH. As shown in Figure 2.20, ABH was able to reduce the protein haptenation significantly when the cells were treated with D-NOH, indicating a role for PRXs in the conversion of D-NOH to D-NO. MMZ, however did not reduce the protein haptenation in NHEK exposed to D-NOH.

2.3.4 Discussion

Numerous xenobiotics have been reported to undergo bioactivation to reactive metabolites that cause cellular toxicity [153, 154]. Such metabolism to reactive intermediates mostly is mediated through enzymatic or chemical oxidation to form the toxic intermediates capable of binding cellular proteins to form covalent adducts [155]. Oxidation of SMX and DDS to their arylhydroxylamine and then subsequently to arylnitroso metabolites is believed to be a critical step in their ability to cause CDRs [88, 156]. Various hepatic enzymes, such as the cytochrome P450-dependent monooxygenases, cyclooxygenases and PRXs have been shown to be active in SMX and DDS metabolism [66, 69, 71, 72]. Though survival of reactive metabolites during transit from liver to skin has not been demonstrated, evidence suggests the presence of the hydroxylamine metabolites of these drugs in plasma and urine after therapeutic doses [66, 69, 157]. Importantly, the concentration of SMX in skin blisters of subjects receiving this drug achieve

82% of those observed in plasma [158]. Hence, it has been demonstrated that the parent compound readily penetrates to the epidermal layer of the skin.

We have proposed the bioactivation of such compounds in the epidermal layer of the skin, primarily in keratinocytes [136]. The ability of NHEK to metabolize DDS and SMX to their hydroxylamine metabolites with the subsequent formation of cellular protein covalent adducts is consistent with this hypothesis [115, 136]. Studies to identify the enzyme or enzymes responsible for DDS and SMX bioactivation in NHEK indicated that neither the CYP450-dependent monooxygenases nor cyclooxygenases are responsible for the observed bioactivation (see sub chapter 2.1 and 2.2). Thus, we sought to identify other enzymes that are known to oxidize arylamines and might be involved in the bioactivation process in keratinocytes.

PRXs have been shown to bioactivate arylamine drugs resulting in the formation of arylhydroxylamine metabolites [68, 71]. A potential role of PRXs in the bioactivation of DDS and SMX in NHEK was demonstrated by the ability of the general PRX inhibitors, ABH and KCZ [146, 147], to significantly reduce DDS-dependent protein haptenation in NHEK. While both MPO and LPO have been shown to specifically oxidize arylamine drugs to their arylhydroxylamine metabolites [68, 150], no data was found to support the presence of either enzyme in keratinocytes. Using both immunoblotting and RT-PCR amplification, we failed to find evidence for the expression of either MPO protein or mRNA in NHEK and MPO activity was not observed using a chlorination assay. In addition, we found no evidence for LPO mRNA in NHEK.

The lack of evidence for MPO or LPO expression in NHEK, in contrast to the evidence for both general PRX activity and SMX- and DDS-dependent protein haptenation, suggests that other peroxidases may be involved in SMX and DDS bioactivation in these cells. Importantly, TPO has been shown to oxidize SMX to its arylhydroxylamine metabolite *in vitro* [151]. This observation, together with evidence for the presence of hypothalamic-pituitary-thyroid axis related genes expressed in skin, suggests TPO may be a good candidate for the PRX-dependent bioactivation of these drugs in NHEK [159]. However, our results showing the absence of TPO in NHEK cells suggests the presence of other oxidizing enzymes which might be inhibited by ABH, play a role in the metabolism of these parent drugs.

Other bioactivating enzymes, such as FMOs, are important for the oxidization of arylamine drugs [160]. As previous studies have suggested the presence of FMOs in keratinocytes [75], we sought to determine the role of these enzymes in the bioactivation of SMX and DDS in NHEK. Using an FMO substrate, MMZ [161], we found a 40-50% reduction in the protein haptenation for both DDS and SMX. *In vitro* studies demonstrated that recombinant FMO1 and FMO3 can oxidize SMX and DDS, though incubation with FMO3 resulted in a higher level of protein haptenation. Immunoblot analysis confirmed the presence of FMO3 in these cells, while FMO1 was not detected. It is possible that the failure to detect this latter FMO is due to the use of low affinity antibodies. While FMO3 (and possibly other unidentified FMO's) seems to be responsible for this bioactivation, our results showing the inability of ABH to inhibit the observed

FMO3 activity (data not shown) and the percent inhibition observed with the various inhibitors, suggested that unidentified PRXs or oxidizing enzymes are responsible for between 30 and 40% of SMX and DDS bioactivation, while FMO3 is responsible for 50 to 60% of this activity in keratinocytes.

As we found that combined exposure of NHEK to MMZ and ABH was neither additive nor synergistic in its ability to inhibit protein haptenation upon exposure to SMX or DDS, we considered the potential that these compounds attenuated sequential steps in the formation of covalent adducts in NHEK. Upon formation, S-NOH and D-NOH can undergo autooxidation leading to their respective nitroso species. It is this latter species that is believed to be the penultimate metabolite for the haptenation of cellular proteins. Our demonstration that ABH but not MMZ attenuates protein haptenation in NHEK exposed to D-NOH suggests that PRXs enhance the oxidation of the arylhydroxylamine to the arylnitroso species (Figure 2.20A).

The results reported herein, together with our companion study, demonstrate that the relative role of various enzymes in the bioactivation of SMX and DDS differ in keratinocytes compared to liver. While CYP2C9 and CYP3A4 are important enzymes mediating the oxidation of these drugs in liver, they do not play a significant role in keratinocytes. Consistent with this conclusion, previous studies failed to demonstrate a clear association between variant *CYP2C9* alleles and the incidence of sulfonamide-induced CDRs [162].

Taken together, these data indicate that FMO3 plays an important role in the oxidation of arylamines in NHEK, while PRXs play an important role in the

subsequent formation of the arylnitroso species. As functional variant *FMO3* alleles have been identified [163], it will be important to determine if such variants influence the predisposition of individuals to sulfonamide-induced CDRs. Similarly, environmental and genetic factors that alter the expression of these enzymes should be probed for their potential role in altering the predisposition to these reactions.

Figure 2.13. DDS-dependent protein haptenation in NHEK in the presence of peroxidase inhibitors. NHEK were incubated for 3 h in the presence of vehicle (1% DMSO), 5 mM ABH, or 100 μM KCZ. After pre-incubation with inhibitors, cells were incubated for an additional 3 h with 250 μM DDS. A. Cells were immunostained followed by confocal imaging and fluorescence intensity of cells exposed to vehicle, DDS or DDS + inhibitors was determined by Image J software. Control represents NHEK incubated with vehicle (1% DMSO) alone. Data presented represent the mean ±SD fluorescence intensity of 9 replicates. B. Covalent adducts in cells exposed to vehicle, DDS, or DDS + inhibitors as determined by ELISA. Data represent the mean ±SD optical density of three different experiments having three replicates in each experiment. Data were analyzed statistically using ANOVA with the Holm-Sidak test for multiple pairwise comparisons. $^{*}p< 0.05$ compared to NHEK incubated with vehicle alone, $^{**}p < 0.05$ compared to NHEK incubated with vehicle and DDS, $^{***}p < 0.05$ compared to NHEK incubated with vehicle, DDS and DDS+KCZ.

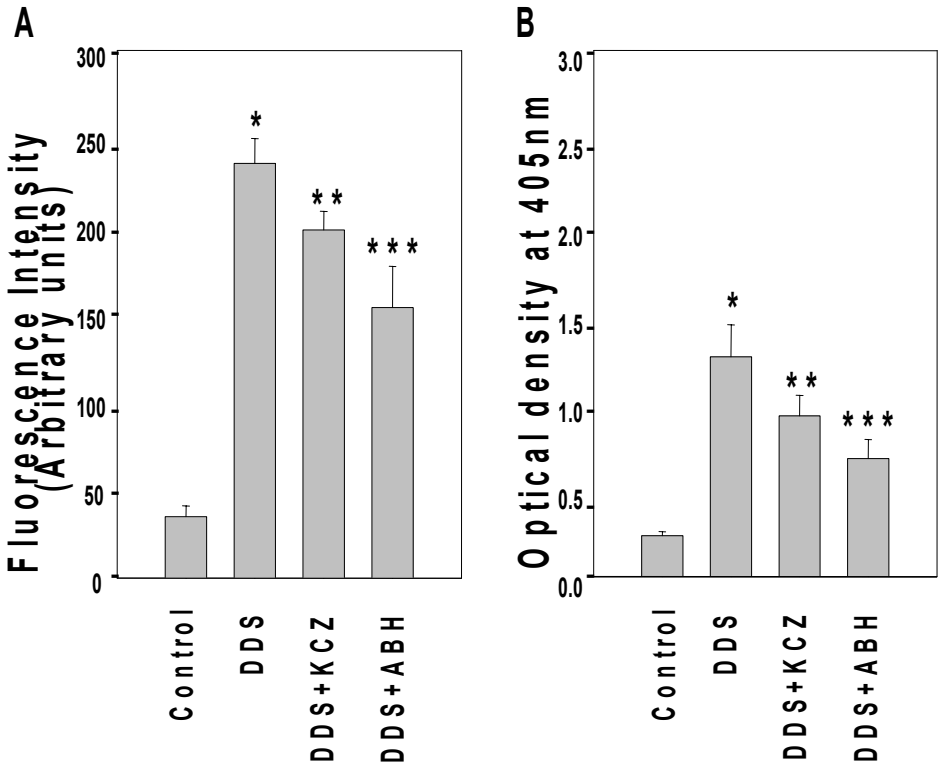
A
Fluorescence Intensity (Arbitrary units)
300
250
200
150
100
50
0
*
**
***
Control
DDS
DDS+KCZ
DDS+ABH
B
Optical density at 405nm
3.0
2.5
2.0
1.5
1.0
0.5
0.0
*
**
***
Control
DDS
DDS+KCZ
DDS+ABH

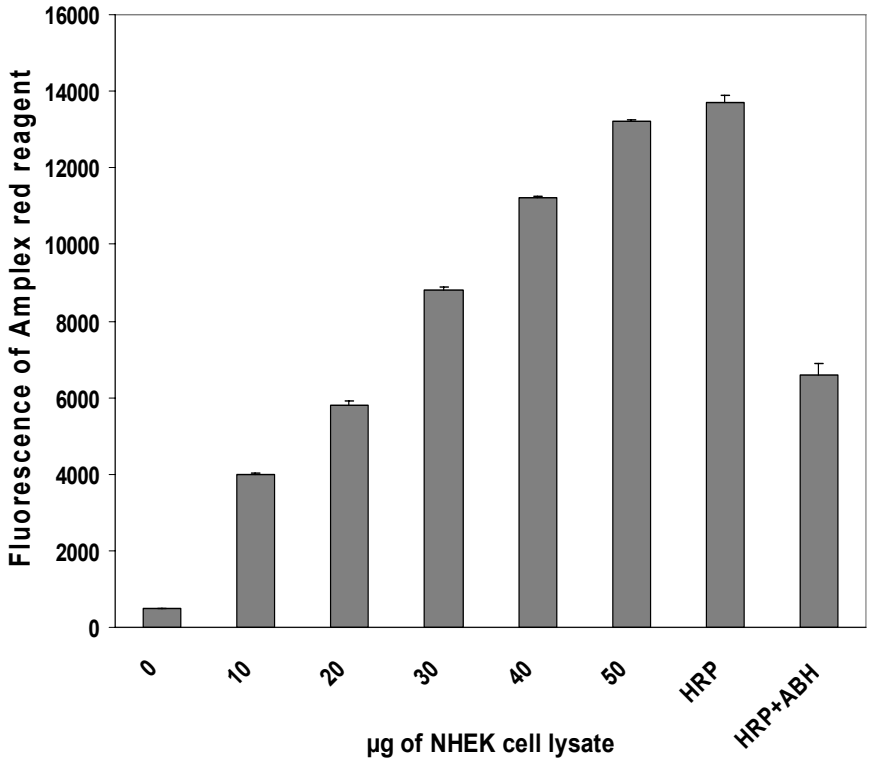

Figure 2.14. Presence of Peroxidases in NHEK. Various amounts of NHEK cell lysate supernatant fraction (10 µg – 50 µg) were mixed with 50 µM Amplex red reagent and 1 mM H_2O_2 in a microtiter plate. Following incubation in the dark for 1 h at room temperature, fluorescence was measured using an excitation wavelength of 530 nm and an emission wavelength of 580 nm. Data represent mean ±SD of 6 replicates.

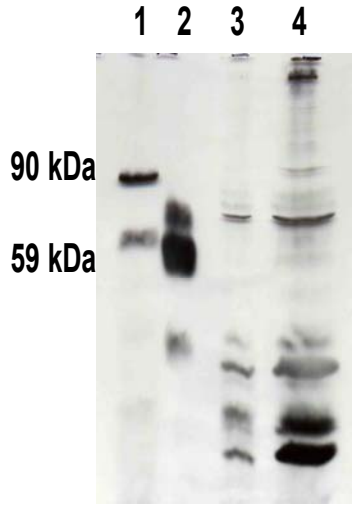

Figure 2.15. Immunoblot analysis for MPO protein expression in NHEK. Fourth passage NHEK cells were probed for MPO proteins using specific primary and secondary antibodies as described in Materials and Methods. Lane 1 represents cultured myeloid cell line as a positive control showing the presence of 90 kDa MPO precursor and 59 kDa MPO heavy subunit. Lane 2 represents pure MPO showing the presence of 59 kDa MPO heavy subunit. Lane 3 and Lane 4 represent 10^5 and 8 x 10^5 NHEK cells respectively in which MPO is absent.

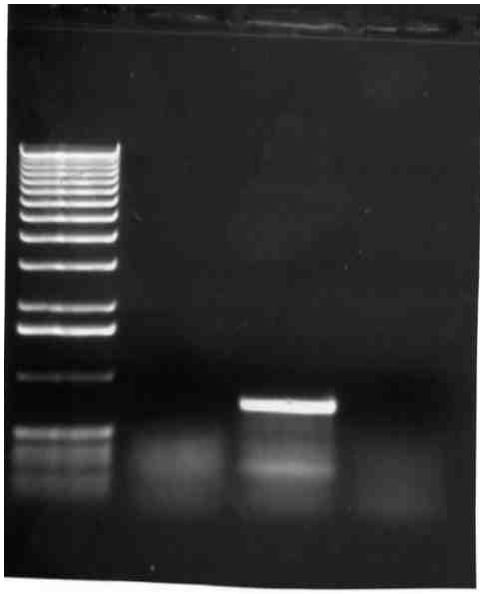

Figure 2.16. Northern blot analysis for LPO mRNA expression in NHEK. Fourth passage NHEK cells were probed for LPO mRNA expression as described in Materials and Methods. Human salivary gland was used as positive control. LPO mRNA was detected as a band at 744 bp. HEK cells were used as negative control.

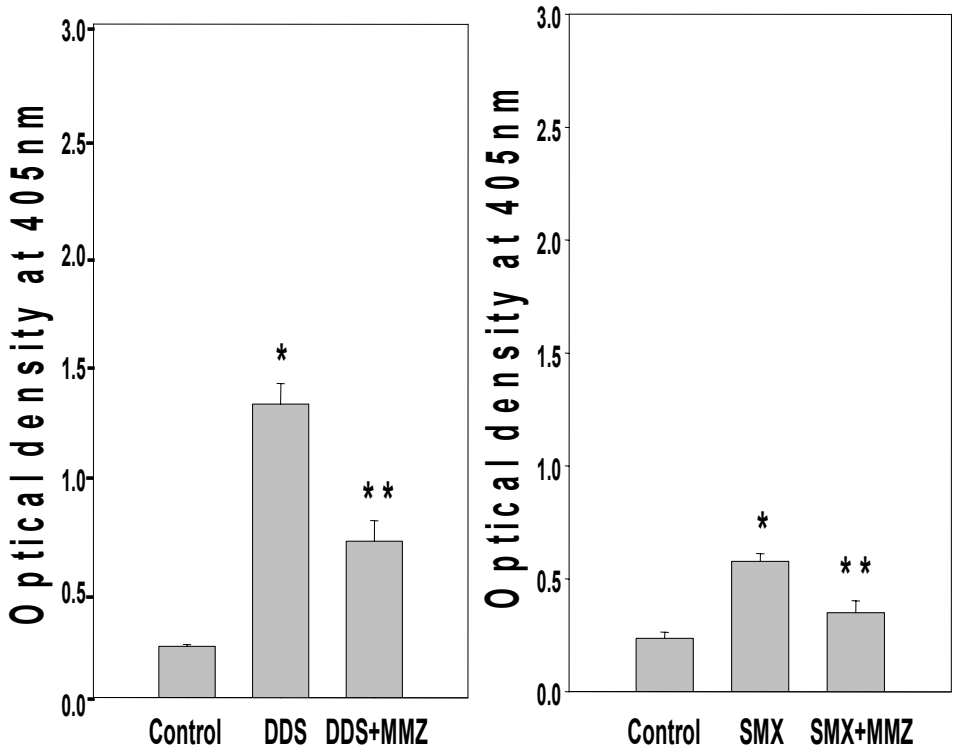

Figure 2.17. SMX- and DDS-dependent protein haptenation in NHEK in the presence of an FMO competitive substrate. NHEK were incubated for 3 h in the presence of vehicle (1% DMSO) or 5 mM methimazole (MMZ). After pre-incubation with inhibitor, cells were incubated for an additional 3 h with 250 μM DDS (A) or SMX (B). Covalent adducts were quantified using ELISA as described in Materials and Methods. Data represent the mean ±SD optical density of three different experiments with three replicates in each experiment. Data were compared using ANOVA with the Holm-Sidak test for multiple pairwise comparisons. $^{*}p< 0.05$ compared to NHEK incubated with vehicle alone, $^{**}p < 0.05$ compared to NHEK incubated with vehicle and DDS/SMX.

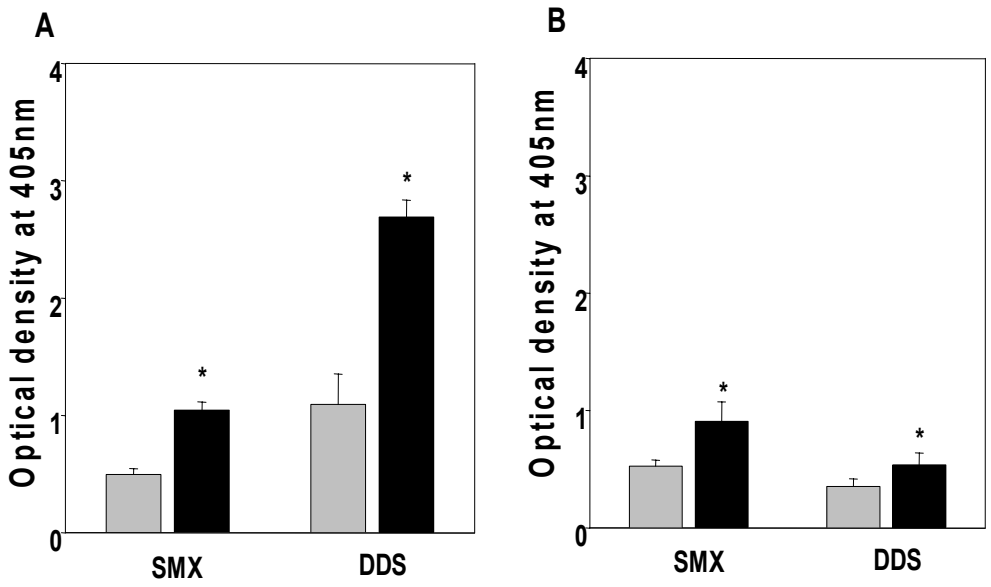

Figure 2.18. Human recombinant FMO mediated DDS and SMX adduct formation. Human recombinant FMO3 (represented in A) or FMO1 (represented in B) was incubated with DDS or SMX (100 μM) in an NADPH regenerating system for 1 h at 37°C as mentioned in Materials and Methods. Heat inactivated FMO3 and FMO1 were used as negative controls (represented by gray bars) versus activated FMO3 and FMO1 (represented by black bars). Covalent adducts were determined by an adduct-specific ELISA as described in Materials and Methods. Data represent mean ±SD of 6 replicates. $^{*}p< 0.05$ compared to the incubation containing heat inactivated FMO3 or FMO1.

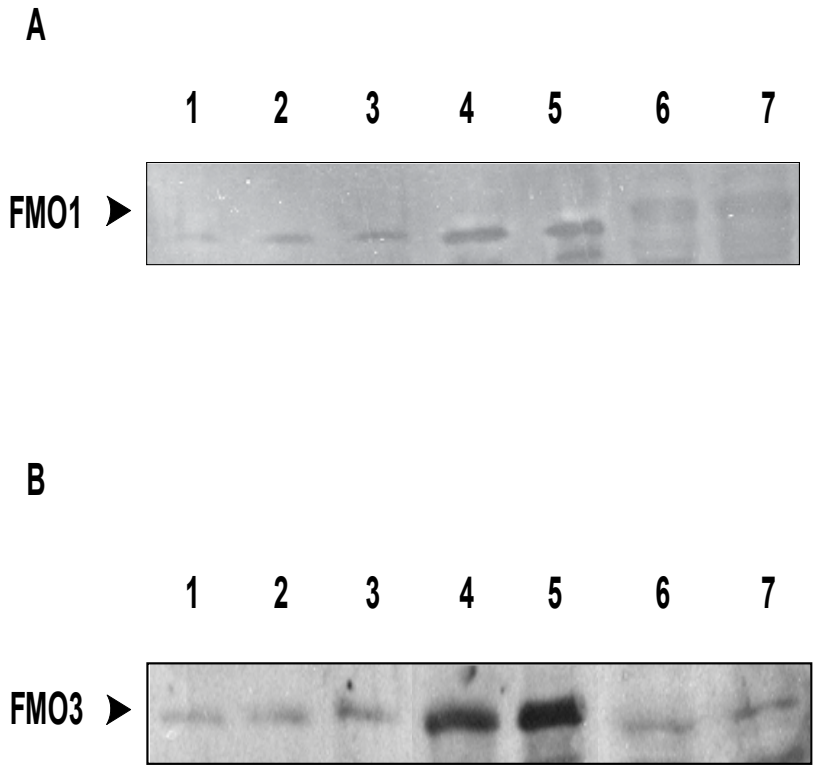

Figure 2.19. FMO3 and FMO1 protein expression in NHEK. Fourth passage NHEK cells were probed for FMO1 and FMO3 proteins using specific primary and secondary antibodies as described in Materials and Methods. A) FMO1 expression: Lane 1-5 represents 25, 100, 250, 350 and 500 fmol of baculovirus-expressed human FMO1 respectively, Lane 6 represents 40 µg and Lane 7 represents 60 µg of NHEK proteins. B) FMO3 expression: Lane 1-5 represents 50, 75, 100, 250 and 500 fmol of baculovirus-expressed human FMO3 respectively, Lane 6 represents 40 µg of NHEK and Lane 7 represents the 60 µg of NHEK proteins.

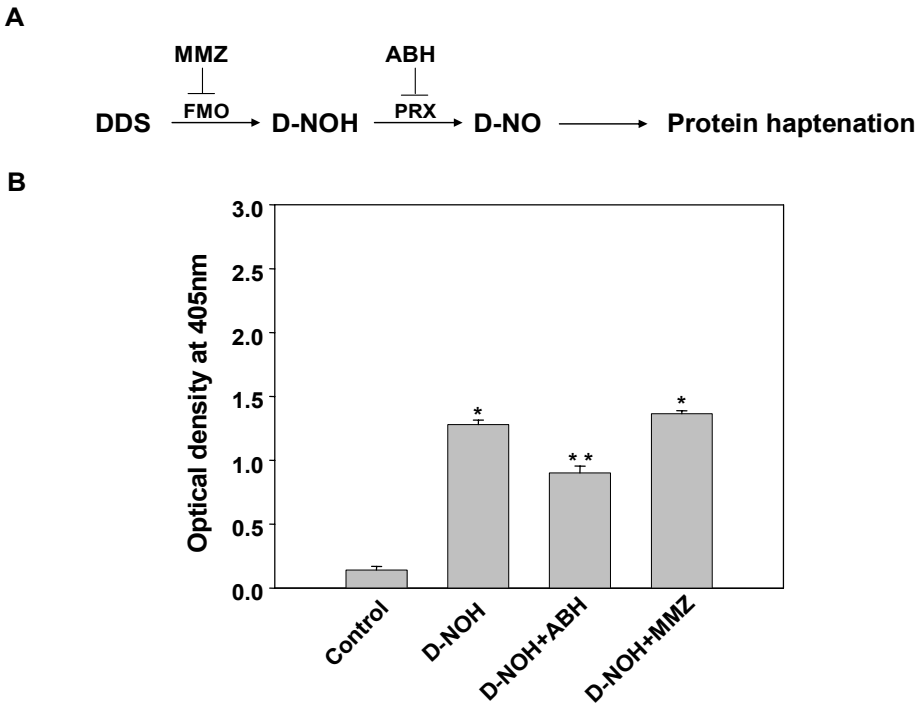

Figure 2.20. D-NOH dependent protein haptenation in NHEK to determine the sequential bioactivation of DDS to D-NO. A. Scheme representing the sequential bioactivation of DDS to D-NO leading to protein haptenation. B. D-NOH dependent protein haptenation in NHEK in the presence of a PRX inhibitor and an FMO competitive substrate. NHEK were incubated with 100 μM D-NOH for 3 h in the presence of 5 mM ABH or 5 mM MMZ. Covalent adducts in cells exposed to vehicle (1% DMSO), D-NOH, or D-NOH + inhibitors were determined by adduct specific ELISA as mentioned in Methods. Data represent the mean ±SD optical density of 6 replicates. Data were analyzed statistically using ANOVA with the Holm-Sidak test for multiple pairwise comparisons. $^{*}p< 0.05$ compared to NHEK incubated with vehicle alone, $^{**}p < 0.05$ compared to NHEK incubated with vehicle, D-NOH and D-NOH+MMZ.

CHAPTER THREE

DETERMINATION OF THE ROLE OF REACTIVE OXYGEN SPECIES (ROS) GENERATION BY THE HYDROXYLAMINE METABOLITES OF SMX AND DDS LEADING TO CELL DEATH *.

3.1 Introduction

Sulfamethoxazole (SMX) is an effective therapeutic agent in the treatment of *Pneumocystis carinii* pneumonia (PCP), resulting in the recovery of approximately 75% of patients suffering from this ailment[164, 165]. Dapsone (DDS) is a useful alternative treatment for PCP, used either alone or in combination with other agents, in patients that cannot tolerate SMX[166-168]. Introduction of the use of these agents for the treatment of PCP in patients infected with the human immunodeficiency virus (HIV) was associated with a high level of adverse reactions, including delayed type hypersensitivity reactions[169-173]. Numerous studies have suggested that these idiosyncratic reactions result from the bioactivation of these agents to arylhydroxylamine metabolites[174-176].

The *in vitro* cytotoxicity of arylhydroxylamine metabolites of SMX (SMX-NOH) and DDS (DDS-NOH) towards peripheral blood mononuclear cells (PBMCs) has been proposed as a marker for delayed-type hypersensitivity reactions associated with these drugs[55, 177, 178]. Although SMX-NOH and DDS-NOH both cause concentration-dependent increases in cell death, DDS-NOH is

---

* Note: Published as: Vyas PM, Roychowdhury S, Woster PM, Svensson CK. Reactive oxygen species generation and its role in the differential cytotoxicity of the arylhydroxylamine metabolites of sulfamethoxazole and dapsone in normal human epidermal keratinocytes. *Biochemical Pharmacology* 70: 275-286, 2005.

significantly more toxic[179]. The *in vitro* cytotoxicity in human PBMCs exhibits an LC_{50} of 325 μM for DDS-NOH and 1752 μM for SMX-NOH. Studies in normal human epidermal keratinocytes (NHEK) demonstrate an LC_{50} of 293 μM for DDS-NOH and LC_{50} of greater than 1500 μM for SMX-NOH [180]. We have recently observed similar differences in the cytotoxicity of these two arylhydroxylamines in normal human dermal fibroblasts[181]. Differential toxicity is also observed with methemoglobin formation *in vitro*, with an EC_{50} of 26.5 μM for DDS-NOH and of 463 μM for SMX-NOH in human red blood cells[182].

Since exposure of cells to SMX-NOH and DDS-NOH have been shown to cause a significant depletion of the major cellular antioxidant (glutathione)[136], ROS accumulation following metabolite exposure may play a causal role in the cytotoxicity observed with these compounds. As other xenobiotics have been shown to be cytotoxic due to their ability to generate reactive oxygen species (ROS)[183-186], we hypothesized that the differential cytotoxicity of DDS-NOH and SMX-NOH may be due to differences in their ability to induce ROS. Arylhydroxylamines such as SMX-NOH and DDS-NOH autooxidize to their respective nitroso compounds (Fig. 3.1).

During this autooxidation, molecular oxygen reduces to superoxide, which is subsequently reduced to hydrogen peroxide (H_2O_2) either spontaneously or catalyzed by superoxide dismutase (SOD). The formed H_2O_2 undergoes the Fenton reaction to form highly cytotoxic hydroxide radicals[187, 188].

We hypothesized that ROS formation is directly correlated to the presence of hydroxylamine (NHOH) functional groups in the molecule. Thus, compounds

having the potential to form two NHOH functional groups may generate a higher level of intracellular ROS. As DDS has two primary amine groups in its molecular structure, while SMX has only one, the former has the *potential* to give rise to a metabolite with two hydroxylamines (Fig. 3.2).

Thus, to probe the proposed hypothesis, in addition to SMX-NOH and DDS-NOH, we synthesized three hydroxylamine metabolites/analogues of DDS: DDS-dihydroxylamine (DDS-diNOH), 4-nitrophenyl-p-tolyl sulfone hydroxylamine (NPTS-NOH) and monoacetyl dapsone hydroxylamine (MADDS-NOH) (Fig. 3.3).

The cytotoxicity and ability to form ROS was then determined for each of these compounds.

3.2 Materials and Methods

Materials. Chemicals for synthesis, including 4-nitrobenzene sulfonyl chloride, 3-amino-5-methyl-isoxazole, 4-(4-nitrophenyl sulfonyl)-aniline, 4-nitrophenylsulfone, 4-nitrophenyl-p-tolylsulfone (NPTS), 4-acetamidophenyl-4'-nitrophenyl sulfone, triethyl phosphite, and platinum oxide, were obtained from Sigma-Aldrich (St. Louis, MO). Rabbit anti-sera were raised against SMX- and DDS-keyhole limpet hemocyanine conjugates and characterized as described previously[180]. Microtiter ELISA plates (96 well) were obtained from Rainin Instruments (Woburn, MA). Goat anti-rabbit antibody conjugated with alkaline phosphatase was purchased from Molecular Probes (Eugene, OR), as was the fluorescent dye Yo-Yo-1. Bradford assay reagent was purchased from PIERCE (Rockford, IL). Trolox was obtained from Oxis International Inc. (Portland, OR).

All other chemicals were purchased from Sigma-Aldrich (St. Louis, MO) or Fisher Scientific (Chicago, IL).

Synthesis of arylhydroxylamine metabolites of SMX and DDS. SMX-NOH and DDS-NOH were synthesized as described previously, with modifications to the purification methods[177, 179, 189]. Briefly, 4-nitrobenzene sulfonyl chloride (4-NSC, 1 mole) was mixed with 3-amino-5-methyl-isoxazole (3-A-5-MI, 1 mole) to obtain the nitro derivative of SMX (Nitro-SMX) which was recrystallized with ethyl acetate and toluene (1:1). Nitro-SMX (4 mmoles) was reduced to SMX-NOH using triethyl phosphate (60 µl) and platinum oxide (12 mg) in a hydrogenator at 40 psi for 4 hr. The synthesized SMX-NOH was purified by preparative TLC using hexane:chloroform:methanol (25:69:6). For synthesis of DDS-NOH, 4-(4-Nitrophenyl sulfonyl)-aniline (NPSA, 7.12 mmoles) was reduced as described above. For purification, DDS-NOH was dissolved in water:ethyl acetate (50:50) and the mixture acidified by hydrochloric acid in a separatory funnel. The acidified water layer containing pure DDS-NOH was separated and then neutralized by addition of sodium carbonate. DDS-NOH was then extracted in ethyl acetate from the water layer and evaporated to dryness to obtain a light yellow solid compound.

For the synthesis of DDS-diNOH, NPTS-NOH and MADDS-NOH, 4 mmoles of 4-nitrophenylsulfone, 4-nitrophenyl-p-tolylsulfone (NPTS) and 4-acetamidophenyl-4'-nitrophenyl sulfone were reduced using triethyl phosphite (60 µl) and platinum oxide (12 mg) as a reducing agent in a hydrogenator. The purity and identity of all metabolites was confirmed by NMR, MS and HPLC techniques.

Cell culture. Adult normal human epithelial keratinocytes (NHEK) (as 1st passage cells), keratinocyte culture media, trypsin, and trypsin neutralizing solution were obtained from CAMBREX (Walkersville, MD). NHEK were grown as we have described previously[180]. Briefly, cells were cultured in 75 cm^2 flasks using keratinocyte basal media (KBM-2) supplemented with bovine pituitary extract (7.5 mg/ml), human epidermal growth factors (0.1 ng/ml), insulin (5 µg/ml), hydrocortisone (0.5 µg/ml), epinephrine, transferrin, gentamicin (50 µg/ml) and amphotericin (50 ng/ml) at 37°C in an atmosphere containing 5% CO_2. Media was replaced every 2-3 days. When cell cultures reached near confluency (70-90%), cells were disaggregated using 0.025% Trypsin/0.01% EDTA in HEPES followed by neutralization with 2 volumes of Trypsin neutralizing solution. Cell suspension was then centrifuged, followed by washing in basal media and re-suspension in KGM-2 (Supplemented growth medium). Cells were then either subjected to sub-culturing or cryo-preservation for later experiments. All experiments were performed using 3rd to 4th passage cells.

Determination of ROS formation. To investigate the differential oxidative stress induced by these arylhydroxylamine metabolites, ROS formation was determined in a cell free system or in NHEK cells using the fluorescent dye 2'-7'-dichlorodihydrofluorescein diacetate (DCHF-DA)[190-192]. For the cell free assay, 2.5 µM of metabolite or parent drug were dissolved in dimethyl sulfoxide (DMSO) and incubated either in sodium phosphate buffer (9.5 mM, pH 7.4) or sodium phosphate buffer containing hydrogen peroxide (H_2O_2, 100 µM) and peroxidase (0.02 U/ml) at room temperature; followed by addition of 2',7'-

dichlorodihydrofluorescein (DCHF) (5 μM). The DCHF used for the cell free assay was obtained by alkaline hydrolysis of DCHF-DA[190]. For the complete hydrolysis of DCHF-DA, 5 μM of DCHF-DA was dissolved in DMSO and incubated with 200 μM of sodium hydroxide (NaOH) for 30 min on ice in a dark cabinet. At the completion of the incubation period, 250 μM of sodium dihydrogen phosphate (NaH_2PO_4) was added to the reaction mixture. Ten μl of this DCHF reaction mixture was added to the final assay volume of 200 μl in 96 well plates. The total concentration of DMSO was not more than 1% v/v in the final assay. ROS formation was measured by the oxidation of DCHF to 2', 7'-dichlorofluorescein (DCF), producing fluorescence which was measured every 5 min for 30 min using a multiwell fluorescence plate reader (Cytofluor®) with an excitation wavelength of 480 nm and emission wavelength of 530 nm. The rate of change in DCF fluorescence was also calculated for these incubations by determining the rate of increase in fluorescence per min over the 30 min period from a plot of fluorescence versus time.

Metabolite-induced ROS formation in NHEK was determined by adding 10^5 cells to each well of a 96 well plate and incubating in 200 μl of KBM-2 media at 37˚C, 5% CO_2 for 24 hr. After 24 hr, KBM-2 was replaced by 200 μl PBS (10 mM) (PBS composition - 0.8% NaCl, 0.02% KCl, 0.01% $MgCl_2.6H_2O$, 0.02% KH_2PO_4, 0.114% Na_2HPO_4, 0.01% $CaCl_2.2H_2O$, pH 7.4). ROS formation was measured in two different conditions. First (designated as preloaded), cells were pre-loaded with DCHF-DA (20μM) and after 30 min the plate was washed to discard extracellular DCHF-DA, followed by the addition of 500 μM of metabolite

or parent drug dissolved in DMSO. Alternatively, 500 μM of metabolite or parent drug were added to the cells followed by the addition of 20 μM DCHF-DA (designated as postloaded). DCF fluorescence was measured as described above.

Effect of ROS scavengers on metabolite-induced ROS formation. The effect of melatonin, Trolox, ascorbic acid, and N-acetylcysteine (NAC) on the ROS formation induced by these metabolites was determined in NHEK. Briefly, 10^5 cells were plated as mentioned above. After 24 hr, melatonin, Trolox, ascorbic acid or NAC (1 mM) were added to cells and the plate was incubated for 1 hr at 37^{o}C prior to addition of metabolites (500 μM) and DCHF-DA (20 μM). DCF fluorescence was determined as previously described. Similarly, the effect of these antioxidants in a cell free system were evaluated using the cell free system described previously.

Cytotoxicity of arylhydroxylamine metabolites and analogues. To assess the relationship between ROS generation and cytotoxicity of these arylhydroxylamines, the cytotoxicity of analogues towards NHEK was compared at an equimolar concentration (500 μM). In addition, the effect of ascorbic acid as an antioxidant on the cytotoxicity was evaluated. Cytotoxicity was determined using an impermeable DNA binding dye, as we have described previously[180]. Briefly, 10^5 NHEK cells were plated on 96-well plates and incubated overnight in 200 μl of KGM-2 media at 37˚C, 5% CO_2. After 24 hr, KGM-2 was replaced by KBM-2 and 1 mM ascorbic acid or vehicle and the plate incubated for 3 hr. After this pre-incubation period, 500 μM of metabolite or parent drug was added and

cells were incubated for an additional 3 hr. After 3 hr incubation with metabolites, the plate was washed once with KBM-2 followed by the addition of fresh KBM-2 containing 4 μM of Yo-Yo-1. Fluorescence was measured for 16 hr in a temperature controlled fluorescent plate reader as described above. After 16 hr, Triton-X (0.1%) was added to all wells and a final reading was taken after a further incubation of 3 hr (total incubation time was 19 hr). The cytotoxicity was determined using the following formula:

$$\% \text{ cell death} = \frac{(\text{Yo-Yo fluorescence})_{16hrs} - (\text{Yo-Yo fluorescence})_{0hrs}}{(\text{Yo-Yo fluorescence})_{19hrs} - (\text{Yo-Yo fluorescence})_{0hrs}} \times 100$$

Adduct formation by arylhydroxylamine metabolites in NHEK with and without ROS scavenger. Formation of metabolite-protein adducts in NHEK following incubation with arylhydroxylamine metabolite in the presence or absence of 1 mM of ascorbic acid was determined as previously described[180]. Briefly, NHEK cells (1 X 10^6 cells) were cultured for 24 hr in 50 ml centrifuge tubes containing 10 ml of KGM-2. Cells were then incubated for 3 hr in the presence or absence of 1 mM ascorbic acid prior to the addition of metabolite (50 μM). After 24 hr, tubes were centrifuged at 220 g for 5 min to pellet the cells. The supernatant containing the medium was drained off and cell pellets were lysed in 1 ml of deionized water, using repeated cycles of freezing and thawing (3 times) and ultrasonication, to ensure complete lysis. The cell suspension was then thoroughly vortexed and centrifuged at 220 *g* for 5 min and the pellet containing the cell debris discarded. The supernatant containing cellular soluble proteins was collected for protein assay and subsequent ELISA.

ELISA analysis for detection of covalent adduct formation was performed as described previously[180], with minor modifications. Following protein content measurement using the Bradford reagent kit, all samples were diluted to contain 250 μg/ml protein. An aliquot of 100 μl was adsorbed onto 96 well polystyrene microtiter plates for 16 hr at 4°C. Wells were washed three times using Tris-casein buffer (0.5% casein, 0.9% NaCl, 0.01% Thimerosal, 10 mM Tris-HCl, pH 7.6) and then blocked with Tris-casein buffer for 1 hr. After an additional wash, wells were incubated for 16 hr at 4°C with 100 μl of anti-SMX or anti-DDS rabbit serum (1:500 diluted with Tris-casein buffer). Wells were subsequently washed 4 times with Tris-casein buffer and incubated with alkaline phosphatase conjugated goat anti-rabbit antibody (1:1000 diluted in Tris-casein buffer) for 2 hr at room temperature. After washing 4 times with Tris-casein buffer, antibody binding was detected with colorimetric alkaline phosphate substrate reagent. After 1 hr of incubation at room temperature, optical density was measured at 405 nm using a V_{max} kinetic micro plate reader (Molecular Devices).

Statistical analysis. Data is presented as mean (SD). Data were analyzed using the Friedman rank sum test or ANOVA with the Holm-Sidak test for multiple comparisons, as appropriate. A value of $p < 0.05$ was considered significant.

3.3 Results

Synthesis of arylhydroxylamine metabolites of SMX and DDS. The product yield for Nitro-SMX, SMX-NOH and DDS-NOH were 95%, 79% and 78%, whereas the determined purities were 99%, 89% and 88%, respectively. As the

obtained purities for SMX-NOH and DDS-NOH were not optimal for biological use, metabolites were further purified using preparative TLC and acidified extraction methods to obtain a purity of greater than 98% for both metabolites. Synthesized DDS-diNOH, NPTS-NOH and MADDS-NOH were found to have yields of 83%, 93% and 85%, with purities of 96%, 99% and 97%, respectively.

ROS generation by arylhydroxylamine metabolites and analogues. In a cell free system, ROS generation was increased by all arylhydroxylamines (Fig. 3.4). The DCF fluorescence in the presence of SMX-NOH, DDS-NOH, DDS-diNOH, NPTS-NOH or MADDS-NOH was increased by 80, 365, 144, 355 and 395%, respectively, as compared to control. All DDS metabolites/analogues exhibited a higher level of ROS generation than SMX-NOH. DCF fluorescence was not increased in incubations containing the parent compounds. The rate of change in fluorescence for each metabolite (which was found to be linear over the 30 min incubation period) was consistent with the cumulative fluorescence observed at 30 min (Fig. 3.5).

To more closely mimic the intracellular conditions and to increase the catalytic cycle for the redox reaction of the oxidation of the arylhydroxylamine metabolites, while at the same time avoiding variability that might arise due to permeability differences in the metabolites, metabolites were also incubated in sodium phosphate buffer with hydrogen peroxide and peroxidase. As expected, in the presence of peroxidase/H_2O_2, the basal level of ROS generation was considerably higher than that observed in buffer alone. The ROS generation by SMX-NOH, DDS-NOH, DDS-diNOH, NPTS-NOH and MADDS-NOH was

increased by 55, 135, 75, 165 and 150%, respectively, as compared to control (Fig. 3.6).

While the absolute DCF fluorescence in the presence of peroxidase/H_2O_2 was markedly elevated compared to the results in the absence of peroxidase/H_2O_2 (Fig. 3.4), the rank order of ROS generation between metabolites was the same.

In NHEK, ROS formation in the presence of the various arylhydroxylamines at a concentration of 2.5 μM was not different from NHEK incubated with vehicle alone (data not shown), which is likely due to the high level of antioxidants in these cells (e.g., glutathione and ascorbic acid). Evaluation of a range of concentrations of SMX-NOH and DDS-NOH (5, 50 and 500 μM) showed that at a concentration of 500 μM, DDS-NOH formed a substantially higher amount (4.5 fold) of ROS (1079% increase as compared to control) compared to 500 μM of SMX-NOH (237% increase as compared to control). At lower concentrations, 5 μM and 50 μM, there was no significant difference in ROS formation between DDS-NOH and SMX-NOH (Fig. 3.7).

When each of the arylhydroxylamines was added to NHEK at a concentration of 500 μM, all metabolites/analogues of DDS induced a similar level of ROS, which was at least two-fold higher than that induced by SMX-NOH (Fig. 3.8).

Importantly, at the concentrations examined, none of the metabolites induced significant cell death within the 30 min time frame of ROS generation assessment (data not shown). Though DDS-diNOH consistently resulted in a

lower level of ROS generation than other metabolites/analogues of DDS in a cell free system, it induced a similar level of ROS in NHEK. While the ROS measured was slightly higher using postloaded DCHF than preloaded DCHF, the pattern between metabolites was similar in both paradigms.

Effect of various ROS scavengers on ROS formation by SMX-NOH and DDS-NOH in NHEK. To further probe the role of ROS generation in the differential cytotoxicity of SMX-NOH and DDS-NOH, we assessed the ability of various antioxidants to suppress the generation of ROS induced by arylhydroxylamine metabolites (Fig. 3.9).

The reduction in DDS-NOH and SMX-NOH induced ROS generation in NHEK with Trolox was found to be 44 and 43%, respectively. In contrast, melatonin did not reduce ROS generation compared to incubation of either metabolite alone. Ascorbic acid reduced DDS-NOH- and SMX-NOH-induced ROS generation by 87 and 69%, respectively. NAC was also found to markedly attenuate arylhydroxylamine-induced ROS generation. The effect of these antioxidants on ROS generation in a cell free system paralleled that observed in NHEK (data not shown).

Cytotoxicity of hydroxylamine metabolites. Cytotoxicity of the compounds toward NHEK was evaluated in presence and absence of ascorbic acid (Fig. 3.10).

As previously observed, DDS-NOH was found to cause a higher level of cell death compared to SMX-NOH at an equimolar concentration (500 μM). Among the other arylhydroxylamine analogues of DDS, NPTS-NOH was found to

be highly toxic compared to all other arylhydroxylamine metabolites evaluated. Ascorbic acid attenuated, but did not completely block, the cytotoxicity of DDS-NOH and NPTS-NOH towards NHEK. Interestingly, neither MADDS-NOH or DDS-diNOH was cytotoxic at this concentration.

Adduct formation by arylhydroxylamine metabolites in NHEK with and without ROS scavenger. Compared with SMX-NOH, DDS-NOH formed a higher amount of metabolite-protein adduct when incubated with NHEK (Fig. 3.11).

Ascorbic acid significantly reduced, but did not prevent, the adduct formation for both of these hydroxylamine metabolites in NHEK cells.

3.4 Discussion

As several studies have suggested that the *in vitro* cytotoxicity of the arylhydroxylamine metabolites of sulfonamides may serve as an indicator of predisposition to hypersensitivity reactions to these compounds[55, 193, 194], it is of interest to note that DDS-NOH has consistently been found to be more cytotoxic *in vitro* than SMX-NOH in cells from normal subjects and those with a history of hypersensitivity to sulfonamides[179, 195]. Importantly, the limited number of direct comparisons have found that SMX is associated with a higher frequency of hypersensitivity reactions than DDS[168, 196, 197]. The basis for the differential cytotoxicity between metabolites is unclear. Studies comparing the methemoglobin forming ability of these two arylhydroxylamines in purified hemoglobin suggest that DDS-NOH more readily oxidizes to reactive species[182]. Hence, we postulated that differences in ROS generation between the metabolites may explain the observed differences in cytotoxicity.

As shown in Fig. 3.2, both SMX and DDS possess arylamine functional groups that are capable of undergoing catalytic oxidation to the corresponding arylhydroxylamine; both of which have been confirmed as metabolites in man after administration of the respective parent compound[60, 198-202]. In contrast to SMX, DDS possesses a second arylamine group that may undergo oxidation to yield a di-arylhydroxylamine. As some cells (e.g., NHEK) in which DDS-NOH has been shown to exhibit a higher level of cytotoxicity have been demonstrated to be capable of bioactivating SMX and DDS to their respective arylhydroxylamine metabolites, the potential exists for further oxidation of DDS-NOH to its di-arylhydroxylamine. As such a metabolite would possess two functional groups capable of giving rise to ROS (Fig. 3.1), this is a potential mechanism for the enhanced toxicity of DDS-NOH in this cell type. Hence, in addition to SMX-NOH and DDS-NOH, we synthesized this potential metabolite of DDS. To assess the impact of functional groups that alter the reactivity of the arylhydroxylamine, we also examined two additional metabolites/analogues of DDS-NOH. MADDS-NOH is a metabolite of DDS that has been isolated in man[198], as well as being formed *in vitro* in liver microsomes[203]. NPTS-NOH is an analogue of DDS-NOH in which the opposing amine has been replaced by a methyl group (Fig. 3.3).

As demonstrated in Fig. 3.4, 3.5 and 3.6, there are clear differences in the ability of these metabolites/analogues to induce ROS generation in a cell free system. Consistent with our hypothesis, ROS generation in the presence of DDS-NOH was substantially greater than that seen with SMX-NOH. MADDS-NOH and NPTS-NOH exhibited a similar level of ROS generation as that seen with DDS-

NOH, while the di-arylhydroxylamine analogue induced a level of ROS more similar to that seen with SMX-NOH. This suggests that a second hydroxylamine functional group attenuates rather than enhances the formation of ROS.

The concentration of metabolite needed to induce a measurable increase in ROS in NHEK was considerably higher than that needed in a cell free system (Fig. 3.7). This observation is expected, since cellular antioxidants serve as an important defense mechanism and rapidly detoxify cellular generated ROS. At a concentration of 500 μM, DDS-NOH produced substantially more ROS than that seen with SMX-NOH. Comparison of all examined metabolites at this concentration in NHEK demonstrated that each of the arylhydroxylamine metabolites/analogues of DDS formed a significantly higher amount of ROS as compared to SMX-NOH (Fig. 3.8). Though the ROS generation induced by DDS-diNOH was consistently lower than that seen with other metabolites/analogues of DDS in each of the cell free systems, it resulted in a similar level of ROS generation in NHEK. This observation may be explained by differences in cellular distribution between the metabolites or the presence of an as yet unidentified enzymatic oxidation of the arylhydroxylamines.

As a component of assessing the role of ROS generation on the differential cytotoxicity of the metabolites examined, we evaluated the ability of several ROS scavengers to attenuate arylhydroxylamine-induced ROS generation in NHEK exposed to either SMX-NOH or DDS-NOH. In particular, Trolox, melatonin, ascorbic acid and NAC, which have demonstrated antioxidant properties and scavenge various free radicals[204-209], were assessed for their

ability to attenuate metabolite-induced ROS generation. The lack of effect of melatonin was somewhat surprising (Fig. 3.9), but may be due to its ability to induce superoxide dismutase[210-212]. The induction of superoxide dismutase leads to increased formation of H_2O_2 and subsequently to elevated levels of hydroxyl radicals in the cells. This pro-oxidant activity might counteract the generalized antioxidant activity of melatonin and thus reduce its intracellular ROS scavenging activity.

If the ROS generation is responsible for the differential cytotoxicity in NHEK cells for DDS-NOH and SMX-NOH, then the reduction in free radical formation should lead to reduced cytotoxicity. As ascorbic acid was found to be the most potent antioxidant reducing ROS generation, we determined the cytotoxicity of the arylhydroxylamines toward NHEK cells in the presence and absence of ascorbic acid (Fig. 3.10). The percent cell death induced by these metabolites was not found to correlate with ROS generation. In particular, though DDS-diNOH and MADDS-NOH induced a similar level of ROS in NHEK as that seen with DDS-NOH and NPTS-NOH, neither of these former metabolites induced significant cell death at a concentration of 500 μM. At this same concentration, DDS-NOH and NPTS-NOH were clearly cytotoxic. Moreover, though DDS-NOH and NPTS-NOH induced a similar level of ROS in NHEK (Fig. 3.8), the later was substantially more cytotoxic than DDS-NOH (71% vs 39% mean cell death). The difference in relative potencies for ROS generation and cell death between these metabolites suggests that differences ROS generation does not explain the relative cytotoxicity of arylhydroxylamine metabolites.

However, the fact that cell death was decreased under conditions of reduced ROS generation for DDS-NOH and NPTS-NOH (i.e., in the presence of ascorbic acid), suggests that ROS may play some role in the cell death observed with these metabolites.

Since previous studies have demonstrated that SMX-NOH and DDS-NOH result in the formation of metabolite-protein adducts in NHEK, we determined whether or not ascorbic acid would reduce the covalent adduct formation. As illustrated in Fig. 3.11, ascorbic acid was able to reduce the adduction that occurred with direct addition of metabolite. As previous studies have demonstrated that ascorbic acid blocks the autooxidation of these arylhydroxylamines, this data supports the suggestion that formation of the nitroso enhances the covalent binding of these metabolites. However, the ability to detect adducts despite concentrations of ascorbic acid shown previously to prevent autooxidation, suggests alternative pathways for covalent adduction to cellular proteins.

In summary, our studies do not support the hypothesis that the formation of ROS serves as a primary means for induction of cell death by arylhydroxylamine metabolites of sulfonamides in NHEK. While there are clear differences in the ROS generation observed with SMX-NOH and DDS-NOH, studies with structural analogues of DDS-NOH demonstrate that ROS formation and cytotoxicity are not directly correlated for these compounds. Elucidation of the mechanism of cell death induced by these agents will be necessary to identify the basis for the differential potency observed. While our studies do not

support a simple connection between cell death and ROS generation induced by these metabolites, they should not be construed to suggest that the increase in ROS generation in such cells is unimportant. Indeed, induction of oxidative stress may result in the release or surface expression of important danger signals that are critical in the provocation of an immune response – an essential step in the immune-mediated idiosyncratic toxicity observed with these drugs. Studies probing this potential are ongoing.

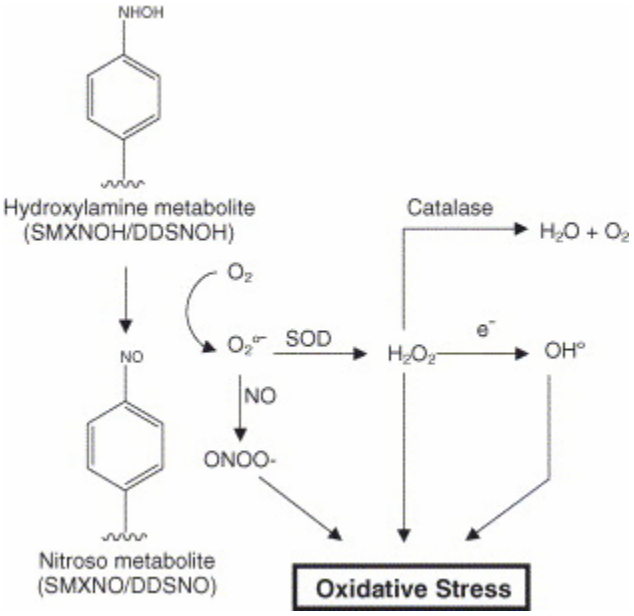

Figure 3.1. Scheme for ROS generation and increase in oxidative stress by arylhydroxylamines. DDS-NO, nitroso metabolite of DDS; SMX-NO, nitroso metabolite of SMX; SOD, superoxide dismutase.

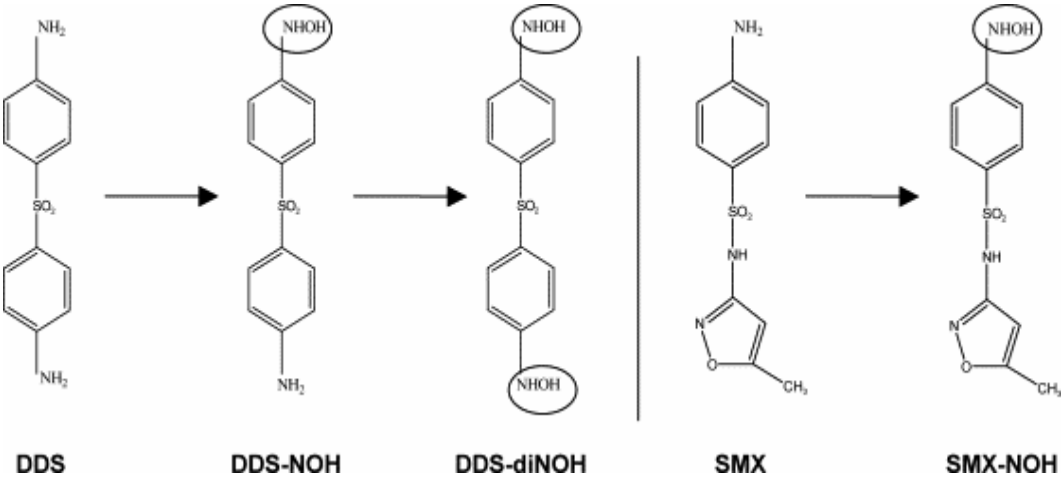

Figure 3.2. Identified and potential metabolites of DDS and SMX which may give rise to ROS. To date, DDS-NOH and SMX-NOH have been isolated from humans, while dapsone dihydroxylamine (DDS-diNOH) has not.

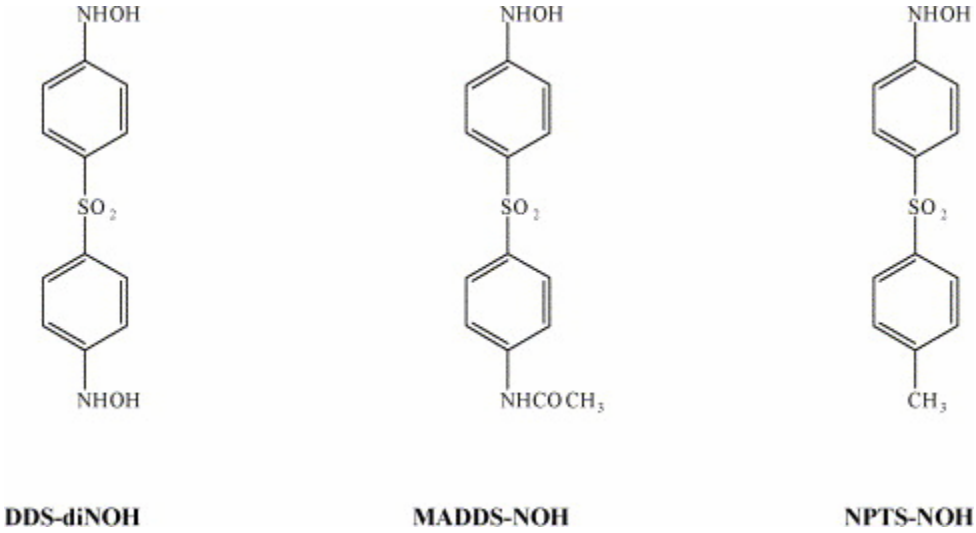

Figure 3.3. Structures of dapsone dihydroxylamine (DDS-diNOH), monoacetyldapsone hydroxylamine (MADDS-NOH), and 4-nitrophenyl-*p*-tolyl sulfone hydroxylamine (NPTS-NOH).

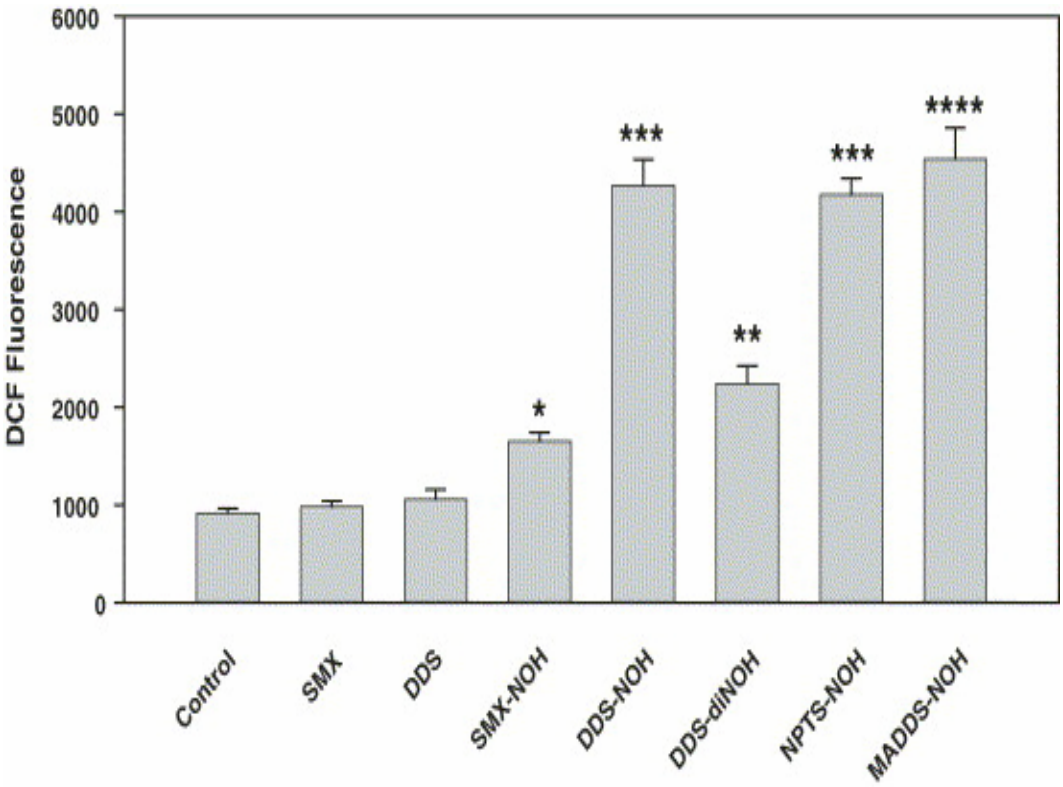

Figure 3.4. Fluorescence of 2′,7′-dichlorofluorescein (DCF) in the presence of various compounds in a cell-free system. Parent compounds or metabolites (2.5 μM) were incubated in phosphate buffer to which 2′,7′-dichlorodihydrofluoroscein (5 μM) was added. Fluorescence was measured every 5 min for 30 min. Data shown are the mean (S.D.) fluorescence of five incubations for each metabolite at 30 min which were analyzed statistically using ANOVA with Holm–Sidak test for multiple comparisons. $^{*}p < 0.05$ compared to control, SMX and DDS; $^{**}p < 0.05$ compared to control, SMX, DDS and SMX-NOH; $^{***}p < 0.05$ compared to control, SMX, DDS, SMX-NOH and DDS-diNOH; $^{****}p < 0.05$ compared to control, SMX, DDS, SMX-NOH, DDS-diNOH and NPTS-NOH.

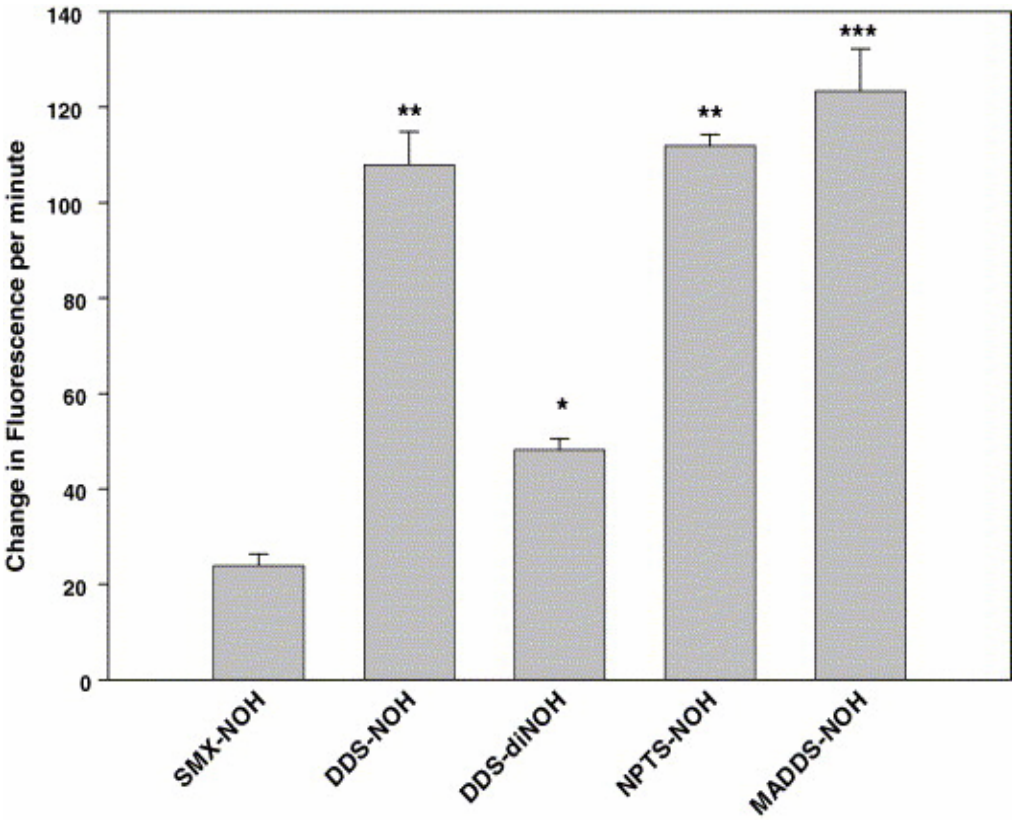

Figure 3.5. Increase of DCF fluorescence per minute in presence of various compounds in a cell-free system. See Fig. 3.4 for experimental details. Data shown are the mean (S.D.) of the rate of change in the fluorescence measured over 30 min. Data were analyzed statistically using ANOVA with the Holm–Sidak test for multiple comparisons. $^{*}p < 0.05$ compared to SMX-NOH; $^{**}p < 0.05$ compared to SMX-NOH and DDS-diNOH; $^{***}p < 0.05$ compared to SMX-NOH, DDS-NOH, DDS-diNOH and NPTS-NOH.

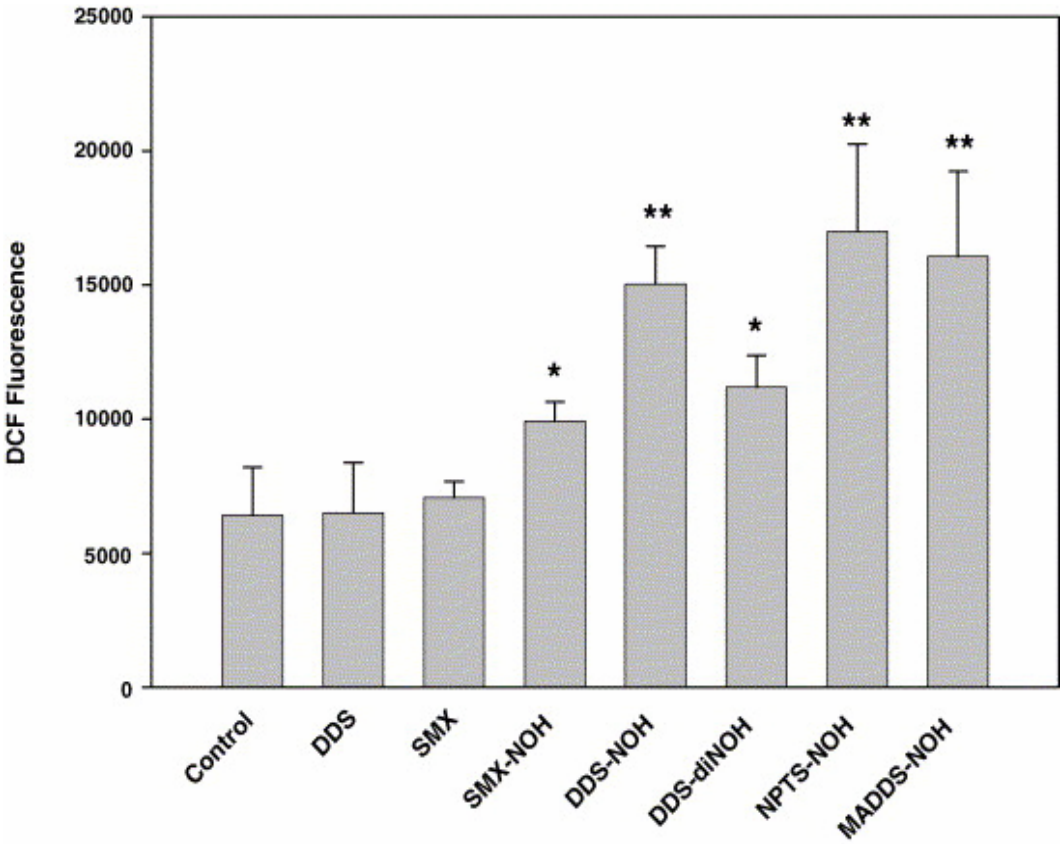

Figure 3.6. Fluorescence of 2′,7′-dichlorofluorescein (DCF) in the presence of various compounds and horseradish peroxidase in a cell-free system. Parent compounds or metabolites (2.5 μM) were incubated in phosphate buffer containing H_2O_2 (100 μM) and horseradish peroxidase (0.02 U/mL) to which 2′,7′-dichloro-dihydrofluoroscein (5 μM) was added. Fluorescence was measured every 5 min for 30 min. Data shown are the mean (S.D.) fluorescence of five incubations at 30 min. (Note difference in scale from Fig. 3.4). Data were analyzed statistically using ANOVA with the Holm–Sidak test for multiple comparisons. $^{*}p < 0.05$ compared to control, SMX and DDS; $^{**}p < 0.05$ compared to control, SMX, DDS, SMX-NOH and DDS-diNOH.

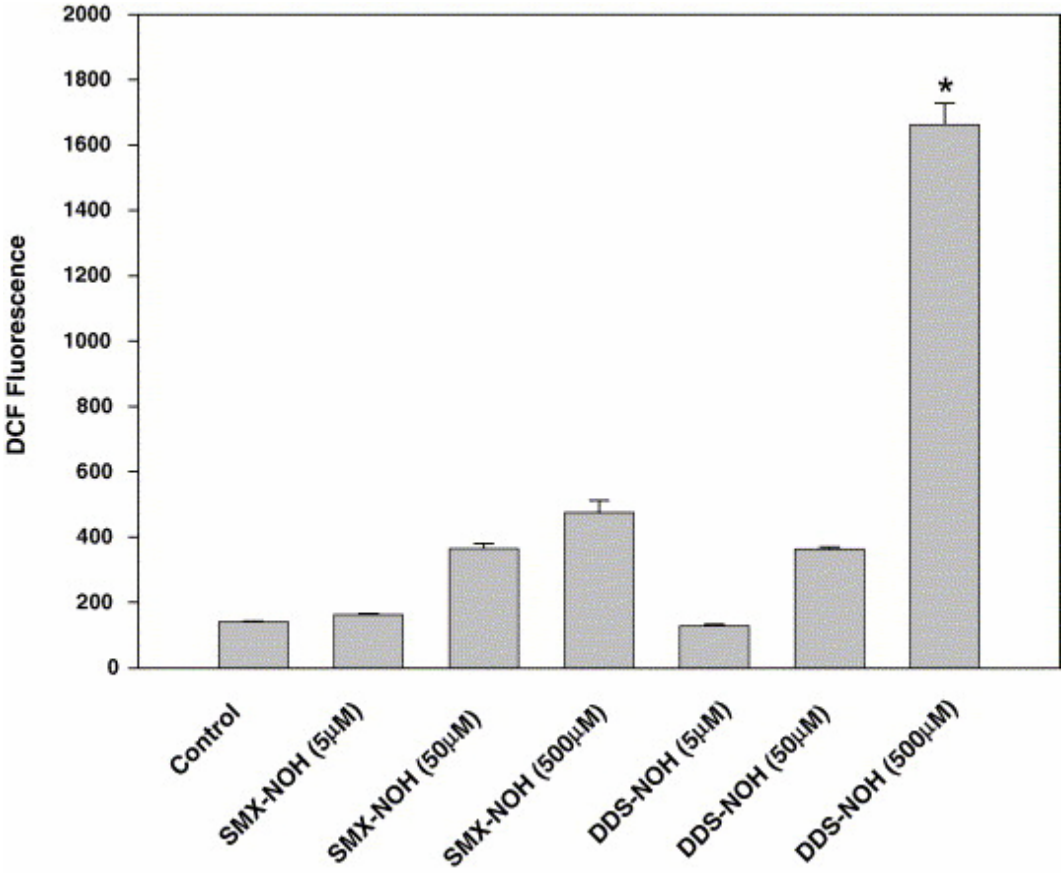

Figure 3.7. Fluorescence of 2′,7′-dichlorofluorescein (DCF) in NHEK incubated with SMX-NOH and DDS-NOH. Metabolites were added to suspensions of NHEK in phosphate buffer to which 2′,7′-dichlorodihydro-fluoroscein diacetate (20 μM) was added. Fluorescence was measured every 5 min for 30 min. Data shown are the mean (S.D.) fluorescence of three incubations at 30 min and were analyzed by Friedman rank sum test. $^{*}p < 0.05$ compared to same concentration of SMX-NOH.

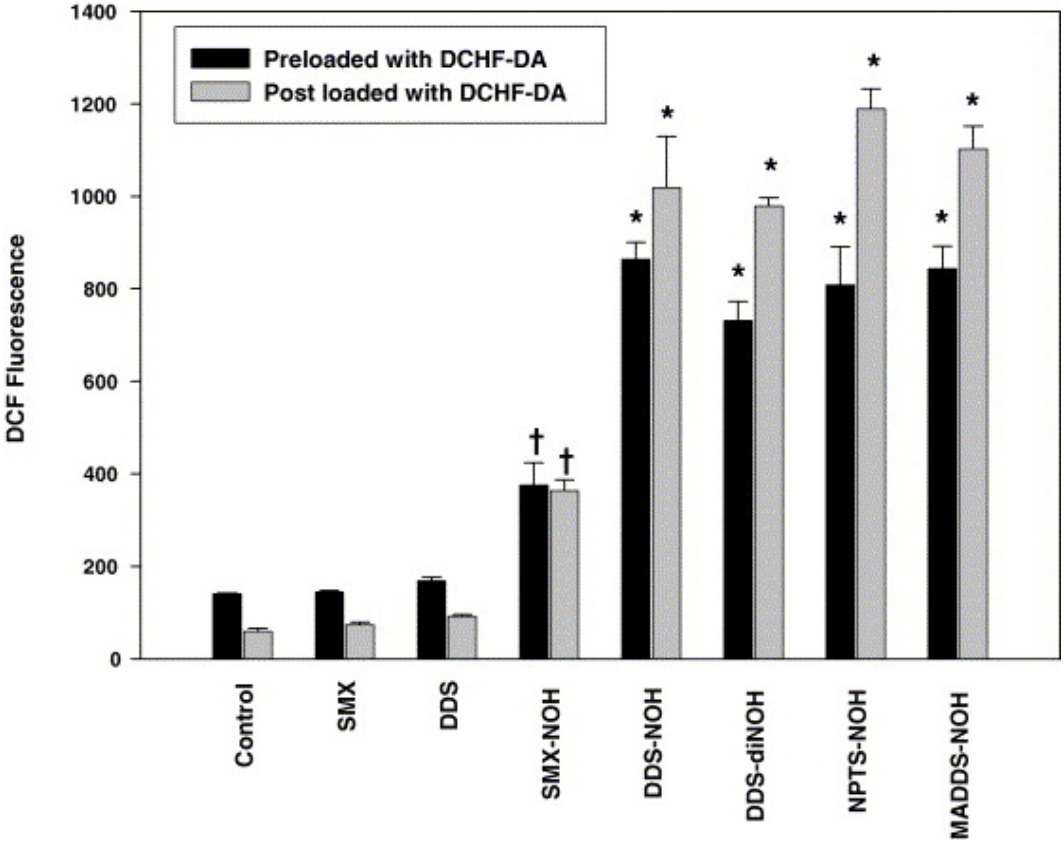

Figure 3.8. Fluorescence of 2′,7′-dichlorofluorescein (DCF) in NHEK preloaded/postloaded with DCHF-DA exposed to various metabolites and analogues. NHEK cells were preloaded or postloaded with 2′,7′-dichlorodihydro-fluoroscein diacetate (20 μM) and exposed to metabolites (500 μM) in phosphate buffer. Fluorescence was measured every 5 min for 30 min. Data shown are the mean (S.D.) fluorescence of three incubations at 30 min and were analyzed statistically using ANOVA with the Holm–Sidak test for multiple comparisons. $^{*}p < 0.05$ compared to control, SMX, DDS and SMX-NOH under same condition; $^{\dagger}p < 0.05$ compared to control, SMX and DDS under same condition.

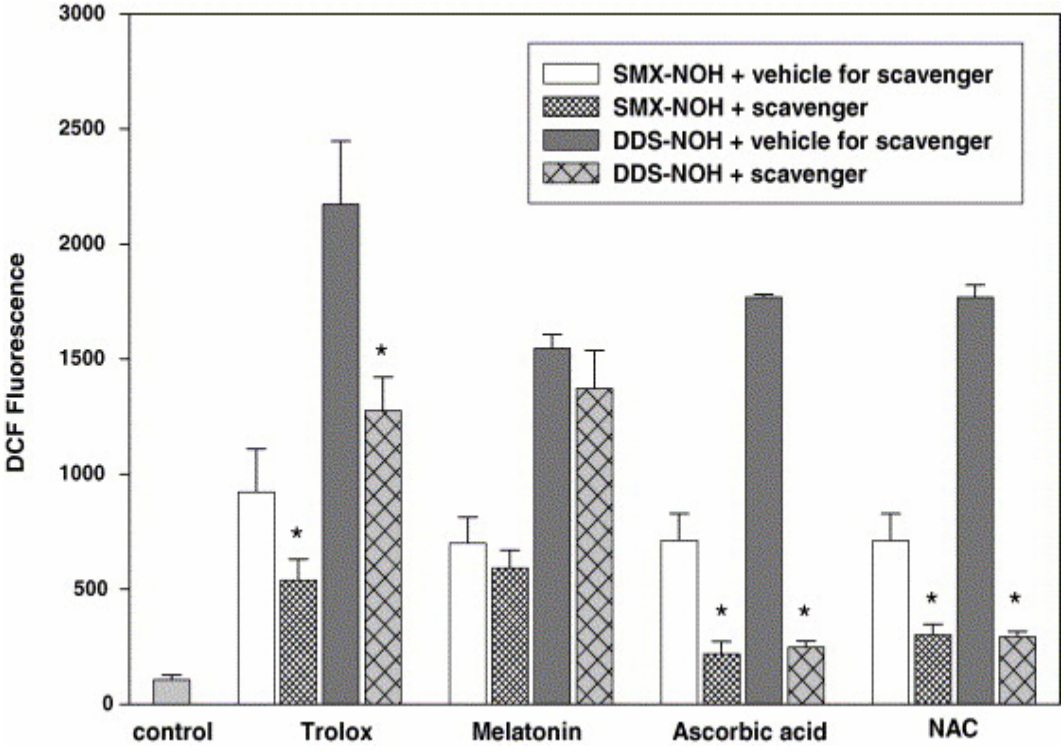

Figure 3.9. ROS generation in NHEK incubated with SMX-NOH or DDS-NOH in presence and absence of ROS scavengers. ROS scavengers, Trolox, melatonin, ascorbic acid and NAC (1 mM), were added to 10^5 NHEK prior to addition of metabolites (500 μM) and DCHF-DA (20 μM). Data presented represent the mean (S.D.) fluorescence at 30 min of three experiments with four replicates of each condition in each experiment. Data were analyzed statistically using ANOVA with the Holm–Sidak test for multiple comparisons. $^{*}p < 0.05$ compared to metabolite without scavenger.

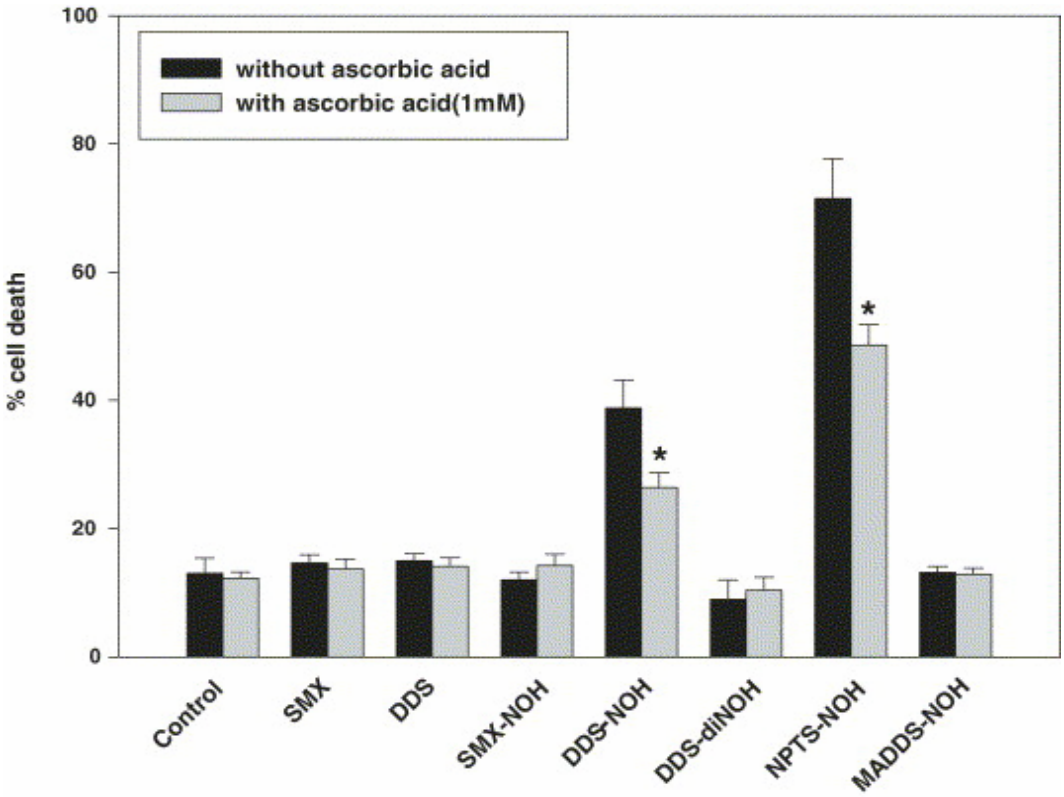

Figure 3.10. Cytotoxicity of various compounds in presence and absence of ascorbic acid in NHEK. 10^5 NHEK cells were plated on 96-well plates and 1 mM ascorbic acid or vehicle was added to cells 3 h prior to addition of 500 μM of metabolite or parent drug. After 3 h incubation with metabolites, the plate was washed with KBM-2 followed by the addition of fresh KBM-2 containing 4 μM of Yo-Yo-1. Fluorescence was measured for 16 h in a temperature controlled fluorescent plate reader followed by the addition of Triton-X (0.1%) for 3 h. The %cytotoxicity was determined as described in Materials and Methods. Data presented represent the mean (S.D.) fluorescence of five replicates of each ndition. Data were analyzed statistically using Friedman rank sum test. $^{*}p < 0.05$ compared to metabolite without ascorbic acid.

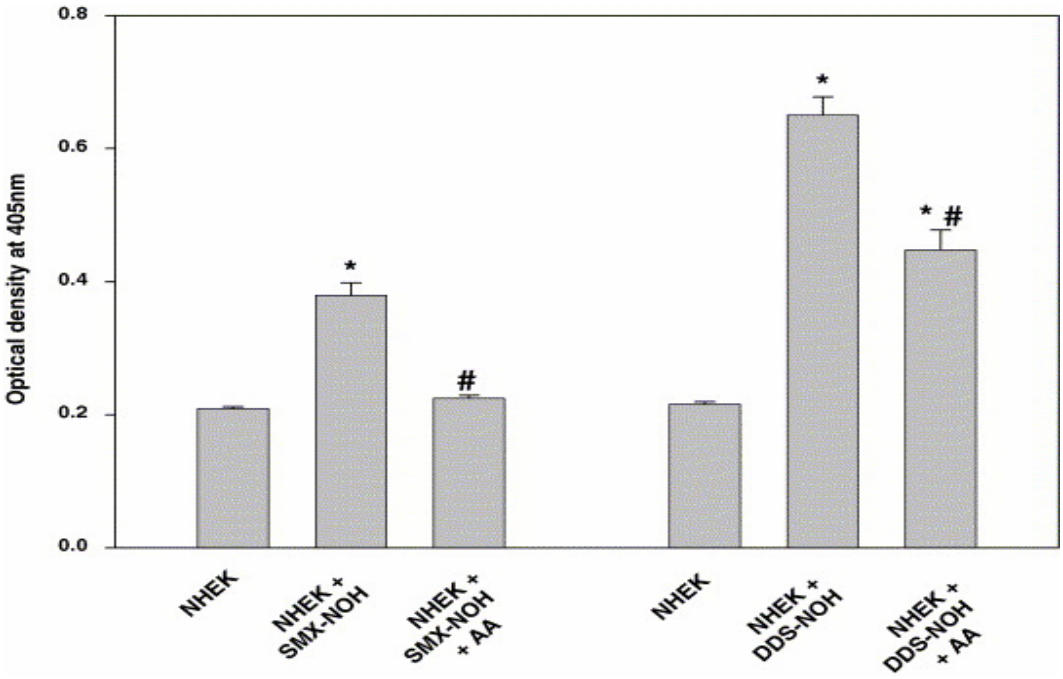

Figure 3.11. Metabolite-protein adducts formation by SMX-NOH and DDS-NOH in presence and absence of ascorbic acid (AA) in NHEK. 10^6 NHEK cells were grown for 24 h in 50 ml centrifuge tubes containing 10 ml of complete growth medium (KGM-2). Cells were then incubated for 3 h in presence or absence of 1 mM ascorbic acid (AA) prior to the addition of metabolite (50 μM). After 24 h, tubes were centrifuged and the cell pellets were lysed in 1 ml of deionized water. Adducts for SMX-NOH and DDS-NOH were determined by the ELISA technique as described in Materials and Methods. Data presented represent the mean (S.D.) optical density of five replicates of each condition. Data were analyzed statistically using ANOVA with the Holm–Sidak test multiple pairwise comparisons. $^{*}p < 0.05$ compared to NHEK without metabolite; $^{\#}p < 0.05$ compared to NHEK + metabolite without ascorbic acid.

CHAPTER FOUR

ROLE OF FOLATE DEFICIENCY AS A PREDISPOSING FACTOR IN CAUSING CDRs

4.1 Introduction

Folic acid is essential for man and is mainly involved in purine synthesis. Dietary folate is converted in to 5-methyl tetrahydrofolate (5-MTHF), which is involved in the methylation of homocysteine (Hcy) to methionine. The methyl group in methionine plays an important role in the methylation of DNA, RNA, histones and proteins. It is also responsible for the synthesis of phospholipids, creatine, carnitine and neurotransmitters (Fig. 4.1)[213-215].

Virtually all food sources are rich in folate including meat, fresh fruits and vegetables. Daily requirement for folates is around 400 µg for adults and 600 µg for pregnant women, according to US recommended daily allowances[216]. Normally, daily diet sufficies to meet this requirement, however, several factors have been associated with folate deficiency.

Folate deficiency has been reported in a variety of populations and shown to be associated with factors such as geographical location, culture, financial status and eating habits[217]. Protracted cooking can destroy around 90% of the folates in dietary food resulting in the reduction in its consumed amount[217]. Age related changes in folate status have also been reported, with lower levels observed in geriatric patients[218]. Certain agents, such as antiepileptic and anticancer drugs, have also been reported to cause folate deficiency[219, 220]. Habits such as smoking and drinking alcohol might affect folate utilization[221].

Moreover, certain populations have been reported to be deficient in their folate status[222, 223]. Polymorphism in MTHF-reductase enzyme has also been reported to cause variable levels of folate [224].

Folate deficiency causes a reduction in methionine leading to the accumulation of Hcy, with a resulting hyperhomocysteinemia (HHcy). HHcy leads to increased cellular oxidative stress in which mitochondrial antioxidants such as thioredoxin and peroxiredoxin are reduced and NADH oxidase activity is upregulated, resulting in the generation of peroxynitrite and nitrotyrosine. The resultant increase in reactive oxygen species (ROS) leads to cellular damage[225]. Zou et al have demonstrated that Hcy increases superoxide (O_2°) production via NADH/NADPH oxidase by stimulating de novo ceramide synthesis and subsequently enhancing Rac GTPase activity in rat renal mesangial cells[226]. Hcy increases Erk (MAPK) activity leading to proliferation and induction of endoplasmic reticulum stress[227]. Folate supplementation has been shown to reduce the Hcy levels and corresponding oxidative stress[228]. Findings supported by Symons et al suggested that severe HHcy evoked by folate-depletion initiates arterial stiffening by a mechanism associated with increased oxidative and glycoxidative stress[229]. Moreover, HHcy due to folate deficiency have been reported as a promoting factor for elevating reactive oxygen species (ROS) and oxidative stress in numerous studies[230-233]. Various disease conditions such as neural tube defects, inflammatory disease, osteoporosis and Alzheimer dementia are associated with folate deficiency due to an increase in oxidative stress [234].

In our lab, we have demonstrated that the arylhydroxylamine metabolites of SMX and DDS generate reactive oxygen species (ROS) leading to an increase in oxidative stress in NHEK (Chapter 3)[80]. As one possible explanation for the idiosyncratic nature of CDRs caused by SMX and DDS, we propose folate deficiency as a predisposing factor for these reactions. As folate deficiency has been shown to elevate Hcy levels leading to an increase in oxidative stress, it can be proposed that those individuals who are folate deficient may have higher oxidative damage when treated with these arylamine drugs. As oxidative stress leads to the activation of antigen presenting cells (APCs) thus leading to the cascade of immune responses terminating in a CDR, those individuals who are folate deficient (and thus having higher oxidative damage) may be more prone to manifest these reactions.

In order to probe this hypothesis, folate deficient and folate supplemented NHEK cells were developed. Folate levels were measured in both the cell types followed by evaluation of protein haptenation, oxidative stress and cytotoxicity of the SMX-NOH and DDS-NOH in these cells to study our hypothesis.

4.2 Materials and Methods

Materials. Folate deficient and folate supplemented RPMI 1640 media were purchased from Invitrogen (Grand Island, NY). Adult normal human epithelial keratinocytes (NHEK) (as 1st passage cells), keratinocyte culture media, trypsin, and trypsin neutralizing solution were obtained from CAMBREX (Walkersville, MD). Rabbit anti-sera were raised against SMX- and DDS-keyhole limpet hemocyanine conjugates and characterized as described previously[180].

Microtiter ELISA plates (96 well) were obtained from Rainin Instruments (Woburn, MA). Goat anti-rabbit antibody conjugated with alkaline phosphatase was purchased from Molecular Probes (Eugene, OR), as was the fluorescent dye Yo-Yo-1. Bradford assay reagent was purchased from PIERCE (Rockford, IL). All other chemicals were purchased from Sigma-Aldrich (St. Louis, MO) or Fisher Scientific (Chicago, IL).

Cell culture. NHEK were grown in folate deficient and folate supplemented RPMI media. Briefly, 3rd passage NHEK cells were cultured in 75 cm^2 flasks using folate deficient and folate supplemented RPMI 1640 basal media supplemented with bovine pituitary extract (7.5 mg/ml), human epidermal growth factors (0.1 ng/ml), insulin (5 µg/ml), hydrocortisone (0.5 µg/ml), epinephrine, transferrin, gentamicin (50 µg/ml) and amphotericin (50 ng/ml) at 37^{o}C in an atmosphere containing 5% CO_2. Media was replaced every 2-3 days. When cell cultures reached near confluency (70-90%), cells were disaggregated using 0.025% Trypsin/0.01% EDTA in HEPES followed by neutralization with 2 volumes of Trypsin neutralizing solution. Cell suspension was then centrifuged, followed by washing in basal media and re-suspension in Supplemented growth medium. Cells were then subjected to experiments. All experiments were performed using 4th passage cells.

Measurement of 5-MTHF in folate deficient and folate supplemented NHEK. 5-methyl tetrahydrofolate levels were determined in folate deficient and folate supplemented NHEK cells by a previously described HPLC method[235] in

the lab of Dr. Schalinske at the Department of Food Science and Human Nutrition, Iowa State University, Ames, IA 50011, USA.

Protein haptenation of arylhydroxylamine metabolite of DDS in folate deficient and folate supplemented NHEK. To determine the effect of folate deficiency on protein haptenation, formation of metabolite-protein adducts in folate deficient and folate supplemented NHEK following incubation with the arylhydroxylamine metabolite of DDS was evaluated as previously described[180]. Briefly, folate deficient and folate supplemented NHEK cells (1 X 10^6 cells) were cultured for 24 hr in 50 ml centrifuge tubes containing 10 ml of respective media. Cells were then incubated for 3 hr in the presence or absence of of DDS-NOH (250 μM). After 24 hr, tubes were centrifuged at 220 g for 5 min to pellet the cells. The supernatant containing the medium was drained off and cell pellets were lysed in 1 ml of deionized water, using repeated cycles of freezing and thawing (3 times) and ultrasonication, to ensure complete lysis. The cell suspension was then thoroughly vortexed and centrifuged at 220 *g* for 5 min and the pellet containing the cell debris discarded. The supernatant containing cellular soluble proteins was collected for protein assay and subsequent ELISA.

ELISA analysis for detection of protein haptenation was performed as described previously[180], with minor modifications. Following protein content measurement using the Bradford reagent kit, all samples were diluted to contain 250 μg/ml protein. An aliquot of 100 μl was adsorbed onto 96 well polystyrene microtiter plates for 16 hr at 4^{o}C. Wells were washed three times using Tris-casein buffer (0.5% casein, 0.9% NaCl, 0.01% Thimerosal, 10 mM Tris-HCl, pH

7.6) and then blocked with Tris-casein buffer for 1 hr. After an additional wash, wells were incubated for 16 hr at 4^{o}C with 100 μl of anti-DDS rabbit serum (1:500 diluted with Tris-casein buffer). Wells were subsequently washed 4 times with Tris-casein buffer and incubated with alkaline phosphatase conjugated goat anti-rabbit antibody (1:1000 diluted in Tris-casein buffer) for 2 hr at room temperature. After washing 4 times with Tris-casein buffer, antibody binding was detected with colorimetric alkaline phosphate substrate reagent. After 1 hr of incubation at room temperature, optical density was measured at 405 nm using a V_{max} kinetic micro plate reader (Molecular Devices).

Cytotoxicity of arylhydroxylamine metabolites of SMX and DDS in folate deficient and folate supplemented NHEK. To assess the relationship between folate deficiency and cytotoxicity, the cytotoxicity of SMX-NOH and DDS-NOH in folate deficient and folate supplemented NHEK was compared at an equimolar concentration (500 μM). Cytotoxicity was determined using an impermeable DNA binding dye, as we have described previously[180]. Briefly, 10^5 folate deficient and folate supplemented NHEK cells were plated on 96-well plates and incubated overnight in 200 μl of respective media at 37˚C, 5% CO_2. After 24 hr, the media was replaced with fresh media and 500 μM of metabolites were added and cells were incubated for an additional 3 hr. After 3 hr incubation with metabolites, the plate was washed once with respective media followed by the addition of fresh media containing 4 μM of Yo-Yo-1. Fluorescence was measured for 16 hr in a temperature controlled fluorescent plate reader as described above. After 16 hr, Triton-X (0.1%) was added to all wells and a final reading was taken after a

further incubation of 3 hr (total incubation time was 19 hr). The cytotoxicity was determined using the following formula:

$$\% \text{ cell death} = \frac{(\text{Yo-Yo fluorescence})_{16hrs} - (\text{Yo-Yo fluorescence})_{0hrs}}{(\text{Yo-Yo fluorescence})_{19hrs} - (\text{Yo-Yo fluorescence})_{0hrs}} \times 100$$

Determination of ROS formation of SMX-NOH and DDS-NOH in folate deficient and folate supplemented NHEK. To investigate the differential oxidative stress in folate deficient and folate supplemented conditions, ROS formation was determined in both the cell types in presence and absence of the hydroxylamine metabolites of SMX and DDS. The fluorescent dye 2'-7'-dichlorodihydrofluorescein diacetate (DCHF-DA) was used to measure the generation of reactive oxygen species in these cells[190-192]. Metabolite-induced ROS formation in folate deficient and folate supplemented NHEK was determined by adding 10^5 cells of each type to each well of a 96 well plate and incubating in 200 µl of respective media at 37˚C, 5% CO_2 for 24 hr. After 24 hr, the media was replaced by 200 µl PBS (10 mM) (PBS composition - 0.8% NaCl, 0.02% KCl, 0.01% $MgCl_2.6H_2O$, 0.02% KH_2PO_4, 0.114% Na_2HPO_4, 0.01% $CaCl_2.2H_2O$, pH 7.4). ROS formation was measured by preloading the cells with DCHF-DA (20 µM) and after 30 min the plate was washed to discard extracellular DCHF-DA, followed by the addition of 500 µM of metabolites (SMX-NOH and DDS-NOH) dissolved in DMSO. The total concentration of DMSO was not more than 1% v/v in the final assay. ROS formation was measured by the oxidation of DCHF-DA to 2', 7'-dichlorofluorescein (DCF), producing fluorescence which was measured every 5 min for 30 min using a multiwell fluorescence plate reader

(Cytofluor®) with an excitation wavelength of 480 nm and emission wavelength of 530 nm. The amount of fluorescence produced was directly related to the amount of oxidative stress generated in these cells.

Determination of formation of DDS and SMX from arylhydroxylamine metabolites in folate deficient and folate supplemented NHEK via high performance liquid chromatography (HPLC). DDS-NOH and SMX-NOH (50 µM) were added to the folate deficient and folate supplemented NHEK cells for 24h at 37°C. Ascorbic acid (1 mM) was included in all incubations to stabilize the arylhydroxylamine from autooxidation. After 24 h, the reaction was terminated by addition of 3 ml of ethyl acetate and the parent drug formation was determined as described previously [98].

Statistical analysis. Data is presented as mean (SD). Data were analyzed using the Friedman rank sum test or ANOVA with the Holm-Sidak test for multiple comparisons, as appropriate. A value of $p < 0.05$ was considered significant.

4.3 Results

Measurement of 5-MTHF in folate deficient and folate supplemented NHEK. Several approaches were taken to develop the folate deficient NHEK cells. Studies were initiated by growing NHEK using DMEM media which were folate deficient or folate supplemented. Using this approach, however, cell viability and growth was found to be low. Including growth supplements for NHEK was also attempted, but showed only 30 to 40% confluency after growing cells for more than 10 days, after which the viability was reduced significantly (40%).

In our next approach, we used RPMI 1640 folate deficient and folate supplemented media. It was found that NHEK growth supplements were the most essential factors for the growth of these cells in any media, without which it was not possible to grow NHEK. Among the NHEK growth supplements, only bovine pituitary extract is undefined for folic acid content, other supplement factors are devoid of folic acid. Growing NHEK cells with folate deficient and folate supplemented RPMI 1640 media with NHEK growth supplements except bovine pituitary extract showed 50% confluency after 9 days. Inclusion of bovine pituitary extract showed remarkable change showing 80-90% confluency in 7 days with 94% viability.

Since the folate content of the bovine pituitary extract was undefined, it was important to demonstrate that this paradigm resulted in cells with reduced folate content. Thus, 5-methyl tetrahydrofolate levels were determined in folate deficient and folate supplemented NHEK cells by HPLC. A significant reduction in the 5-MTHF level was observed in folate deficient cells as compared to folate supplemented cells (Fig. 4.3). This substantiated the ability to use these cells to test our hypothesis.

Protein haptenation of arylhydroxylamine metabolite of DDS in folate deficient and folate supplemented NHEK. In order to determine the effect of folate deficiency on protein haptenation, the difference in the formation of covalent adducts in folate deficient and folate supplemented NHEK following incubation with arylhydroxylamine metabolite of DDS was evaluated. As shown in

Figure 4.4, there was no difference in the extent of protein haptenation in folate deficient and folate supplemented NHEK cells exposed to DDS-NOH.

Cytotoxicity of arylhydroxylamine metabolites of SMX and DDS in folate deficient and folate supplemented NHEK. To determine if folate deficiency predisposed NHEK to the cytotoxic effects of arylhydroxylamines, the cytotoxicity of SMX-NOH and DDS-NOH in folate deficient and folate supplemented NHEK was compared at an equimolar concentration (500 μM). As shown in Figure 4.5, there was no difference in the cytotoxicity of SMX-NOH and DDS-NOH between folate deficient and folate supplemented cells.

Determination of ROS formation of SMX-NOH and DDS-NOH in folate deficient and folate supplemented NHEK. To investigate the differential oxidative stress in folate deficient and folate supplemented conditions, ROS formation was determined in both cell types in presence and absence of the hydroxylamine metabolites of SMX and DDS.

The data shown in Fig. 4.5 suggests that there is significant reduction in the oxidative stress in folate deficient cells compared to that of folate supplemented cells when treated with the arylhydroxylamine metabolites. This observation may be explained by enhanced reduction of the arylhydroxylamine metabolite (which is mediated via cytochrome b5 reductase) in folate deficient cells. Interestingly, an induction in CYP 450 reductase has been reported in folate deficient in rats[236].

Formation of DDS and SMX from arylhydroxylamine metabolites in folate deficient and folate supplemented NHEK via high performance liquid

chromatography (HPLC). In order to determine folate deficient NHEK exhibit an increased ability to reduce the arylhydroxylamine metabolites, conversion of DDS-NOH and SMX-NOH back to their respective parent drugs (DDS and SMX) was evaluated in the folate deficient and folate supplemented NHEK cells.

As shown in Fig. 4.6, there was no difference in the conversion of the arylhydroxylamine metabolites to their parent drugs between folate deficient and folate supplemented cells. These results suggest that reductases were not induced in folate deficient conditions in NHEK.

4.4 Discussion

The basis for the idiosyncratic nature of CDRs caused by a variety of xenobiotics is unclear. Certain factors which are important in the detoxification pathways of reactive metabolites have been suggested as responsible factors for the idiosyncratic nature of these reactions. Glutathione (GSH) has been shown to contribute to the detoxification of reactive metabolites of sulfonamides[237] and our lab has shown that GSH deficiency predisposes keratinocytes to SMX-NOH-induced cytotoxicity[136]. These results suggested that oxidative stress may, in general, serve as a predisposing factor for arylhydroxylamine-induced toxicity. Therefore, we postulated that the increase in oxidative stress due to HHcy secondary to folate deficiency would be a predisposing factor for the toxic effects of these metabolites. Moreover, HHcy due to folate deficiency have been reported as a promoting factor for elevating reactive oxygen species (ROS) and oxidative stress in numerous studies[230-233].

In order to probe this hypothesis, folate deficient and folate supplemented NHEK cells were developed and 5-MTHF levels were determined to confirm the folate deficiency in these cells. Subsequently, differences in the protein haptenation, cytotoxicity and oxidative stress of the arylhydroxylamine metabolites of SMX and DDS between the folate deficient and folate supplemented NHEK cells were measured and compared to evaluate the proposed hypothesis.

5-MTHF levels were reduced in the folate deficient NHEK - thus supporting the method for the development of this model. As we determined the reduction in the 5-MTHF levels in the NHEK cells which were grown successfully in folate deficient RPMI media with all of the growth supplements including bovine pituitary extract, we selected this paradigm as a method of choice for growing folate deficient cells. Folate supplemented cells were grown in the same manner using folate supplemented RPMI media which showed higher folate levels.

Covalent adduct formation in cells exposed to DDS-NOH did not differ between folate deficient and folate supplemented cells. Determination of the oxidative stress induced by the arylhydroxylamine metabolites of SMX and DDS in the folate deficient and supplemented NHEK cells showed a significant reduction in the oxidative stress (16%) in folate deficient cells compared to folate supplemented cells. While unexpected, the magnitude of this reduction was small and unlikely to be biologically relevant. Possible explanations for this unexpected finding include induction of certain antioxidants such as GSH, thioredoxin or

NADPH in folate deficient cells, which in turn reduce the ROS. As we have recently found that peroxidases are able to enhance the oxidation of DDS-NOH to DDS-NO (see Chapter 2), it is also possible that folate deficiency reduces the activity of cellular peroxidases. Alternatively, folate deficiency may result in the induction of detoxification pathways. Interestingly, CYP450 reductase has been shown to be induced in the liver of rats fed a folate deficient diet[236]. As reductase mediated conversion of SMX-NOH to SMX has been shown to be an important detoxification pathway in liver, we determined the conversion of the arylhydroxylamine metabolites to their respective parent drugs in folate deficient and folate supplemented cells. We found no change in the conversion of the hydroxylamine metabolites to the parent drugs between the two types of cells.

Thus, though folate deficiency is a clinical manifestation in AIDS patients[238-242] and has also been observed in cutaneous disorders such as psoriasis[243, 244], our results do not suggest that folate deficiency alters the bioactivation, detoxification, or protein haptenation in keratinocytes exposed to either parent sulfonamides or their arylhydroxylamine metabolites. Unexplored is the impact of folate deficiency on the immune response to antigens.

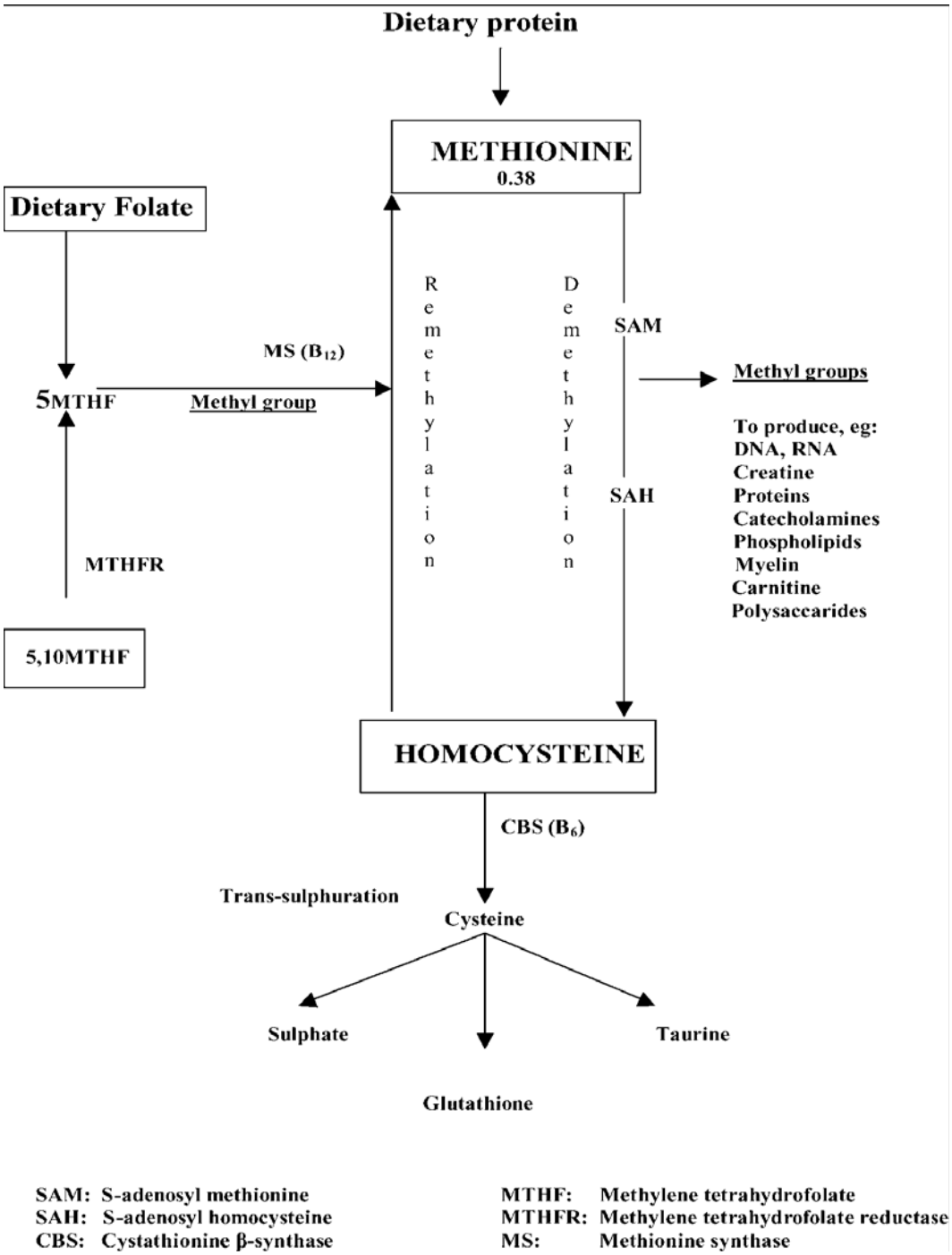

Figure 4.1. Folate, Methionine and Homocysteine Metabolism.

(Figure Reproduced from[213])

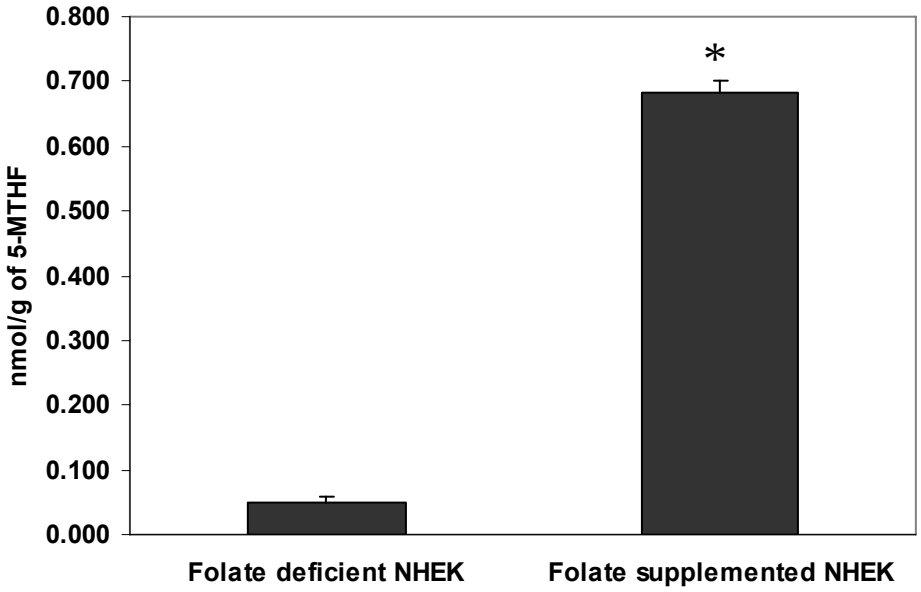

Figure 4.2 Measurement of 5-MTHF in folate deficient and folate supplemented NHEK. Data presented as mean (SD) of 6 incubations. *$p<0.05$ compared to folate deficient NHEK.

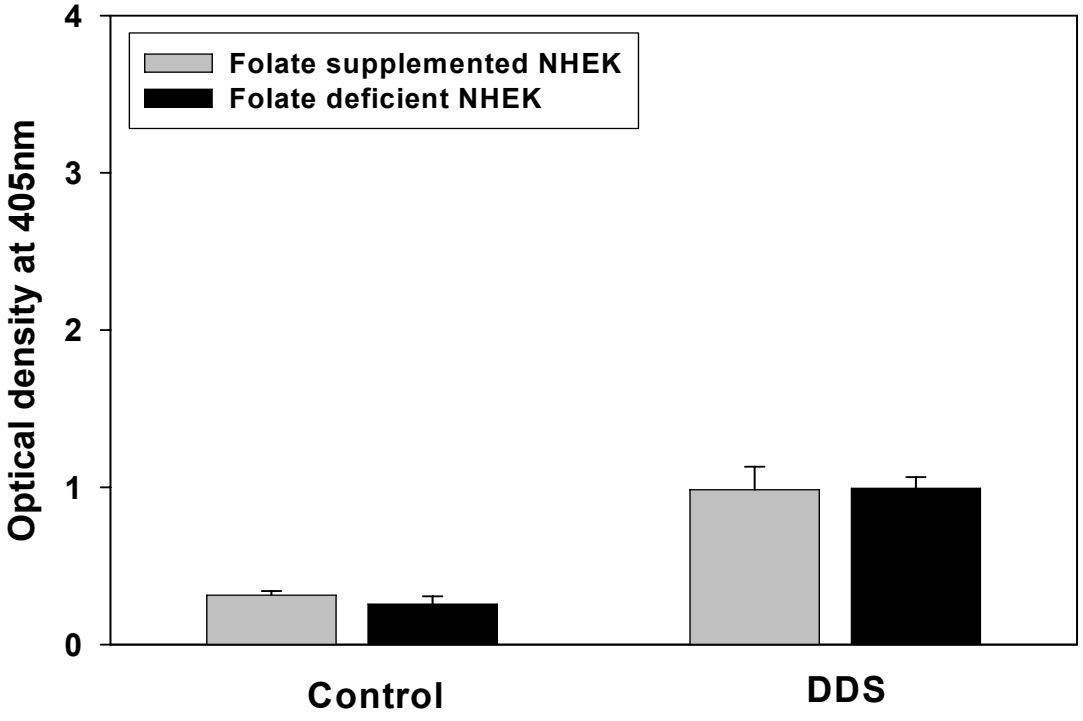

Figure 4.3. Protein haptenation by DDS-NOH in folate deficient and folate supplemented NHEK. 10^6 NHEK cells were grown for 24 h in 50 ml centrifuge tubes containing 10 ml of folate deficient and folate supplemented RPMI 1640 medium. After 24 h, both the cells types were incubated with 250 μM of DDS-NOH for additional 24 h followed by centrifugation of the tubes to obtain the cell pellet and lysing them in 1 ml of deionized water. Adducts for DDS-NOH were determined by the ELISA technique. Data presented represent the mean (S.D.) optical density of five replicates of each condition. Data were analyzed statistically using Friedman rank sum test and found not to differ between groups.

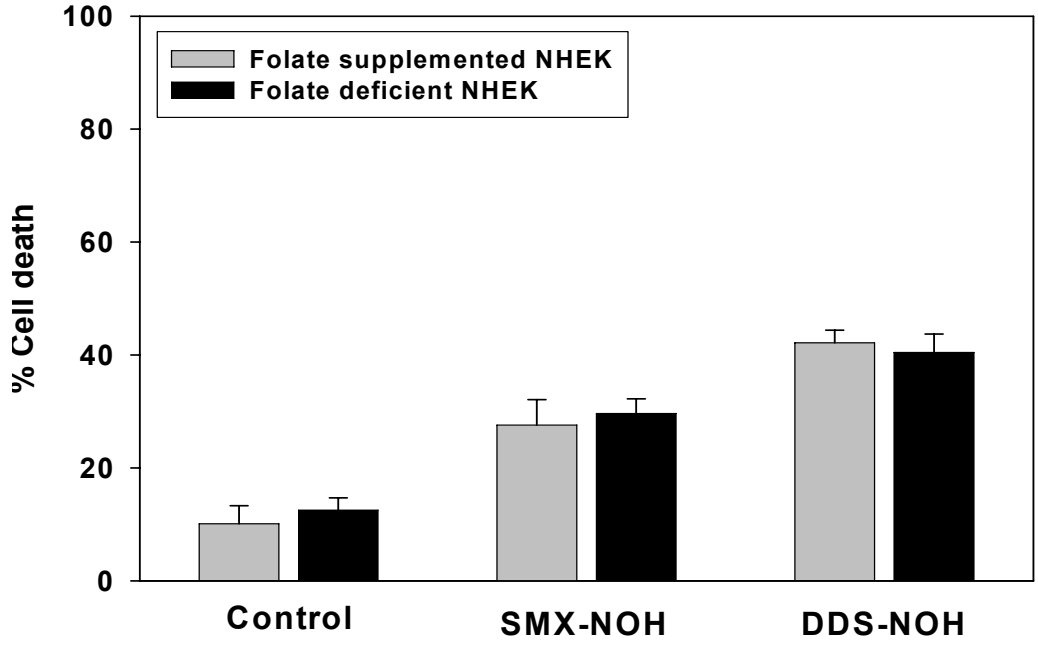

Figure 4.4. Cytotoxicity of SMX-NOH and DDS-NOH in folate deficient and folate supplemented NHEK. 10^5 NHEK cells were plated on 96-well plates and plate was incubated for 24 h. Following the 24 h incubation period, 500 μM of metabolites were added and plate was incubated for additional 3 h. After 3 h incubation with metabolites, the plate was washed with respective media followed by the addition of fresh media containing 4 μM of Yo-Yo-1. Fluorescence was measured for 16 h in a temperature controlled fluorescent plate reader followed by the addition of Triton-X (0.1%) for 3 h. The %cytotoxicity was determined as described in Materials and Methods. Data presented represent the mean (S.D.) fluorescence of five replicates of each condition. Data were analyzed statistically using Friedman rank sum test and found not to differ.

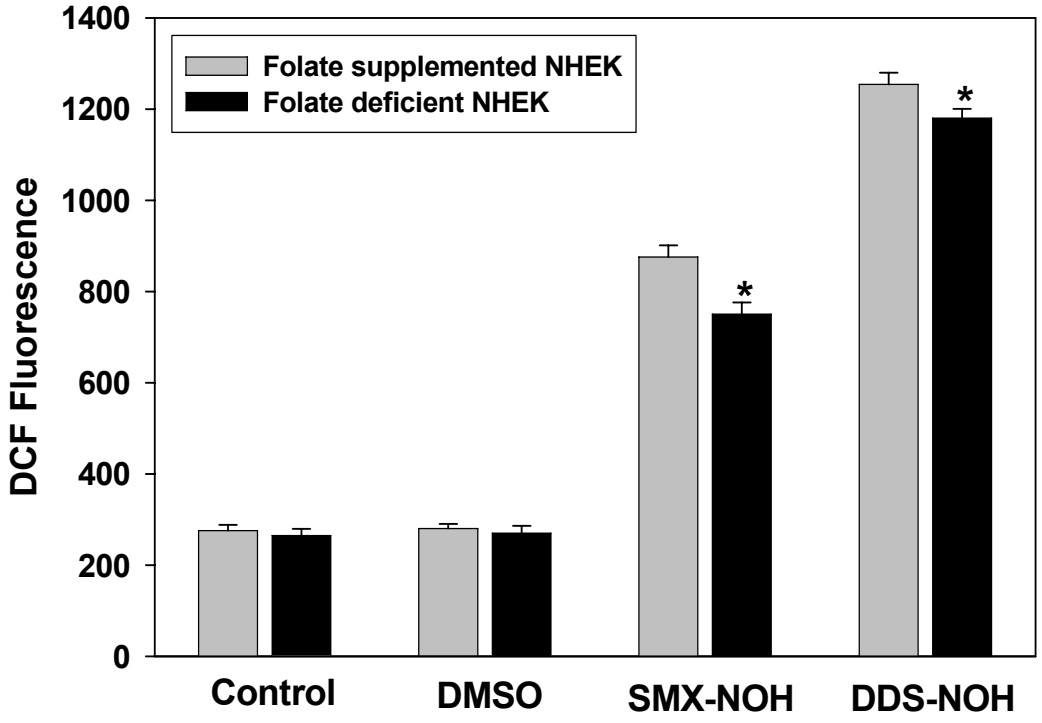

Figure 4.5. ROS formation of SMX-NOH and DDS-NOH in folate deficient and folate supplemented NHEK. 10^5 folate deficient and supplemented NHEK cells were incubated and ROS formation measured by preloading the cells with DCHF-DA (20 μM), followed by washing the plate after 30 min to discard extracellular DCHF-DA. 500 μM of metabolites (SMX-NOH and DDS-NOH) were then added. ROS formation was measured by fluorescence using a multiwell fluorescence plate reader (Cytofluor®) with an excitation wavelength of 480 nm and emission wavelength of 530 nm. Data were analyzed statistically using Friedman rank sum test. $^{*}p < 0.05$ compared to folate supplemented NHEK.

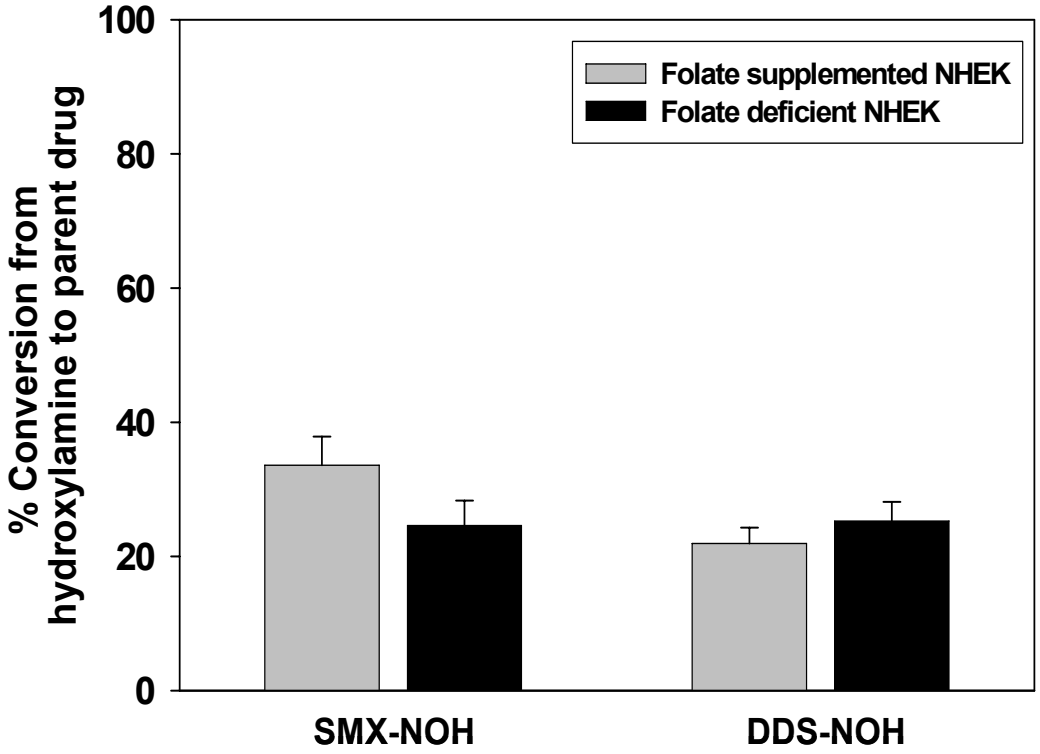

Figure 4.6. Formation of the parent drugs from the arylhydroxylamines in folate deficient and folate supplemented NHEK cells by HPLC. SMX-NOH or DDS-NOH (50 μM) were incubated in folate deficient and folate supplemented NHEK cells for 24 h at 37°C. Ascorbic acid (1 mM) was included in all incubations to stabilize the arylhydroxylamine. After 24 h, the reaction was terminated by addition of 3 ml of ethyl acetate and the parent drug formation was determined by HPLC technique as described previously [98]. Data were analyzed statistically using Friedman rank sum test and groups were found not to differ.

CHAPTER FIVE

SUMMARY AND CONCLUSION

Cutaneous drug reactions (CDRs) are responsible for numerous minor to life-threatening and fatal complications. These CDRs range from transient, mild erythema to toxic epidermal necrolysis, which often results in disability and death. Though the exact mechanism for CDRs is not completely understood, evidence suggests that the bioactivation of drugs to reactive oxygen or nitrogen species is an important factor in the initiation of these reactions [245]. According to the hapten hypothesis, small molecular weight molecules are unable to initiate the immune response on their own. Upon binding with cellular proteins, however, such compounds can act as an antigen which can then initiate an immune response[246]. Several drugs having an arylamine functional group can undergo bioactivation to reactive arylhydroxylamine metabolites[65, 69, 177, 247, 248]. These metabolites can bind to cellular proteins forming an antigen, which can then initiate the immune response ultimately causing CDRs.

The antimicrobial drugs sulfamethoxazole (SMX) and dapsone (DDS) are reported to cause adverse reactions of an idiosyncratic nature due to their bioactivation to arylhydroxylamine metabolites[65, 69, 177, 247, 248]. However, it is unclear whether such reactive species generated in the liver can survive transit to the skin to precipitate CDRs. Therefore, it has been proposed that the bioactivation of these parent drugs may be taking place at or near the site of the adverse effect, especially in keratinocytes of the skin[136]. The bioactivation of SMX and DDS to their respective hydroxylamine metabolites in normal human

epidermal keratinocytes (NHEK) and the adducts formed by these hydroxylamine metabolites with cellular proteins has been reported previously[136]. However, the mechanism behind the mentioned bioactivation was still unclear. Whether it is enzymatic or chemical mediated oxidation which is responsible for converting the parent arylamine drugs to their hydroxylamine metabolites was of question. Studies in specific aim 1 (Chapter 2) were focused to determine the enzyme which is responsible for causing this bioactivation and the results showed that it is flavin containing monooxygenases (FMOs) and non-specific peroxidases (PRXs). Moreover, chemical mediated oxidation by hydrogen peroxide is also a mechanism by which these parent drugs are oxidized – though it is unclear if this is an important intracellular mechanism.

As several clinical studies have used the strategy of enzyme inhibition to treat specific diseases[249, 250], inhibition of FMOs and PRXs enzymes by their inhibitors might be a viable approach to inhibit the bioactivation of these parent drugs to their reactive metabolites and thus prevent the development of CDRs. Moreover, polymorphism in the FMOs and PRXs phenotype might be important as predisposing risk factors responsible for the idiosyncratic nature of these reactions. The insignificant role of CYP450s in NHEK, which is the major metabolizing enzyme for SMX and DDS in liver, suggests tissue specific bioactivation may exhibit varying importance of specific enzymes.

As protein haptenation was utilized as the major parameter in these bioactivation studies, it may be used for screening a library of compounds to eliminate the future toxic compounds leading to high adduct formation. However,

further studies are required in order to evaluate protein haptenation as an objective measurement for the evaluation of new drug molecules.

Bioactivation of arylamine xenobiotics to the reactive hydroxylamine metabolites induce various toxic reactions producing variety of reactive oxygen species (ROS) and nitrogen species (RNS)[78, 79] (Chapter 3, specific aim 2). However, the level of ROS and RNS after cells were exposed to parent compounds was insignificant. In contrast, exposure of cells to preformed metabolite readily elevated ROS. This suggests that the level of intracellular bioactivation is insufficient to produce measurable oxidative stress, but that exposure to liver-generated metabolites may result in meaningful elevations in ROS.

The ROS and RNS formed may lead to the imbalance of the redox status of the cellular system resulting in the oxidation of proteins, lipid peroxidation and DNA oxidation[251-254]. Human immunodeficiency virus (HIV)-infected individuals have been found to be more susceptible to drug-induced cutaneous DTH reactions[255]. A lowered antioxidant (e.g., glutathione) status in HIV-infected individuals has been suggested as a predisposing factor in the higher frequency of CDRs in this population[256]. Exposure to reactive metabolites of SMX and DDS, drugs known to cause CDRs, have been shown to cause depletion of reduced glutathione[136]. Taken together, these data indicate that reduced antioxidant status and/or higher ROS generation in skin cells may predispose individuals to CDRs.

Our results suggested that both SMX-NOH and DDS-NOH are able to generate ROS and thus elevate oxidative stress in NHEK which might be an important factor for the activation of antigen presenting cells (APCs) leading to CDRs. However, our results indicate that the extent of ROS generation does not appear to depend upon the number of NHOH functional groups on the molecule, but might depend upon other functional groups, especially at the para position of the NHOH group. It was also found that the antioxidants such as ascorbic acid and N-acetylcysteine were able to reduce the oxidative stress and protein haptenation caused by these metabolites and hence might be a choice for therapeutic strategies to reduce the occurrence of CDRs.

Studies relating oxidative stress and related cytotoxicity showed that they are not directly correlated, but there are other factors such as the absorption of the molecule and also the type of cell death, that might be determining factors for cytotoxicity. Generation of oxidative stress by these metabolites may play an important role by acting as danger signals for the immune system. Studies are ongoing in our lab to probe these implications.

CDRs caused by SMX, DDS, carbamazepine and other drugs are idiosyncratic in nature, meaning only few individuals exhibit these reactions. Certain factors which are important in the detoxification pathways of these reactive metabolites such as slow acetylation phenotype, GSH deficiency have been shown as possible responsible factors for the idiosyncratic nature of these reactions[59, 257, 258].

Studies in our lab have shown that GSH deficiency predisposes NHEK, making them more susceptible to SMX-NOH toxicity[136]. As GSH is a primary intracellular antioxidant, GSH deficiency leads to the elevation in the oxidative stress causing more oxidative damage by ROS. Folate deficiency also leads to increase in the oxidative stress due to hyperhomocysteinemia (HHcy) [230-233]. We postulated that the increase in oxidative stress caused by folate deficiency might be a predisposing factor for the idiosyncratic nature of these reactions. However, the results obtained in our protein haptenation, cytotoxicity and oxidative stress studies do not support our hypothesis as there was no difference in the measured parameters between folate deficient and folate supplemented cells.

The mechanism by which systemically administered drug provokes a CDR is unknown. The proposed role of the keratinocyte as a target site provides potential insight into the mechanism for CDRs. However, many gaps in our knowledge need to be filled to prove the proposed hypothesis. The results of this dissertation project have identified the cutaneous enzymes that are important in mediating the bioactivation of these drugs. These results suggest that previous pharmacogenetic studies, which have focused on cytochrome P450s and acetyltransferases, may have failed to observe associations by not considering tissue specific enzyme-mediated bioactivation. Indeed, the results presented herein suggest the need to evaluate the role of polymorphisms in FMO-3 as a predisposing factor for the development of CDRs. Future studies are also needed to determine if the protein haptenation observed *in vitro* is observed in patients receiving these drugs.

REFERENCES

1. DeSwarte RD, Drug allergy - Problems and strategies. *J Allergy Clin Immunol* **1984,** 74, 209-221.

2. Jick H, Adverse drug reactions: The magnitude of the problem. *J Allergy Clin Immunol* **1984,** 74, 555-557.

3. Gardner P; Watson LJ, Adverse drug reactions: A pharmacist-based monitoring system. *Clin Pharmacol Ther* **1970,** 11, 802-877.

4. Simmons M; Parker JM; Gowdey CW, Adverse drug reactions during hospitalization. *Can Med Assoc J* **1968,** 98, 175.

5. Smidt WA; McQueen EG, Adverse drug reactions to drugs: A comprehensive hospital in-patient survery. *N Z Med J* **1972,** 76, 397-402.

6. Nolan L; O'Malley K, Adverse drug reactions in the elderly. *Br J Hosp Med* **1989,** 41, 446-457.

7. Black AJ; Somers K, Drug related illness resulting in hospital admissions. *J R Coll Physicians* **1984,** 18, 40-41.

8. Levy M; Kewitz H; Altwein W et al, Hospital admissions due to adverse drug reactions: a comparative study from Jerusalem and Berlin. *Eur J Clin Pharmacol* **1980,** 17, 25-31.

9. McKenney JM; Harrison WL, Drug-related hospital admissions. *Am J Hosp Pharm* **1976,** 33, 792-795.

10. Davies DM(ed.), *Textbook of adverse drug reactions.* 3 ed.; Oxford University Press: Oxford, 1985; p 1-11.

11. Williamson J; Chopin JM, Adverse reactions to the prescribed drugs in the elderly: a multicentre investigation. *Age Ageing* **1980,** 9, 73-80.

12. Battegay M; Opravil M et al, Rash with amoxycillin-clavulanate therapy in HIV-infected patients. *Lancet* **1989,** ii, 1100.

13. van der Ven, A. J.; Koopmans, P. P.; Vree, T. B.; van der Meer, J. W., Adverse drug reaction to co-trimoxazole in HIV infection. *Lancet* **1991,** 338, 431-433.

14. Hughes, W., Treatment and prophylaxis for Pneumocystis carinii pneumonia. *Parasitol Today* **1987,** 3, 332-335.

15. Champion RH; Greaves MW; (eds.), K. B. A., *The Urticarias*. Churchill Livingstone: Edinburgh, 1985.

16. Schwartz LB, Mast cells and their role in urticaria. *J Am Acad Dermatol* **1991,** 25, 190-204.

17. Gary M; Ilfeld D; Kelton JG, Correlation of a quinidine-induced platelet specific antibody with development of thrombocytopenia. *Am J Med* **1985,** 79, 253-255.

18. Erffmeyer JE, Serum sickness syndrome. *Ann Allergy* **1986,** 56, (105-109).

19. Roitt I; Brostoff J; Male D (eds), *Immunology*. 2 ed.; Gower medical publishing: London, 1989.

20. Erffmeyer JE, Penicillin allergy. *Clin Rev Allergy* **1986,** 4, 171 -188.

21. Arndt KA; Jick H, Rates of cutaneous drug reactions to drugs. A report from the Boston Collaborative Drug Surveillance Program. *JAMA* **1976,** 235, 918-922.

22. Bigby M; Jick S; Jick H et al, Drug-induced cutaneous reactions: a report from the Boston Collaborative Drug Surveillance Program on 15,438 consecutive inpatients, 1975 to 1982. *JAMA* **1986,** 256, 3358- 3363.

23. Hilgard P; Hossfeld DK, Transient bleomycin induced thrombocytopenia. A clinical study. *Eur J Cancer* **1978,** 14, 1261-1264.

24. Miescher PA; Graf J, Drug-induced thrombocytopenia. *Clin Haematol* **1980,** 9, 505-519.

25. Porter J; Jick H, Amoxicillin and ampicillin rashes equally likely. *Lancet* **1980,** i, 1037.

26. Naik RPC; Srinivas CR; Das PC, Generalized drug reaction sparing nevus depigmentosus. *Arch Dermatol* **1986,** 122, 509-510.

27. Basak P; Kanwar AJ; Mistri G, Drug rash in hemiplegic. *Arch Dermatol* **1990,** 126, (688-689).

28. Gebel K; Hornstein OP, Drug-induced erythema multiforme. Results of a long-term retrospective study. *Dermatologica* **1984,** 168, (35-40).

29. Stern R; Bigby M, An expanded profile of cutaneous reactions to non-steroidal antiinflammatory drugs. *JAMA* **1984,** 252, 1433-1437.

30. Bianchine JR; Macaraeg PVJ; Lasagna L et al, Drugs at etiologic factors in the Stevens-Johnson syndrome. *Am J Med* **1968,** 44, 390-405.

31. Nethercott JR; Choi BC, Erythema multiforme (Stevens-Johnson syndrome)-chart review of 123 hospitalized patients. *Dermatologica* **1985,** 171, 383-396.

32. Lever WF; Schaumburg-Lever G, *Histopathology of the skin.* 7 ed.; JB Lippincott: Philadelphia, 1990.

33. Reed RJ, Erythema multiforme. A clinical syndrome and a histologic complex. *Am J Dermatopathol* **1985,** 8, 143-152.

34. Merk HF, Diagnosis of drug hypersensitivity: lymphocyte transformation test and cytokines. *Toxicology* **2005,** 209, 217 - 220.

35. Yawalkar N, Drug-induced exanthems. *Toxicology* **2005,** 209, 131 - 134.

36. Mauri-Hellweg D; Bettens F; Mauri D; Brander C; Hunziker T; Pichler WJ, Activation of drug-specific CD4 and CD8+ T cells in individuals allergic to sulfonamides, phenytoin, and carbamazepine. *J Immunol* **1995,** 155, 462–472.

37. Schnyder B; Burkhart C; Schnyder-Frutig K et al, Recognition of sulfamethoxazole and its reactive metabolites by drug-specific CD4+ T cells from allergic individuals. *J Immunol* **2000,** 164, 6647 - 6654.

38. Zanni MP; von Greyerz S; Schnyder B et al, HLA-restricted, processing- and metabolism-independent pathway of drug recognition by human alpha beta T lymphocytes. *J Clin Invest* **1998,** 102, 1591 - 1598.

39. Naisbitt DJ, Drug hypersensitivity reactions in skin: understanding mechanisms and the development of diagnostic and predictive tests. *Toxicology* **2004,** 194(3), 179-196.

40. Stejskal VDM; Forsbeck M; Olin R, Side chain-specific lymphocytes responses in workers with occupational allergy induced by penicillins. *Int Arch Allergy Appl Immunol* **1987,** 82, 461-464.

41. Sogn DD, Penicillin allergy. *J Allergy Clin Immunol* **1984,** 74, 589-593.

42. Weiss ME; Adkinson NF, Immediate hypersensitivity reactions to penicillin and related antibiotics. *Clin Allergy* **1989,** 18, 515-540.

43. Idsoe O; Guthe T; Willcox R et al, Nature and extent of penicillin side-reactions, with particular reference to fatalities from anapylactic shock. *Bull WHO* **1968,** 38, 159-188.

44. Belley L, Allergy to penicillin. *Br Med J* **1984,** 288, 511-512.

45. Gerber D, Adverse reactions to piroxicam. *Drug Intell Clin Pharm* **1987,** 21, 707-710.

46. Pitts N, Efficacy and safety of piroxicam. *Am J Med* **1982,** 72(Suppl 2A), 77-87.

47. Valsecchi R; Cainelli T, Nonpigmenting fixed drug reaction to piroxicam. *J Am Acad Dermatol* **1989,** 21, 1300.

48. Kochevar IE; Morison WL; Lamm JL et al, Possible mechanism of piroxicam induced photosensitivity. *Arch Dermatol* **1986,** 122, 1283-1287.

49. Katayama H; Kawada A, Exacerbation of psoriasis induced by indomethacin. *J Dermatol (Tokyo)* **1981,** 8, 323-327.

50. Smith F; Lindberg P, Life-threatening hypersensitivity to sulindac. *JAMA* **1980,** 244, 269-270.

51. Wright AL; Bleehen SS; Champion AE, Reticulate pigmentation due to bleomycin: light and electron-microscopic studies. *Dermatologica* **1990,** 181, 255-257.

52. Lincke-Plewig H, Bleomycin-exanthem. *Hautarzt* **1980,** 31, 616-618.

53. Kukla LJ; McGuire WP, Heat induced recall of bleomycin skin changes. *Cancer* **1982,** 50, 2283-2284.

54. Bennet JP; Burns CP, Absence of progression of recurrent bleomycin skin toxicity without postponement or attenuation of therapy. *Am J Med* **1988,** 85, 585-586.

55. Rieder, M. J.; Uetrecht, J.; Shear, N. H.; Cannon, M.; Miller, M.; Spielberg, S. P., Diagnosis of sulfonamide hypersensitivity reactions by in-vitro "rechallenge" with hydroxylamine metabolites. *Annals of Internal Medicine* **1989,** 110, 286-9.

56. Cribb AE; Lee BL; Trepanier LA et al, Adverse reactions to sulphonamide and sulphonamide-trimethoprim antimicrobials:
clinical syndromes and pathogenesis. *Adverse Drug React Toxicol Rev Port Imunoalergol* **1996,** 15, 9 - 50.

57. Cribb AE; Spielberg SP, An invitro investigation of predisposition to sulphonamide idiosyncratic toxicity in dogs. *Veterinary Research Communications* **1990,** 14, 241-252.

58. Chan H-L; Stern RS; Arndt KA; Langlois J; Jick SA; Jick H; AM, W., The incidence of erythema multiforme, Stevens-Johnson syndrome, and toxic epidermal necrolysis. A population-based study with particular reference to reactions caused by drugs among outpatients. *Arch Dermatol* **1990,** 126, 43–47.

59. Rieder, M.; Shear, N.; Kanee, A.; Tang, B.; Spielberg, S., Prominence of slow acetylator phenotype among patients with sulfonamide hypersensitivity reactions. *Clin Pharmacol Ther* **1991,** 49, 13-17.

60. Cribb, A. E.; Spielberg, S. P., Sulfamethoxazole is metabolized to the hydroxylamine in humans. *Clinical Pharmacology & Therapeutics* **1992,** 51, 522-6.

61. Walsh JS; Reese MJ; Thurmond LM, The metabolic activation of abacavir by human liver cytosol and expressed human alcohol dehydrogenase isozymes. *Chem Biol Interact* **2002,** 142, 135 - 154.

62. Claesen M; Moustafa MA; Adline J; Vandervorst D; Poupaert JH, Evidence for an arene oxide-NIH shift pathway in the metabolic conversion of phenytoin to 5-(4-hydroxyphenyl)-5-phenylhydantoin in the rat and in man. *Drug Metab. Dispos* **1982,** 10, 667–671.

63. Madden S; Maggs JL; Park BK, Bioactivation of carbamazepine in the rat in vivo: evidence for the formation of reactive arene oxide(s). *Drug Metab Dispos* **1996,** 24, 469 - 479.

64. Maggs JL; Naisbitt DJ; Tettey JN; Pirmohamed M; Park BK, Metabolism of lamotrigine to a reactive arene oxide intermediate. *Chem Res Toxicol* **2000,** 13, 1075–1081.

65. Cribb, A.; Spielberg, S.; Griffin, G., N4-hydroxylation of sulfamethoxazole by cytochrome P450 of the cytochrome P4502C subfamily and reduction of sulfamethoxazole hydroxylamine in human and rat hepatic microsomes. *Drug Metab Dispos* **1995,** 23, 406-414.

66. Mitra, A.; Thummel, K.; Kalhorn, T.; Kharasch, E.; Unadkat, J.; Slattery, J., Metabolism of dapsone to its hydroxylamine by CYP2E1 in vitro and in vivo. *Clin Pharmacol Ther* **1995,** 58, 556-566.

67. Uetrecht, J.; Shear, N.; Zahid, N., N-chlorination of sulfamethoxazole and dapsone by the myeloperoxidase system. *Drug Metab Dispos* **1993,** 21, (5), 830-834.

68. Uetrecht, J.; Zahid, N.; Shear, N.; Biggar, W., Metabolism of dapsone to a hydroxylamine by human neutrophils and mononuclear cells. *J Pharmacol Exp Ther* **1988,** 245, (1), 274-279.

69. Winter, H.; Wang, Y.; Unadkat, J., CYP 2C8/9 mediate dapsone N-hydroxylation at clinical concentrations of dapsone. *Drug Metab Dispos* **2000,** 28, 865-868.

70. Cashman JR; Zhang J, Human flavin-containing monooxygenases. *Annu Rev Pharmacol Toxicol* **2006,** 46, 65-100.

71. Cribb, A.; Miller, M.; Tesoro, A.; Spielberg, S., Peroxidase-dependent oxidation of sulfonamides by monocytes and neutrophils from humans and dogs. *Mol Pharmacol* **1990,** 38, 744-751.

72. Goebel, C.; Vogel, C.; Wulferink, M.; Mittmann, S.; Sachs, B.; Schraa, S.; Abel, J.; Degen, G.; Uetrecht, J.; leichmann, E., Procainamide, a drug causing lupus, induces prostaglandin H synthase-2 and formation of T cell-sensitizing drug metabolites in mouse macrophages. *Chem Res Toxicol* **1999,** 12, 488-500.

73. Liu, Y.; Levy, G., Activation of heterocyclic amines by combinations of prostaglandin H synthase-1 and -2 with N-acetyltransferase 1 and 2. *Cancer Lett* **1998,** 133, 115-123.

74. Baron, J.; Holler, D.; Schiffer, R.; Frankenberg, S.; Neis, M.; Jugert, F., Expression of multiple cytochrome P450 enzymes and multidrug resistance-associated transport proteins in human skin keratinocytes. *J Invest Dermatol* **2001,** 116, 541-548.

75. Janmohamed, A.; Dolphin, C.; Phillips, I.; Shephard, E., Quantification and cellular localization of expression in human skin of genes encoding flavin-containing monooxygenases and cytochromes P450. *Biochem Pharmacol* **2001,** 62, 777-786.

76. Kanekura, T.; Laulederkind, S.; Kirtikara, K.; Goorha, S.; Ballou, L., Cholecalciferol induces prostaglandin E2 biosynthesis and transglutaminase activity in human keratinocytes. *J Invest Dermatol* **1998,** 111, 634-639.

77. Park, B.; Kitteringham, N.; Powell, H.; Pirmohamed, M., Advances in molecular toxicology-towards understanding idiosyncratic drug toxicity. *Toxicology* **2000,** 153, 39–60.

78. Rav RS; Mehrotra S; Shanker U; Babu GS; Joshi PC; Hanss RK, Evaluation of UV-induced superoxide radical generation potential of some common antibiotics. *Drug Chem Toxicol* **2001,** 24, 191–200.

79. Naito Y; Yoshikawa T; Yoshida N; Kondo M, Role of oxygen radical and lipid peroxidation in indomethacin-induce d gastricmucosal injury. *Dig Dis Sci* **1998,** 43, 30S–34S.

80. Vyas, P.; Roychowdhury, S.; Woster, P.; Svensson, C., Reactive oxygen species generation and its role in the differential cytotoxicity of the arylhydroxylamine metabolites of sulfamethoxazole and dapsone in normal human epidermal keratinocytes. *Biochem Pharmacol* **2005,** 70, 275-286.

81. Fuchs J; Zollner TM; Kaufmann R, e. a., Redox-modulated pathways in infl ammatory skin diseases. *Free Radic Biol Med* **2001,** 30, 337 - 353.

82. Roychowdhury, S.; Svensson, C., Mechanisms of drug-induced delayed-type hypersensitivity reactions in the skin. *AAPS Journal* **2005,** 7(4), Article 80, DOI: 10.1208/aapsj070480.

83. Kantengwa S; Jornot L; Devenoges C, e. a., Superoxide anions induce the maturation of human dendritic cells. *Am J Respir Crit Care Med* **2003,** 167, 431 - 437.

84. Verhasselt V; Goldman M; Willems F, Oxidative stress up-regulates IL-8 and TNF-alpha synthesis by human dendritic cells. *Eur J Immunol* **1998,** 28, 3886 - 3890.

85. Matsue H; Edelbaum D; Shalhevet D, e. a., Generation and function of reactive oxygen species in dendritic cells during antigen presentation. *J Immunol* **2003,** 171, 3010 - 3018.

86. Chen KH; Reece LM; Leary JF, Mitochondrial glutathione modulates TNF-alpha-induced endothelial cell dysfunction. *Free Radic Biol Med* **1999,** 27, 100 - 109.

87. De Smedt AC; Van Den Heuvel RL; Van Tendeloo VF et al, Capacity of CD34+ progenitor-derived dendritic cells to distinguish between sensitizers and irritants. *Toxicol Lett* **2005,** 156, 377 - 389.

88. Svensson, C.; Cowen, E.; Gaspari, A., Cutaneous drug reactions. *Pharmacol Rev* **2001,** 53, 357-379.

89. Cribb AE; Lee BL; Trepanier LA; Spielberg SP, Adverse reactions to sulphonamide and sulphonamide-trimethoprim antimicrobials: clinical syndromes and pathogenesis. *Adv Drug React Toxicol Rev* **1996,** 15, 9-50.

90. Goldie SJ; Kaplan JE; Losina E; Weinstein MC; Paltiel AD; Seage GR; Craven DE; Kimmel AD; Zhang H; Cohen CJ; Freedberg KA, Prophylaxis for human immunodeficiency virus-related Pneumocystis carinii pneumonia: using

simulation modeling to inform clinical guidelines. *Arch Intern Med* **2002,** 162, (8), 921-8.

91. Hughes WT, Treatment and prophylaxis for Pneumocystis carinii pneumonia. *Parasitol Today* **1987,** 3, (11), 332-5.

92. Rieder MJ; Uetrecht J; Shear NH; Cannon M; Miller M; Spielberg SP, Diagnosis of sulfonamide hypersensitivity reactions by in-vitro "rechallenge" with hydroxylamine metabolites. *Ann Intern Med* **1989,** 110, (4), 286-289.

93. Dujovne D; Chan C; Zimmerman H, Sulfonamide hepatic injury. *N Engl J Med* **1967,** 377, 785-788.

94. Svensson CK; Cowen EW; Gaspari AA, Cutaneous drug reactions. *Pharmacol. Rev.* **2001,** 53, 357-379.

95. Berg P., a. D., P., Co-trimoxazole-induced liver injury - an analysis of cases with hypersensitivity-like reactions. *Infection* **1987,** 15, S259-S263.

96. Reilly TP, J. C., Mechanistic perspectives on sulfonamide-induced cutaneous drug reactions. *Curr Opin Allergy Clin Immunol* **2002,** 2, 307-315.

97. Svensson CK, Do arylhydroxylamine metabolites mediate the idiosyncratic reactions associated with sulfonamides and sulfones? *Chem Res Toxicol* **2003,** 16, 1034-1043.

98. Reilly TP; Lash LH; Doll MA; Hein DW; Woster PM; Svensson CK, A role for bioactivation and covalent binding within epidermal keratinocytes in sulfonamide-induced cutaneous drug reactions. *J Invest Dermatol* **2000,** 114, (6), 1164-73.

99. Roychowdhury S; Vyas PM; Reilly TP; Gaspari AA; Svensson CK, Characterization of the formation and localization of sulfamethoxazole and dapsone-associated drug-protein adducts in human epidermal keratinocytes. *J Pharmacol Exp Ther* **2005,** 314, (1), 43-52.

100. Rys-Sikora R; Konger R; Schoggins J; Malaviya R; Pentland A, Coordinate expression of secretory phospholipase A2 and cyclooxygenase -2 in activated human keratinocytes. *Am J Physiol Cell Physiol.* **2000,** 278, C822-C833.

101. Kanekura T; Laulederkind S; Kirtikara K; Goorha S; Ballou L, Cholecalciferol induces prostaglandin E2 biosynthesis and transglutaminase activity in human keratinocytes. *J Invest Dermatol* **1998,** 111, 634-639.

102. Janmohamed A; Dolphin CT; Phillips IR; Shephard EA, Quantification and cellular localization of expression in human skin of genes encoding flavin-containing monooxygenases and cytochromes P450. *Biochem Pharmacol.* **2001,** 62, (6), 777-786.

103. Baron JM; Holler D; Schiffer R; Frankenberg S; Neis, M. M. H.; Jugert FK, Expression of multiple cytochrome p450 enzymes and multidrug. *J Invest Dermatol* **2001,** 116, (4), 541-548.

104. Saeki M; Saito Y; Nagano M; Teshima R; Ozawa S; Sawada J, mRNA expression of multiple cytochrome P450 isozymes in four types of cultured skin cells. *Int Arch Allergy Immunol* **2002,** 127, 333-336.

105. Cribb AE; Spielberg SP; Griffin GP, N4-hydroxylation of sulfamethoxazole by cytochrome P450 of the cytochrome P4502C subfamily and reduction of sulfamethoxazole hydroxylamine in human and rat hepatic microsomes. *Drug Metab Dispos* **1995,** 23, (3), 406-414.

106. Gill H; Tija J; Kitteringham N; Pirmohamed M; Back D; Park B, The effect of genetic polymorphism in CYP2C9 on sulphamethoxazole N- hydroxylation. *Pharmacogenetics* **1999,** 9, (1), 43-53.

107. Winter H; Wang Y; Unadkat J, CYP 2C8/9 mediate dapsone N-hydroxylation at clinical concentrations of dapsone. *Drug Metab Dispos* **2000,** 28, (8), 865-868.

108. Mitra AK; Thummel KE; Kalhorn TF; Kharasch ED; Unadkat JD; Slattery JT, Metabolism of dapsone to its hydroxylamine by CYP2E1 in vitro and in vivo. *Clin Pharmacol Ther* **1995,** 58, 556-566.

109. Liu Y; Levy G, Activation of heterocyclic amines by combinations of prostaglandin H synthase-1 and -2 with N-acetyltransferase 1 and 2. *Cancer Lett* **1998,** 133, 115-123.

110. Goebel C; Vogel C; Wulferink M; Mittmann S; Sachs B; Schraa S; Abel J; Degen G; Uetrecht J; leichmann E, Procainamide, a drug causing lupus, induces prostaglandin H synthase-2 and formation of T cell-sensitizing drug metabolites in mouse macrophages. *Chem Res Toxicol* **1999,** 12, (6), 488-500.

111. Vyas PM; Roychowdhury S; Woster PM; Svensson CK, Reactive oxygen species generation and its role in the differential cytotoxicity of the arylhydroxylamine metabolites of sulfamethoxazole and dapsone in normal human epidermal keratinocytes. *Biochem Pharmacol* **2005,** 70, (2), 275-286.

112. Beaune, P.; P. Kremers; F. Letawe-Goujon; J.E. Gielen, Monoclonal antibodies against human liver cytochrome P-450. *Biochem Pharmacol* **1985,** 34, 3547-3552.

113. Kuehl P; Zhang J; Lin Y; Lamba J; Assem M; Schuetz J; Watkins PB; Daly A; Wrighton SA; Hall SD; Maurel P; Relling M; Brimer C; Yasuda K; Venkataramanan R; Strom S; Thummel K; Boguski MS; Schuetz E, Sequence diversity in CYP3A promoters and characterization of the genetic basis of polymorphic CYP3A5 expression. *Nat Genet* **2001,** 27, 383-391.

114. Haufroid V; Toubeau F; Clippe A; Buysschaert M; Gala JL; Lison D, Real-time quantification of cytochrome P4502E1 mRNA in human peripheral blood lymphocytes by reverse transcription-PCR: method and practical application. *Clin Chem* **2001,** 47, (6), 1126-1129.

115. Roychowdhury, S.; Vyas, P.; Reilly, T.; Gaspari, A.; Svensson, C., Characterization of the formation and localization of sulfamethoxazole and dapsone-associated drug-protein adducts in human epidermal keratinocytes. *J Pharmacol Exp Ther* **2005,** 314, 43-52.

116. Goldstein, J.; Faletto, M.; Romkes-Sparkes, M.; Sullivan, T.; Kitareewan, S.; Raucy, J.; Lasker, J.; Ghanayem, B., Evidence that CYP2C19 is the Major (S)-Mephenytoin 4'-hydroxylase in humans. *Biochemistry* **1994,** 33, (7), 1743-1752.

117. Cribb AE; Nuss CE; Alberts DW; Lamphere DB; Grant DM; Grossman SJ; Spielberg SP, Covalent binding of sulfamethoxazole reactive metabolites to human and rat liver subcellular fractions assessed by immunochemical detection. *Chem Res Toxicol* **1996,** 9, 500-507.

118. Cribb AE; Miller M; Tesoro A; Spielberg SP, Peroxidase-dependent oxidation of sulfonamides by monocytes and neutrophils from humans and dogs. *Mol Pharmacol* **1990,** 38, (5), 744-751.

119. Uetrecht JP, Drug metabolism by leukocytes and its role in drug-induced lupus and other idiosyncratic drug reactions. *Crit Rev Toxicol.* **1990,** 20, (4), 213-235.

120. Yengi LG; Xiang Q; Pan J; Scatina J; Kao J; Ball SE; Fruncillo R; Ferron G; Wolf CR, Quantitation of cytochrome P450 mRNA levels in human skin. *Anal Biochem* **2003,** 316, 103-110.

121. Saeki, M.; Saito, Y.; Nagano, M.; Teshima, R.; Ozawa, S.; Sawada, J., mRNA expression of multiple cytochrome P450 isozymes in four types of cultured skin cells. *Int Arch Allergy Immunol* **2002,** 127, 333-336.

122. Wurster W; Nemes R; Lamba J; Schuetz EG; Blaisdell J; Goldstein JA; Reilly TP; Svensson CK, Bioactivation of sulfamethoxazole (SMX) and dapsone (DDS) in normal human epidermal keratinocytes (NHEK) results in the formation of drug-protein adducts. *Allergologie* **2004,** 4, 169.

123. Balani SK; Zhu T; Yang TJ; Liu Z; He B; Lee FW, Effective Dosing Regimen of 1-Aminobenzotriazole for Inhibition of Antipyrine Clearance in Rats, Dogs, and Monkeys. *Drug Metab Dispos* **2002,** 30, (10), 1059-1062.

124. Vyas PM; Roychowdhury S; Svensson CK, Role of human cyclooxygenase-2 in the bioactivation of dapsone and sulfemethoxazole. *Drug Metab Dispos* **2005,** In press.

125. Du, L.; Neis, M.; Ladd, P.; Lanza, D.; Yost, G.; Keeney, D., Effects of the differentiated keratinocyte phenotype on expression levels of CYP1-4 family genes in human skin cells. *Toxicol Appl Pharmacol* **2006,** 213, (2), 135-144.

126. Rieder MJ; Krause R; Bird IA, Time-course of toxicity of reactive sulfonamide metabolites. *Toxicology* **1995,** 95, (1-3), 141-146.

127. Manchanda T; Hess D; Dale L; Ferguson SG; Rieder MJ, Haptenation of sulfonamide reactive metabolites to cellular proteins. *Mol Pharmacol* **2002,** 62, (5), 1011-1026.

128. Naisbitt DJ; Farrell J; Gordon SF; Maggs JL; Burkhart C; Pichler WJ; Pirmohamed M; Park BK, Covalent binding of the nitroso metabolite of sulfamethoxazole leads to toxicity and major histocompatibility complex-restricted antigen presentation. *Mol Pharmacol* **2002,** 62, (3), 628-637.

129. Cashman JR; Xiong YN; Xu L; Janowsky A, N-oxygenation of amphetamine and methamphetamine by the human flavin-containing monooxygenase (form 3): role in bioactivation and detoxication. *J Pharmacol Exp Ther* **1999,** 288, (3), 1251-60.

130. Golly I; Hlavica P, N-Oxidation of 4-chloroaniline by prostaglandin synthase. Redox cycling of radical intermediate(s). *Biochem J* **1985,** 226, (3), 803-809.

131. Maier J; Hla T; Maciag T, Cyclooxygenase is an immediate early gene induced by interleukin -1 in human endothelial cells. *J Biol Chem* **1990,** 265, 10805-10808.

132. Buckman S; Gresham A; Hale P; Hruza G; Anast J; Masferrer J; Pentland A, COX-2 expression is induced by UVB exposure in human skin: Implications for the development of skin cancer. *Carcinogenesis* **1998,** 19, 723-729.

133. Rubin RL; Curnette JT, Metabolism of procainamide to the cytotoxic hydroxylamine by neutrophils activated in vitro. *J Clin Invest* **1989,** 83, 1336-1343.

134. Khan, F.; Roychowdhury, S.; Nemes, R.; Vyas, P.; Woster, P.; Svensson, C., Effect of pro-Inflammatory cytokines on the toxicity of the arylhydroxylamine metabolites of sulphamethoxazole and dapsone in normal human keratinocytes. *Toxicology* **2006,** 218, (2-3), 90-99.

135. Uetrecht, J., The role of leukocyte-generated reactive metabolites in the pathogenesis of idiosyncratic drug reactions. *Drug Metab Rev* **1992,** 24, 299-366.

136. Reilly, T.; Lash, L.; Doll, M.; Hein, D.; Woster, P.; Svensson, C., A role for bioactivation and covalent binding within epidermal keratinocytes in sulfonamide-induced cutaneous drug reactions. *J Invest Dermatol* **2000,** 114, 1164-1173.

137. Vyas, P.; Roychowdhury, S.; Svensson, C., Role of human cyclooxygenase-2 in the bioactivation of dapsone and sulfamethoxazole. *Drug Metab Dispos* **2006,** 34, (1), 16-18.

138. Tucker, K.; Lilly, M.; Heck, L. J.; Rado, T., Characterization of a new human diploid myeloid leukemia cell line (PLB-985) with granulocytic and monocytic differentiating capacity. *Blood* **1987,** 70, (2), 372-378.

139. Nauseef, W.; Root, R.; Malech, H., Biochemical and immunologic analysis of hereditary myeloperoxidase deficiency. *J Clin Invest* **1983,** 71, (5), 1297-1307.

140. Kettle, A.; Winterbourn, C., Assays for the chlorination activity of myeloperoxidase. *Meth Enzymo* **1994,** 233, 502-512.

141. Borregaard, N.; Heiple, J.; Simons, E.; Clark, R., Subcellular localization of the b-cytochrome component of the human neutrophil microbicidal oxidase: translocation during activation. *J Cell Biol* **1983,** 97, 52-61.

142. Henderson, M.; Krueger, S.; Siddens, L.; Stevens, J.; Williams, D., S-oxygenation of the thioether organophosphate insecticides phorate and

disulfoton by human lung flavin-containing monooxygenase 2. *Biochem Pharmacol* **2004,** 68, 959-967.

143. Krueger, S.; Siddens, L.; Henderson, M.; Andreasen, E.; Tanguay, R.; Pereira, C.; Cabacungan, E.; Hines, R.; Ardlie, K.; Williams, D., Haplotype and functional analysis of four flavin-containing monooxygenase isoform 2 (FMO2) polymorphisms in Hispanics. *Pharmacogenet Genomics* **2005,** 15, 245-256.

144. Laemmli, U., Cleavage of structural proteins during the assembly of the head of the bacteriophage T4. *Nature* **1970,** 227, 680–685.

145. Towbin, H.; Staehelin, T.; Gordon, J., Electrophoretic transfer of proteins from polyacrylamide gels to nitrocellulose sheets: Procedure and some applications. *Proc Natl Acad Sci U S A* **1979,** 76, 4350–4354.

146. Cornejo, L.; Lopez de Blanc, S.; Femopase, F.; Azcurra, A.; Calamari, S.; Battellino, L.; Dorronsoro de Cattoni, S., Evolution of saliva and serum components in patients with oral candidosis topically treated with Ketoconazole and Nystatin. *Acta Odontol Latinoam* **1998,** 11, (1), 15-25.

147. Kettle, A.; Gedye, C.; Winterbourn, C., Mechanism of inactivation of myeloperoxidase by 4-aminobenzoic acid hydrazide. *Biochem J* **1997,** 321, 503-508.

148. Ator, M.; David, S.; Ortiz de Montellano, P., Structure and catalytic mechanism of horseradish peroxidase. Regiospecific meso alkylation of the prosthetic heme group by alkylhydrazines. *J Biol Chem* **1987,** 262, (31), 14954-14960.

149. Kettle, A.; Gedye, C.; Hampton, M.; Winterbourn, C., Inhibition of myeloperoxidase by benzoic acid hydrazides. *Biochem J* **1995,** 308 (Pt 2), 559-563.

150. Gorlewska-Roberts, K.; Teitel, C.; Lay, J. J.; Roberts, D.; Kadlubar, F., Lactoperoxidase-catalyzed activation of carcinogenic aromatic and heterocyclic amines. *Chem Res Toxicol* **2004,** 17, (12), 1659-1666.

151. Gupta, A.; Eggo, M.; Uetrecht, J.; Cribb, A.; Daneman, D.; Rieder, M.; Shear, N.; Cannon, M.; Spielberg, S., Drug-induced hypothyroidism: the thyroid as a target organ in hypersensitivity reactions to anticonvulsants and sulfonamides. *Clin Pharmacol Ther* **1992,** 51, (1), 56-67.

152. Chung WG; Park CS; Roh HK; Lee WK; Cha YN, Oxidation of ranitidine by isozymes of flavin-containing monooxygenase and cytochrome P450. *Jpn J Pharmacol* **2000,** 84, (2), 213-220.

153. Svensson, C., Do arylhydroxylamine metabolites mediate the idiosyncratic reactions associated with sulfonamides and sulfones? *Chem Res Toxicol* **2003,** 16, 1034-1043.

154. Uetrecht, J., Drug metabolism by leukocytes and its role in drug-induced lupus and other idiosyncratic drug reactions. *Crit Rev Toxicol* **1990,** 20, 213-235.

155. Lin, C.; Boland, B.; Lee, Y.; Salemi, M.; Morin, D.; Miller, L.; Plopper, C.; Buckpitt, A., Identification of proteins adducted by reactive metabolites of naphthalene and 1-nitronaphthalene in dissected airways of rhesus macaques. *Proteomics* **2006,** 6, (3), 972-982.

156. Naisbitt, D.; Hough, S.; Gill, H.; Pirmohamed, M.; Kitteringham, N.; Park, B. Cellular disposition of sulphamethoxazole and its metabolites: implications for hypersensitivity. *Br J Pharmacol* **1999,** 126, (6), 1393-1407.

157. Coleman MD; Rhodes LE; Scott AK; Verbov JL; Friedmann PS; Breckenridge AM; Park BK, The use of cimetidine to reduce dapsone-dependent methaemoglobinaemia in dermatitis herpetiformis patients. *Br J Clin Pharmacol* **1992,** 34, (3), 244-249.

158. Krolicki, A., Skin penetration of sulfamethoxazole and trimethoprim after oral administration. *Ann Acad Med Stetin* **2002,** 48, 59-73.

159. Slominski, A.; Wortsman, J.; Kohn, L.; Ain, K.; Venkataraman, G.; Pisarchik, A.; Chung, J.; Giuliani, C.; Thornton, M.; Slugocki, G.; Tobin, D., Expression of hypothalamic-pituitary-thyroid axis related genes in the human skin. *J Invest Dermatol* **2002,** 119, (6), 1449-1455.

160. Cashman, J., Human flavin-containing monooxygenase: substrate specificity and role in drug metabolism. *Curr Drug Metab* **2000,** 1, (2), 181-191.

161. Nace, C.; Genter, M.; Sayre, L.; Crofton, K., Effect of methimazole, an FMO substrate and competitive inhibitor, on the neurotoxicity of 3,3'-iminodipropionitrile in male rats. *Fundam Appl Toxicol* **1997,** 37, (2), 131-140.

162. Pirmohamed, M.; Alfirevic, A.; Vilar, J.; Stalford, A.; Wilkins, E. G. L.; Sim, E.; Park, B. K., Association analysis of drug metabolizing enzyme gene polymorphisms in HIV-positive patients with co-trimoxazole hypersensitivity. *Pharmacogenetics* **2000,** 10, 705-713.

163. Koukouritaki, S. B.; Hines, R. N., Flavin-containing monooxygenase genetic polymorphism: impact on chemical metabolism and drug development. *Pharmacogenomics* **2005,** 6, (8), 807-822.

164. Hughes, W. T., Treatment and prophylaxis for Pneumocystis carinii pneumonia. *Parasitology Today* **1987,** 3, 332-335.

165. Goldie, S. J.; Kaplan, J. E.; Losina, E.; Weinstein, M. C.; Paltiel, A. D.; Seage, G. R.; Craven, D. E.; Kimmel, A. D.; Zhang, H.; Cohen, C. J.; Freedberg, K. A., Prophylaxis for human immunodeficiency virus-related Pneumocystis carinii pneumonia: using simulation modeling to inform clinical guidelines. *Archives of Internal Medicine* **2002,** 162, 921-928.

166. Hughes, W., Use of dapsone in the prevention and treatment of *Pneumocystis carinii* pneumonia: A review. *Clinical Infectious Diseases* **1998,** 27, 191-204.

167. Bozette, S. A.; Finkelstein, D. M.; Spector, S. A.; Frame, P.; Powderly, W. G.; He, W.; Phillips, L.; Craven, D.; van der Horst, C.; Feinberg, J., A randomized trial of three antipneumocystis agents in patients with advanced human

immunodeficiency virus infection. *New England Journal of Medicine* **1995,** 332, 693-699.

168. Blum, R. N.; Miller, L. A.; Gaggini, L. C.; Cohn, D. L., Comparative trial of dapsone versus trimethoprim/sulfamethoxazole for primary prophylaxis of *Pneumocystis carinii* pneumonia. *Journal of Acquired Immunodeficiency Syndrome* **1992,** 5, 341-347.

169. Carr, A.; Cooper, D. A.; Penny, R., Allergic manifestations of human immunodeficiency virus (HIV) infection. *Journal of Clinical Immunology* **1991,** 11, 55-64.

170. Kovacs, J.; Hiemenz, J.; Macher, A.; Stover, D.; Murray, H.; Shelhamer, J.; Lane, H.; Urmacher, C.; Honig, C.; Longo, D.; Parker, M.; Natanson, C.; Parrillo, J.; Fauci, A.; Pizzo, P.; Masur, H., *Pneumocystis carinii* pneumonia: A comparison between patients with the acquired immunodeficiency syndrome and patients with other immunodeficiencies. *Annals of Internal Medicine* **1984,** 100, 663-671.

171. Roudier, C.; Caumes, E.; Rogeaux, O.; Bricaire, F.; Gentilini, M., Adverse cutaneous reactions to trimethoprim-sulfamethoxazole in patients with the acquired immunodeciency syndrome and *Pneumocystis carinii* pneumonia. *Archives of Dermatology* **1994,** 130, 1383-1386.

172. Gordin, F. M.; Simon, G. L.; Wofsy, C. B.; Mills, J., Adverse reactions to trimethoprim-sulfamethoxazole in patients with the acquired immunodeficiency syndrome. *Annals of Internal Medicine* **1984,** 100, 495-499.

173. Jaffe, H. S.; Abrams, D. L.; Ammann, A. J.; Lewis, B. J.; Golden, J. A., Complications of co-trimoxazole in treatment of AIDS-associated *Pneumocystis carinii* pneumonia in homosexual men. *Lancet* **1984,** 2, 1009-1011.

174. Cribb, A. E.; Lee, B. L.; Trepanier, L. A.; Spielberg, S. P., Adverse reactions to sulphonamide and sulphonamide-trimethoprim antimicrobials: clinical syndromes and pathogenesis. *Adverse Drug Reactions & Toxicological Reviews* **1996,** 15, 9-50.

175. Reilly, T. P.; Ju, C., Mechanistic perspectives on sulfonamide-induced cutaneous drug reactions. *Current Opinion in Allergy & Clinical Immunology* **2002,** 2, 307-315.

176. Svensson, C. K., Do arylhydroxylamine metabolites mediate the idiosyncratic reactions associated with sulfonamides and sulfones? *Chemical Research in Toxicology* **2003,** 16, 1034-1043.

177. Rieder, M. J.; Uetrecht, J.; Shear, N. H.; Spielberg, S. P., Synthesis and in vitro toxicity of hydroxylamine metabolites of sulfonamides. *Journal of Pharmacology & Experimental Therapeutics* **1988,** 244, 724-8.

178. Rieder, M. J., In vivo and in vitro testing for adverse drug reactions. *Pediatric Clinics of North America* **1997,** 44, 93-111.

179. Reilly, T. P.; Bellevue, F. H.; Woster, P. M.; Svensson, C. K., Comparison of the in vitro cytotoxicity of hydroxylamine metabolites of sulfamethoxazole and dapsone. *Biochemical Pharmacology* **1998,** 55, 803-810.

180. Reilly, T. P.; Lash, L. H.; Doll, M. A.; Hein, D. W.; Woster, P. M.; Svensson, C. K., A role for bioactivation and covalent binding within epidermal keratinocytes in sulfonamide-induced cutaneous drug reactions. *Journal of Investigative Dermatology* **2000,** 114, 1164-1173.

181. Bhaiya P; Roychowdhury S; Vyas PM; Doll MA; Hein DW; Svensson CK, Bioactivation, protein haptenation, and toxicity of sulfamethoxazole and dapsone in normal human dermal fibroblasts. *Toxicol Appl Pharmacol* **2006,** 215, (2), 158-167.

182. Reilly, T. P.; Woster, P. M.; Svensson, C. K., Methemoglobin formation by hydroxylamine metabolites of sulfamethoxazole and dapsone: Implications for differences in adverse drug reactions. *Journal of Pharmacology and Experimental Therapeutics* **1999,** 288, 951-959.

183. Shangari, N.; O'Brien, P. J., The cytotoxic mechanism of glyoxal involves oxidative stress. *Biochemical Pharmacology* **2004,** 68, 1433-1442.

184. Tafazoli, S.; O'Brien, P. J., Prooxidant activity and cytotoxic effects of indole-3-acetic acid derivatives radicals. *Chemical Research in Toxicology* **2004,** 17, 1350-1355.

185. Atsumi, T.; Ishihara, M.; Kadoma, Y.; Tonosaki, K.; Fujisawa, S., Comparative radical production and cytotoxicity induced by camphorquinone and 9-fluorenone against human pulp fibroblasts. *Journal of Oral Rehabilitation* **2004,** 31, 1155-1164.

186. Yang, J.; Li, H.; Chen, Y. Y.; Wang, X. J.; Shi, G. Y.; Hu, Q. S.; Kang, X. L.; Lu, Y.; Tang, X. M.; Guo, Q. S.; Yi, J., Anthraquinones sensitize tumor cells to arsenic cytotoxicity in vitro and in vivo via reactive oxygen species-mediated dual regulation of apoptosis. *Free Radical Biology and Medicine* **2004,** 37, 2027-2041.

187. Cribb, A. E.; Miller, M.; Leeder, J. S.; Hill, J.; Spielberg, S. P., Reactions of the nitroso and hydroxylamine metabolites of sulfamethoxazole with reduced glutathione. Implications for idiosyncratic toxicity. *Drug Metabolism & Disposition* **1991,** 19, 900-6.

188. Bradshaw, T. P.; McMillan, D. C.; Crouch, R. K.; Jollow, D. J., Formation of free radicals and protein mixed disulfides in rat cells exposed to dapsone hydroxylamine. *Free Radical Biology and Medicine* **1997,** 22, 1183-1193.

189. Vage, C.; Saab, N.; Woster, P. M.; Svensson, C. K., Dapsone-induced hematologic toxicity: comparison of the methemoglobin-forming ability of hydroxylamine metabolites of dapsone in rat and human blood. *Toxicology & Applied Pharmacology* **1994,** 129, 309-16.

190. Myhre, O.; Andersen, J. M.; Aarnes, H.; Fonnum, F., Evaluation of probes 2',7'-dichlorofluorescin diacetate, luminol, and lucigenin as indicators of reactive species formation. *Biochemical Pharmacology* **2003,** 65, 1575-1582.

191. Hempel, S. L.; Buettner, G. R.; O'Malley, Y. Q.; Wessels, D. A.; Flaherty, D. M., Dihydrofluorescein diacetate is superior for detecting intracellular oxidants: Comparision with 2',7'-dichlorodihydrofluorescein diacetate, 5(and 6)-carboxy-2',7'-dichlorodihydrofluorescein diacetate, and dihydrorhodamine 123. *Free Radical Biology and Medicine* **1999,** 27, 146-159.

192. Chignell, C. F.; Sik, R. H., A photochemical study of cells loaded with 2',7'-dichlorofluoroscein: implications for detection of reactive oxygen species generated during UVA irradiation. *Free Radical Biology and Medicine* **2003,** 34, 1029-1034.

193. Carr, A.; Tindall, B.; Penny, R.; Cooper, D. A., In vitro cytotoxicity as a marker of hypersensitivity to sulphamethoxazole in patients with HIV. *Clinical & Experimental Immunology* **1993,** 94, 21-5.

194. Wolkenstein, P.; Charue, D.; Laurent, P.; Revuz, J.; Roujeau, J. C.; Bagot, M., Metabolic predisposition to cutaneous adverse drug reactions. Role in toxic epidermal necrolysis caused by sulfonamides and anticonvulsants. *Archives of Dermatology* **1995,** 131, 544-51.

195. Reilly, T. P.; MacArthur, R. D.; Farrough, M. J.; Crane, L. R.; Woster, P. M.; Svensson, C. K., Is hydroxylamine-induced cytotoxicity a valid marker for hypersensitivity reactions to sulfamethoxazole in HIV-infected individuals? *Journal of Pharmacology and Experimental Therapeutics* **1999,** 291, 1356-1364.

196. Pertel, P.; Hirschtick, R., Adverse reactions to dapsone in persons infected with human immunodeficiency virus. *Clinical Infectious Diseases* **1994,** 18, 630-2.

197. Medina, L.; Mills, J.; Leoung, G.; Hopewell, P.; Lee, B.; Modin, G.; Benowitz, N., Oral therapy for *Pneumocystis carinii* pneumonia in the acquired immunodeficiency syndrome. *New England Journal of Medicine* **1990,** 323, 776-782.

198. Israili, Z. H.; Cucinell, S. A.; Vaught, J.; Davis, E.; Lesser, J. M.; Dayton, P. G., Studies of the metabolism of dapsone in man and experimental animals: formation of N-hydroxy metabolites. *Journal of Pharmacology and Experimental Therapeutics* **1973,** 187, 138-151.

199. Gordon, G. R.; Murray, J. F.; Peters, J. H.; Gelber, R. H.; Jacobson, R. R., Studies on the urinary metabolites of dapsone in man. *International Journal of Leprosy* **1979,** 47, 681-682.

200. Coleman, M. D.; Scott, A. K.; Breckenridge, A. M.; Park, B. K., The use of cimetidine as a selective inhibitor of dapsone N-hydroxylation in man. *British Journal of Clinical Pharmacology* **1990,** 30, 761-7.

201. van der Ven, A. J.; Mantel, M. A.; Vree, T. B.; Koopmans, P. P.; van der Meer, J. W., Formation and elimination of sulphamethoxazole hydroxylamine after oral administration of sulphamethoxazole. *British Journal of Clinical Pharmacology* **1994,** 38, 147-50.

202. van der Ven, A. J.; Vree, T. B.; van Ewijk-Beneken Kolmer, E. W.; Koopmans, P. P.; van der Meer, J. W., Urinary recovery and kinetics of

sulphamethoxazole and its metabolites in HIV-seropositive patients and healthy volunteers after a single oral dose of sulphamethoxazole. *British Journal of Clinical Pharmacology* **1995,** 39, 621-5.

203. Vage, C.; Svensson, C. K., Evidence that the biotransformation of dapsone and monoacetyldapsone to their respective hydroxylamine metabolites in rat liver microsomes is mediated by cytochrome P450 2C6/2C11 and 3A1. *Drug Metabolism & Disposition* **1994,** 22, 572-7.

204. Carr, A.; Frei, B., Does vitamin C act as a pro-oxidant under physiological conditions? *FASEB J* **1999,** 13, 1007-1024.

205. Chaudiere, J.; Ferrari-Iliou, R., Intracellular antioxidants: From chemical to biochemical mechanisms. *Food and Chemical Toxicology* **1999,** 37, 949-962.

206. Bolkenius, F. N.; Grisar, J. M.; DeJong, W., A water-soluble quaternary ammonium analog of alpha-tocopherol that scavenges lipoperoxyl, superoxyl and hydroxyl radicals. *Free Radical Research Communications* **1991,** 14, 363-372.

207. Dinis, T. C.; Maderia, V. M.; Almeida, L. M.; Bolkenius, F. N.; Grisar, J. M.; DeJong, W., Action of phenolic derivatives (acetaminophen, salicylate, and 5-aminosalicylate) as inhibitors of membrane lipid peroxidation and as peroxyl radical scavengers. *Archives of Biochemistry and Biophysics* **1994,** 315, 161-169.

208. Kang, J. O.; Slivka, A.; Slater, G.; Cohen, G., In vivo formation of hydroxyl radicals following intragastric administration of ferrous salt in rats. *Journal of Inorganic Biochemistry* **1989,** 35, 55-69.

209. Pedraza-Chaverri, J.; Barrera, D.; Maldonado, P. D.; Chirino, Y. I.; Macias-Ruvalcaba, N. A.; Medina-Campos, O. N.; Castro, L.; Salcedo, M. I.; Hernandez-Pando, R.; Jang, J. H.; Aruma, O. I.; Jen, L. S.; Chung, H. Y.; Surh, Y. J., S-allylmercaptocysteine scavenges hydroxyl radical and singlet oxygen in vitro and attenuates gentamicin-induced oxidative and nitrosative stress and renal damage in vivo. *BMC Clinical Pharmacology* **2004,** 4, 5.

210. Juknat, A. A.; Kotler, M. L.; Quaglino, A.; Carrillo, N. M.; Hevor, T., Necrotic cell death induced by delta-aminolevulinic acid in mouse astrocytes. Protective role of melatonin and other antioxidants. *Journal of Pineal Research* **2003,** 35, 1-11.

211. Reiter, R. J.; Tan, D. X.; Mayo, J. C.; Sainz, R. M.; Leon, J.; Czarnocki, Z., Melatonin as an antioxidant: biochemical mechanisms and pathophysiological implications in humans. *Acta Biochimica Polonica* **2003,** 50, 1129-1146.

212. Rodriguez, C.; Mayo, J. C.; Sainz, R. M.; Antolin, I.; Herrara, F.; Martin, V.; Reiter, R. J., Regulation of antioxidant enzymes: a significant role for melatonin. *Journal of Pineal Research* **2004,** 36, 1-9.

213. Graham IM; O'Callaghan P, Vitamins, homocysteine and cardiovascular risk. *Cardiovasc Drugs Ther* **2002,** 16, (5), 383-389.

214. Mason JB, Biomarkers of nutrient exposure and status in one-carbon (methyl) metabolism. *J Nutr* **2003,** 133 (Suppl 3), 941S–947S.

215. Stover PJ, Physiology of folate and vitamin B12 in health and disease. *Nutr Rev* **2004,** 62, S3–S12.

216. Institute of Medicine, Dietary reference intakes for thiamin, riboflavin, niacin, vitamin B6, folate, vitamin B12, pantothenic acid, biotin and choline. *National Academy Press* **1998**, 203.

217. Dawson DW; Waters HM, Malnutrition: folate and cobalamin deficiency. *Br J Biomed Sci* **1994,** 51, (3), 221-227.

218. Grinblat J, Folate status in the aged. *Clin Geriatr Med* **1985,** 1, (4), 711-728.

219. Morgan SL; Baggott JE; Lee JY; Alarcon GS, Folic acid supplementation prevents deficient blood folate levels and hyperhomocysteinemia during longterm, low dose methotrexate therapy for rheumatoid arthritis: implications for cardiovascular disease prevention. *J Rheumatol* **1998,** 25, (3), 441-446.

220. Semczuk-Sikora A; Semczuk M, Effect of anti-epileptic drugs on human placenta and the fetus. *Ginekol Pol* **2004,** 75, (2), 166-169.

221. Bailey LB, Folate status assessment. *J Nutr* **1990,** 120 Suppl 11, 1508-1511.

222. Herrmann W; Obeid R; Jouma M, Hyperhomocysteinemia and vitamin B-12 deficiency are more striking in Syrians than in Germans--causes and implications. *Atherosclerosis* **2003,** 166, (1), 143-150.

223. Villalpando S; Latulippe ME; Rosas G; Irurita MJ; Picciano MF; O'Connor DL, Milk folate but not milk iron concentrations may be inadequate for some infants in a rural farming community in San Mateo, Capulhuac, Mexico. *Am J Clin Nutr* **2003,** 78, (4), 782-789.

224. Marshall KG; Howell S; Badaloo AV; Reid M; Farrall M; Forrester T; McKenzie CA, Polymorphisms in genes involved in folate metabolism as risk factors for oedematous severe childhood malnutrition: a hypothesis-generating study. *Ann Trop Paediatr* **2006,** 26, (2), 107-114.

225. Tyagi N; Moshal KS; Ovechkin AV; Rodriguez W; Steed M; Henderson B; Roberts AM; Joshua IG; Tyagi SC, Mitochondrial mechanism of oxidative stress and systemic hypertension in hyperhomocysteinemia. *J Cell Biochem* **2005,** 96, (4), 665-671.

226. Yi F; Zhang AY; Janscha JL; Li PL; Zou AP, Homocysteine activates NADH/NADPH oxidase through ceramide-stimulated Rac GTPase activity in rat mesangial cells. *Kidney Int* **2004,** 66, (5), 1977-1987.

227. Ingram AJ; Krepinsky JC; James L; Austin RC; Tang D; Salapatek AM; Thai K; Scholey JW, Activation of mesangial cell MAPK in response to homocysteine. *Kidney Int* **2004,** 66, (2), 733-745.

228. Das UN, Folic acid says NO to vascular diseases. *Nutrition* **2003,** 19, (7-8), 686-692.

229. Symons JD; Mullick AE; Ensunsa JL; Ma AA; Rutledge JC, Hyperhomocysteinemia evoked by folate depletion: effects on coronary and carotid arterial function. *Arterioscler Thromb Vasc Biol* **2002,** 22, (5), 772-780.

230. Heydrick SJ; Weiss N; Thomas SR; Cap AP; Pimentel DR; Loscalzo J; Keaney JF Jr, L-Homocysteine and L-homocystine stereospecifically induce endothelial nitric oxide synthase-dependent lipid peroxidation in endothelial cells. *Free Radic Biol Med* **2004,** 36, (5), 632-640.

231. Huang RF; Hsu YC; Lin HL; Yang FL, Folate depletion and elevated plasma homocysteine promote oxidative stress in rat livers. *J Nutr* **2001,** 131, (1), 33-38.

232. Rodrigo R; Passalacqua W; Araya J; Orellana M; Rivera G, Implications of oxidative stress and homocysteine in the pathophysiology of essential hypertension. *J Cardiovasc Pharmacol* **2003,** 42, (4), 453-461.

233. Wang G; Mao JM; Wang X; Zhang FC, Effect of homocysteine on plaque formation and oxidative stress in patients with acute coronary syndromes. *Chin Med J (Engl)* **2004,** 117, (11), 1650-1654.

234. Muskiet FA, The importance of (early) folate status to primary and secondary coronary artery disease prevention. *Reprod Toxicol* **2005,** 20(3), 403-410.

235. Ozias MK; Schalinske KL, All-trans-Retinoic Acid Rapidly Induces Glycine N-methyltransferase in a Dose-Dependent Manner and Reduces Circulating Methionine and Homocysteine Levels in Rats. *J Nutr* **2003,** 133, (12), 4090-4094.

236. Zhang J; Henning SM; Heber D; Choi J; Wang Y; Swendseid ME; Go VL, NADPH-cytochrome P-450 reductase, cytochrome P-450 2C11 and P-450 1A1, and the aryl hydrocarbon receptor in livers of rats fed methyl-folate-deficient diets. *Nutr Cancer* **1997,** 28, (2), 160-164.

237. Cribb AE; Miller M; Leeder JS; Hill J; Spielberg SP, Reactions of the nitroso and hydroxylamine metabolites of sulfamethoxazole with reduced glutathione. Implications for idiosyncratic toxicity. *Drug Metab Dispos* **1991,** 19, 900–906.

238. Blair JA; Heales SR, Folate deficiency and demyelination in AIDS. *Lancet* **1987,** 2, 509.

239. Israel DS; Plaisance KI, Neutropenia in patients infected with human immunodeficiency virus. *Clinical Pharmacology* **1991,** 10, 268-279.

240. Purdy BD; Plaisance KI, Infection with the human immunodeficiency virus: epidemiology, pathogenesis, transmission, diagnosis, and manifestations. *Am J Hosp Pharm* **1989,** 46, 1185-1209.

241. Smith I; Howells DW; Kendall B; Levinsky R; Hyland K, Folate deficiency and demyelination in AIDS. *Lancet* **1987,** 2, 215.

242. Zarazaga A; Garcia de Lorenzo A; Montanes P; Culebras JM, Folates in human nutrition, Different clinical situations in which folate deficiencies exist. *Nutr Hosp* **1991,** 6, 207-226.

243. Fry L; Macdonald A; Almeyda J; Griffin CJ; Hoffbrand AV, The mechanism of folate deficiency in psoriasis. *Br J Dermatology* **1971,** 84, 539-544.

244. Touraine R; Revuz J; Zittoun J; Jarret J; Tulliez M, Study of folate in psoriasis: blood levels, intestinal absorption and cutaneous loss. *Br J Dermatology* **1973,** 89, 335-341.

245. Blum RN; Miller LA; Gaggini LC; Cohn DL (1992), Comparative trial of dapsone versus trimethoprim/sulfamethoxazole for primary prophylaxis of Pneumocystis carinii pneumonia. *J Acquir Immune Defic Syndr* **1992,** 5, 341–347.

246. Landsteiner K; Jacobs J, Studies on the sensitization of animals with simple chemical compounds. *Journal of Experimental Medicine* **1935,** 61, 643-656.

247. Coleman MD; Breckenridge AM; Park BK, Bioactivation of Dapsone to a cytotoxic metabolite by human hepatic microsomal enzymes. *British Journal of Clinical Pharmacology* **1989,** 28, 389-395.

248. Gill, H.; Tija, J.; Kitteringham, N.; Pirmohamed, M.; Back, D.; Park, B., The effect of genetic polymorphism in CYP2C9 on sulphamethoxazole N-hydroxylation. *Pharmacogenetics* **1999,** 9, 43-53.

249. Moody DE; Walsh SL; Rollins DE; Neff JA; Huang W, Ketoconazole, a cytochrome P450 3A4 inhibitor, markedly increases concentrations of levo-acetyl-alpha-methadol in opioid-naive individuals. *Clin Pharmacol Ther* **2004,** 76, (2), 154-166.

250. Ridtitid W; Wongnawa M; Mahatthanatrakul W; Raungsri N; M., S., Ketoconazole increases plasma concentrations of antimalarial mefloquine in healthy human volunteers. *J Clin Pharm Ther* **2005,** 30, (3), 285-290.

251. Atsumi T; Ishihara M; Kadoma Y; Tonosaki K; Fujisawa S, Comparative radical production and cytotoxicity induced by camphorquinone and 9-fluorenone against human pulp fibroblasts. *J Oral Rehabil* **2004,** 31, 1155–1164.

252. Shangari N; O'Brien PJ, The cytotoxic mechanism of glyoxal involves oxidative stress. *Biochem Pharmacol* **2004,** 68, 1433–1442.

253. Tafazoli S; O'Brien PJ, Prooxidant activity and cytotoxic effects of indole-3-acetic acid derivatives radicals. *Chem Res Toxicol* **2004,** 17, 1350–1355.

254. Kannan K; Jain SK, Oxidative stress and apoptosis. *Pathophysiology* **2000,** 7, 153 - 163.

255. Coopman SA; Johnson RA; Platt R, e. a., Cutaneous disease and drug reactions in HIV infection. *N Engl J Med* **1993,** 328, 1670 - 1674.

256. Buhl R; Jaffe HA; Holroyd KJ, e. a., Systemic glutathione deficiency in symptom-free HIV-seropositive individuals. *Lancet* **1989,** 2, 1294 - 1298.

257. Carr A; Gross A; Hoskins J; Penny R; Cooper D, Acetylation phenotype and cutaneous hypersensitivity to trimethoprim-sulphamethoxazole in HIV infected patients. *AIDS* **1994,** 8, 333-337.

258. Wolkenstein, P.; Loriot, M.; Aractingi, S.; Cabelguenne, A.; Beaune, P.; Chosidow, O., Prospective evaluation of detoxification pathways as markers of cutaneous adverse reactions to sulphonamides in AIDS. *Pharmacogenetics* **2000,** 10, 821-828.